Evaluation of random temperature fluctuation problems with frequency response approach

(Research Report)

January 2000

Japan Nuclear Cycle Development Institute

O-arai Engineering Center

Ⓚ

JNC TN9400 2001－004
January 2000

Evaluation of random temperature fluctuation problems with frequency response approach

(Research Report)

Yves LEJEAIL* and Naoto KASAHARA**

Abstract

Since thermal striping is a coupled thermohydraulic and thermomechanical phenomenon, sodium mock-up tests were usually required to confirm structural integrity. Authors have developed the frequency response function to establish design-by-analysis methodology for this phenomenon. Applicability of this method to sinusoidal fluctuation was validated through two benchmark problems with FAENA and TIFFSS facilities under EJCC contract. This report describes the extension of the frequency response method to random fluctuations. As an example of application, fatigue strength of a Tee junction of PHENIX secondary piping system was investigated.

* CEA-Cadarache DER/SERSI/LECC
** Structure and Material Research Group, System Engineering Division, OEC, JNC

JNC TN9400 2001－004
２０００年１月

周波数応答関数法によるランダム温度ゆらぎの評価

（研究報告書）

Yves LEJEAIL*、笠原 直人**

要　旨

流体温度ゆらぎによる構造物の熱疲労現象はサーマルストライピングと呼ばれ、従来その評価にはナトリウムモックアップテストが必要であった。これを解析的評価法に置き換えるため、著者らは周波数応答関数法を提案し、FAENA試験とTIFFSS試験データを用いて正弦波温度ゆらぎに対する適用性を検証した。本報告書では、周波数応答関数法の拡張とランダム温度ゆらぎ問題への適用方法について述べる。また例として、フェニックス二次系配管の合流部の熱疲労問題を取り上げ、周波数応答関数法による評価を行った。

尚、本内容は1999年9月から2000年8月までの期間にCEAカダラッシュ研究所にて実施した業務の一部である。

*）　CEAカダラッシュ研究所　炉心機器研究室
**）大洗工学センター　システム技術開発部　構造材料技術開発グループ

Contents

List of tables

List of figures

NOMENCLATURE

$T_f(t)$: Temperature of fluid

ΔT_f: Amplitude of sinusoidal temperature fluctuation of fluid

ΔT_s: Amplitude of sinusoidal temperature fluctuation on the structural surface

$\sigma(t)$: Stress in structure

$\Delta\sigma|_{x=0}$: Amplitude of sinusoidal stress fluctuation on the structural surface

$\Delta\sigma_i$: Ideal stress range converted from hundred percent of fluid temperature amplitude

$G(x,t)$: Time response function of structure to fluid temperature fluctuation

$T_f(j\omega)$: Expression of $T_f(t)$ in frequency domain

$\sigma(j\omega)$: Expression of stress in frequency domain

$G(B_i, jf^*)$: Frequency response function of structural surface to fluid temperature fluctuation

$Bi = \frac{hL}{\lambda}$: Biot number

$t^* = \frac{ta}{L^2}$: Fourier number

$f^* = \frac{fL^2}{a}$: Non-dimensional frequency

x: Length from the surface of structure

t: Time

f: Frequency of sinusoidal fluctuation

ω: Rotational frequency of sinusoidal fluctuation

ϕ: Phase delay

h: Heat transfer coefficient

L: Wall thickness of structure

A: Area

V: Volume

a: Thermal diffusivity of structural material

λ: Heat conductivity of structural material

c: Specific heat

ρ: Density

E : *Young's* modulus of structural material

α: Linear expansion coefficient of structural material

ν: *Poisson's* ratio of structural material

K: Stress index determined by mechanical boundary conditions and material properties

$K = 1/(1-\nu)$ in the case of biaxial plane stress condition

D_f: Fatigue damage factor

N: Cycle number

N_f: Allowable cycle number of structural material

$\Delta \varepsilon_{tot}$: Strain range

1. INTRODUCTION

At an incomplete mixing area of high and low temperature fluids near the structural surface, temperature fluctuation of fluid gives thermal fatigue damage on the walls of structures. This coupled thermohydraulic and thermomechanical phenomenon is called thermal striping, which has so complex mechanism and sometimes causes crack initiation on the structural surfaces that sodium mock-up tests are usually required to confirm structural integrity of components. From recent needs of cost reduction, design-by-analysis methodology is strongly desired for thermal striping.

One of main difficulties to apply numerical approach to evaluate temperature attenuation is thermal hydraulic calculation near walls, where temperature attenuation puts influence on structural integrity. It is required detailed turbulent calculation methods such as DNS and LES with fine meshes less than laminar sub-layers [1]. Those require so huge computational resources that simulation time is usually insufficient to evaluate long time phenomena. Another problem in mechanical side is shortage of high cycle fatigue data to evaluate large number of strain cycles caused from high frequency fluctuation and uncertainty of extrapolation of fatigue strength to long time under random loading.

In order to overcome above difficulties, author paid attention to following structural characteristics. Wall structures can not respond to high frequency fluctuation of fluid temperature because of heat transfer loss and low frequency components of fluctuation may not cause large thermal stresses since thermal homogenization occurs in materials as in Fig.1.1. By utilizing these characteristics, authors have proposed the frequency response method, where stress amplitude of structures can be predicted against the temperature fluctuation with a constant frequency and a heat convection factor [2]. Advantages of this approach are a significant reduction of stress calculation time and an understanding of damageable frequency. This method was validated through two benchmark problems with FAENA and TIFFSS facilities under EJCC contract [3][4][5].

This report describes evaluation methods of random temperature fluctuation problems with the frequency response approach to random fluctuations. An evaluation method in time domain is proposed and possibility of evaluation in frequency domain is discussed. For example, temperature fluctuation of a Tee junction of PHENIX secondary piping system [6] is investigated. An inverse function of the frequency response function can predict fluid and inner surface temperature fluctuations from outer surface measurements. It is possible to utilize these data for validation of thermal hydraulic calculations.

Since simulation time is often not sufficient to give an accurate mechanical evaluation, several ways to extrapolate random signals are investigated.

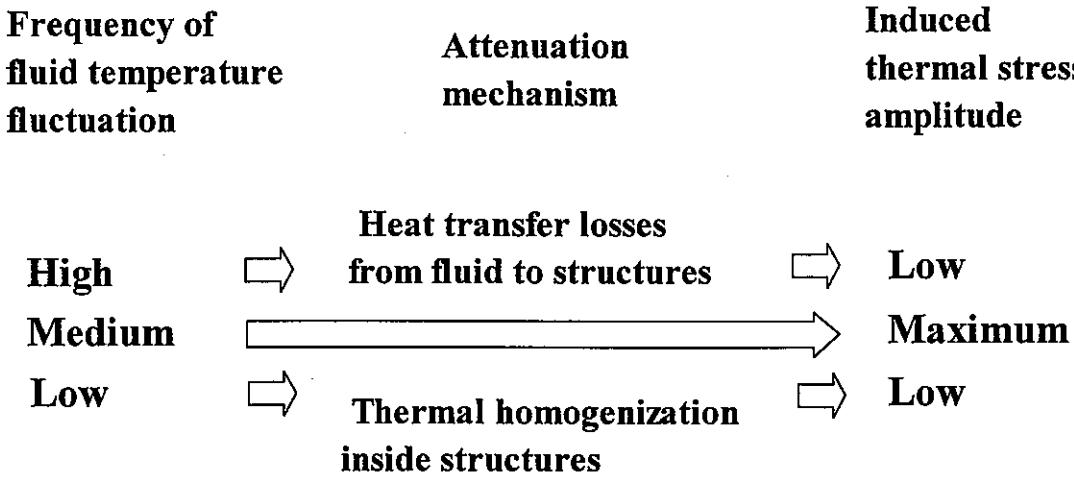

Fig.1.1 General tendency of structural response to fluid temperature fluctuation

2. ANALYSIS METHOD WITH FREQUENCY RESPONSE FUNCTIONS

2.1. STRESS ANALYSIS PROCEDURE

By using the frequency transfer function[2], we can predict stress response to fluid temperature $T_f(t)$ on both time and frequency domain.

Fourier transform of fluid temperature $T_f(t)$ is

$$\Im[T_f(t)] = T_f(jf) \tag{2.1}$$

Stress response $\sigma(jf)$ in frequency domain is calculated with the frequency response function $G(B_i, jf^*)$ as,

$$\sigma(jf) = KE\alpha\Delta G(B_i, jf^*) * T_f(jf) \tag{2.2}$$

where K is stress index determined by mechanical boundary conditions and material properties, and becomes

$$K = 1/(1-\nu) \tag{2.3}$$

in the case of biaxial plane stress condition.

Summary of the frequency response function is explained here. It is a function of non-dimensional frequency $f^* = \frac{fL^2}{a}$ and Biot number $Bi = \frac{hL}{\lambda}$.

Both formulae and the following diagrams provide gains and phase delay of frequency response functions for three kinds of constraint conditions.

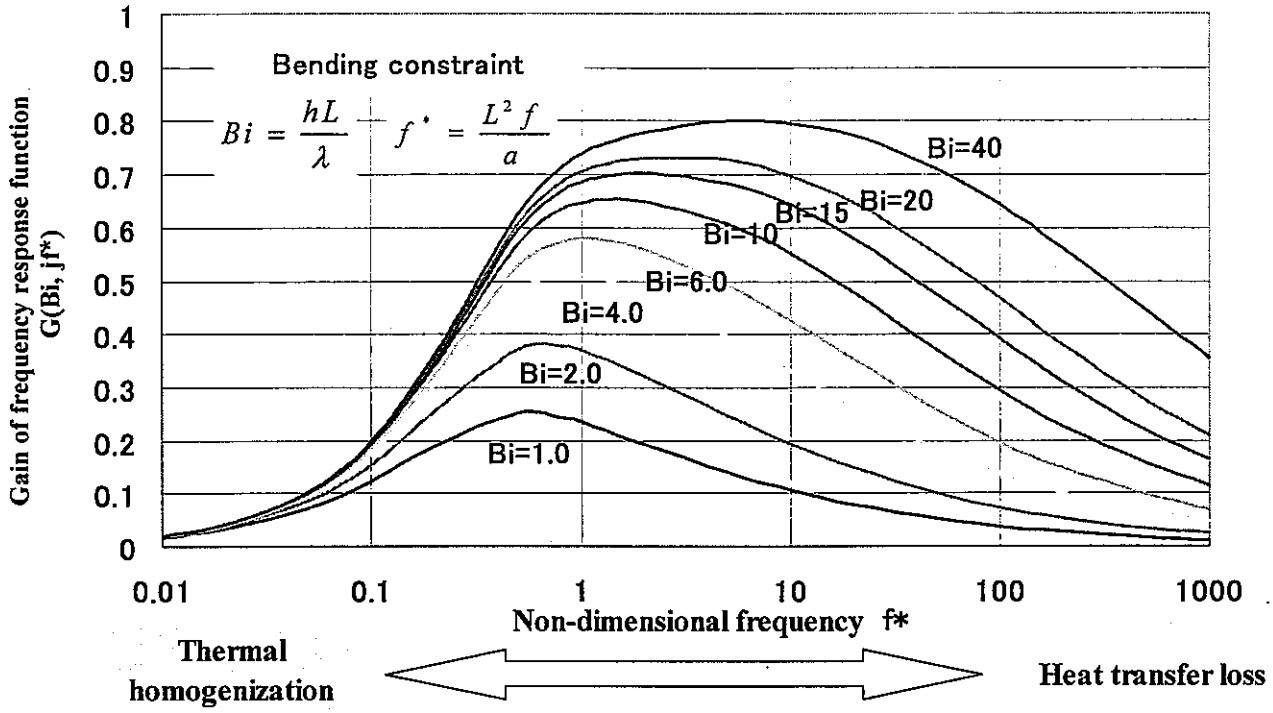

Fig.2.1 Gain of frequency stress response to fluid temperature fluctuation
(Bending constraint condition)

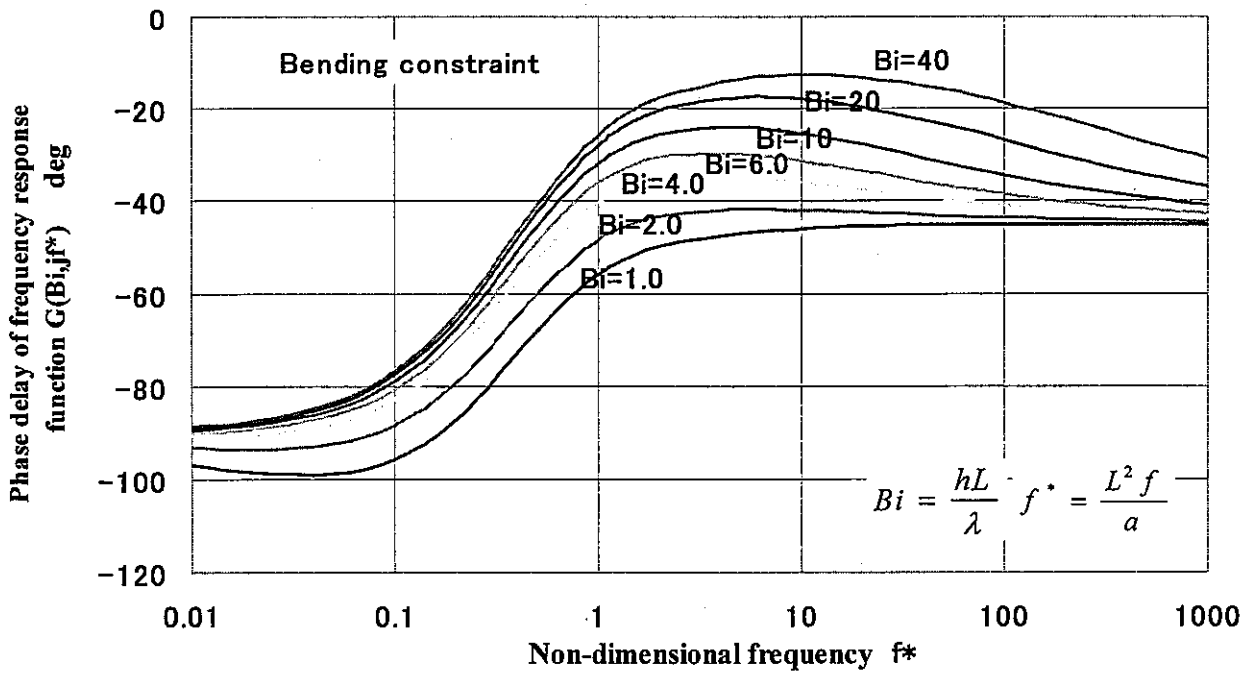

Fig.2.2 Phase delay of frequency stress response to fluid temperature fluctuation
(Bending constraint condition)

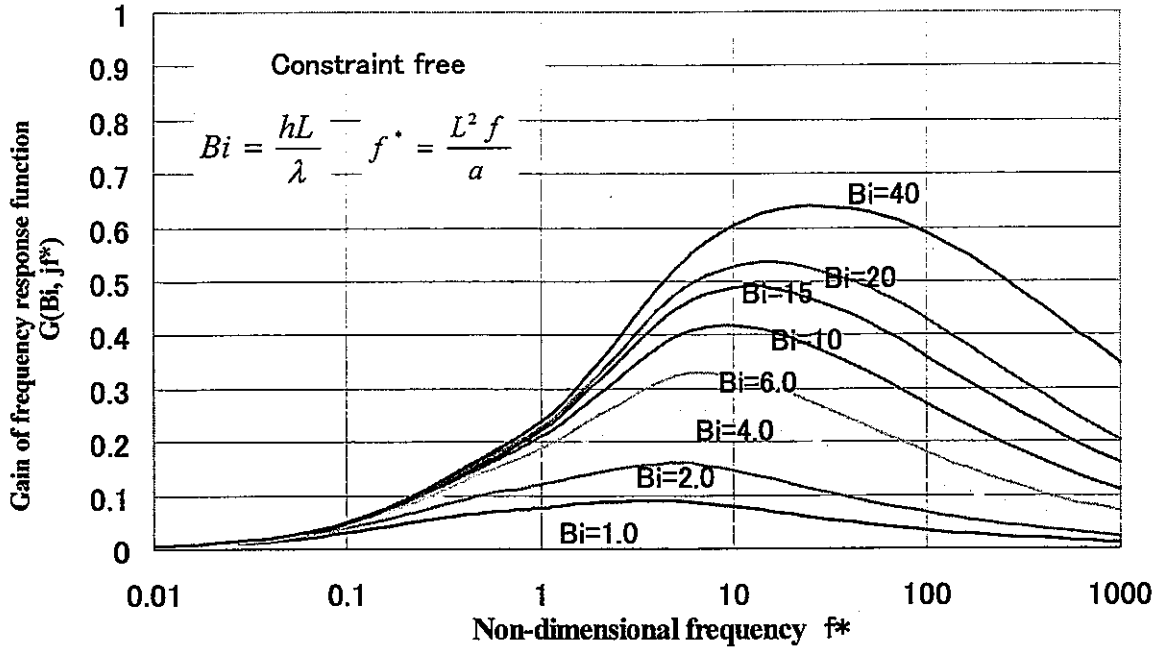

Fig.2.3 Gain of frequency stress response to fluid temperature fluctuation
(Constraint free condition)

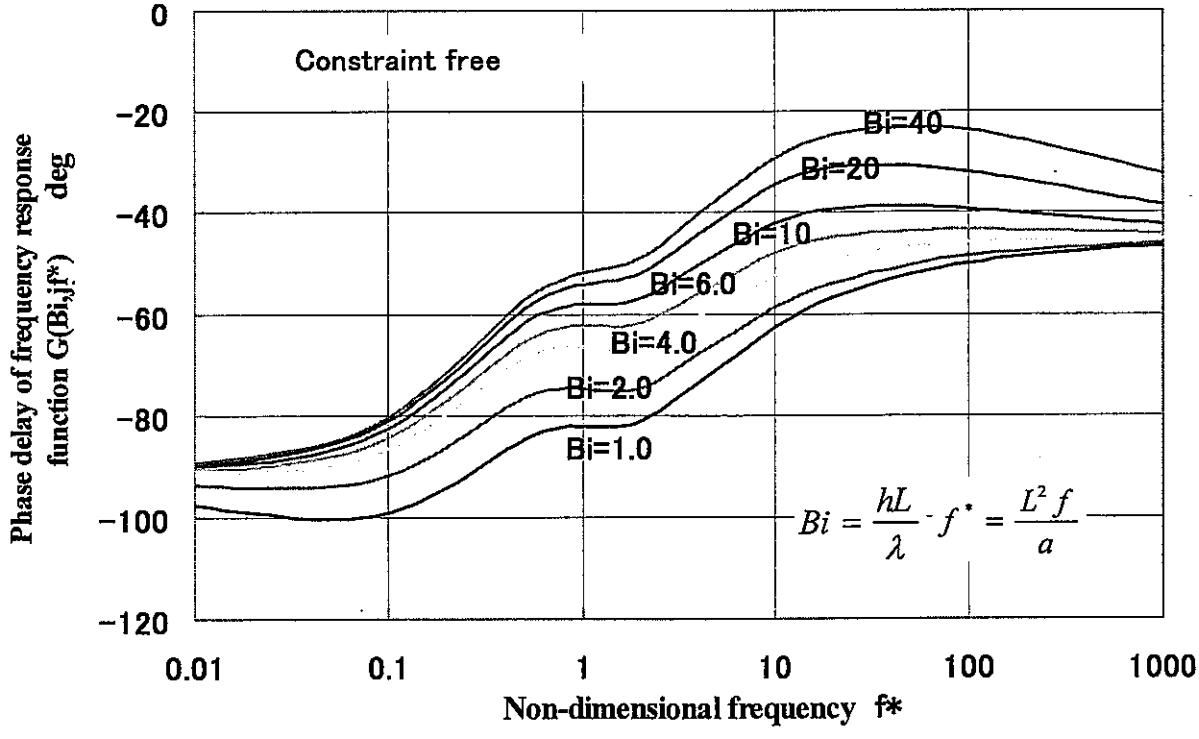

Fig.2.4 Phase delay of frequency stress response to fluid temperature fluctuation
(Constraint free condition)

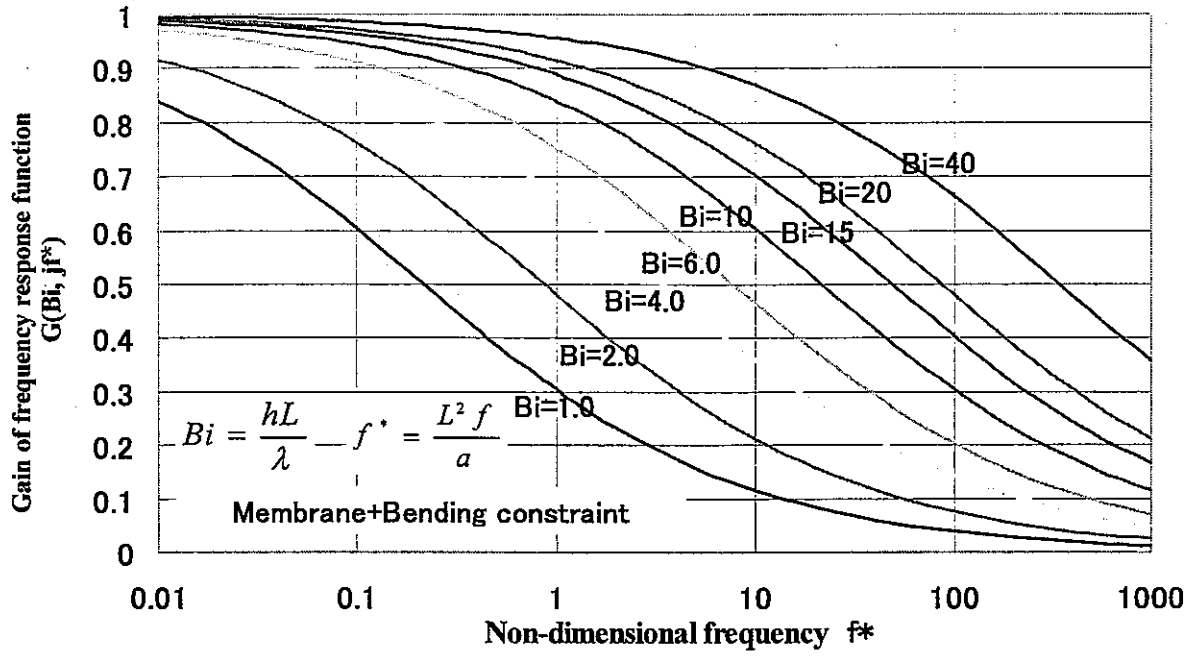

Fig.2.5 Gain of frequency stress response to fluid temperature fluctuation
(Membrane plus bending constraint condition)

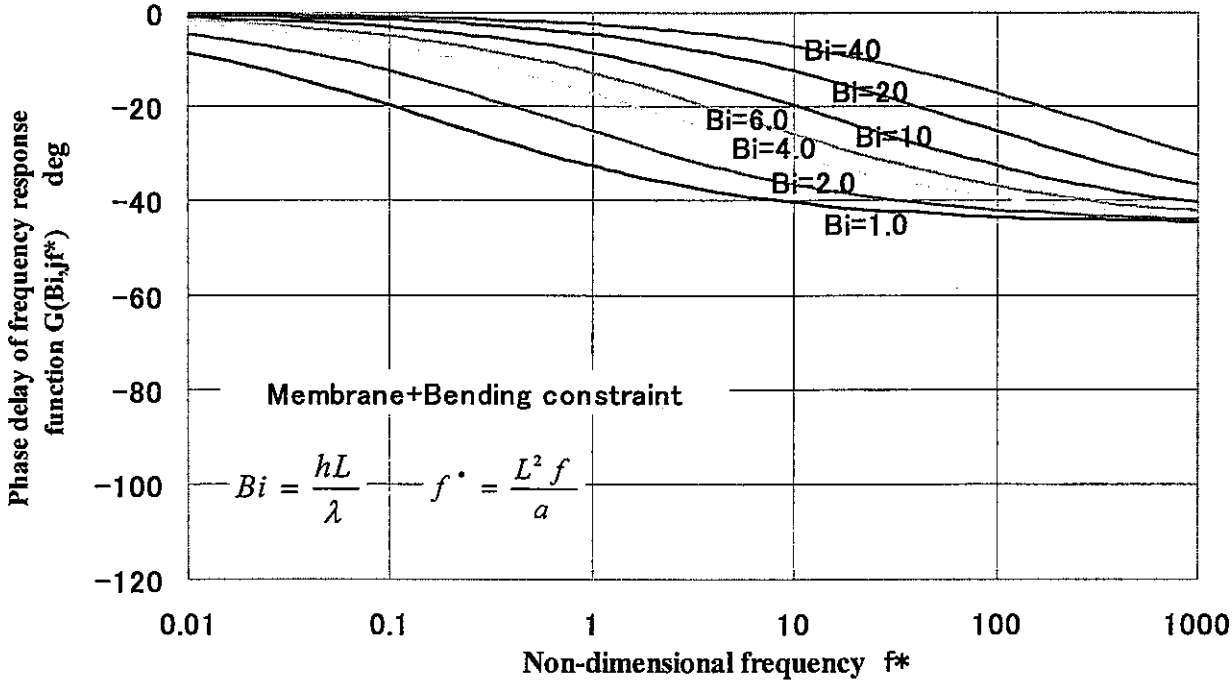

Fig.2.6 Phase delay of frequency stress response to fluid temperature fluctuation
(Membrane plus bending constraint condition)

We can get stress response $\sigma(t)$ in time domain by inverse Fourier analysis.

$$\mathfrak{I}^{-1}[\sigma(jf)] = \sigma(t) \tag{2.4}$$

In Eq.(2.3), the frequency response function $G(B_i, jf^*)$ works as a band pass filter. Therefore, we can limit frequency range for fatigue evaluation.

2.2 FATIGUE STRENGTH ANALYSIS PROCEDURE IN TIME DOMAIN

When time series of stress are obtained, the Rainflow wave counting technique can evaluate pairs of stress ranges $\overline{\Delta\sigma}^{i}$ and their cycle numbers N_i.

Considering strain enhancement from plasticity, JNC procedure estimates total strain range $\overline{\Delta\varepsilon_{tot}}$ from elastically calculated equivalent stress range $\overline{\Delta\sigma}$ [7].

$$\overline{\Delta\varepsilon_{tot}} = Ke' \overline{\Delta\varepsilon_e} \tag{2.5}$$

$$\overline{\Delta\varepsilon_e} = \frac{\overline{\Delta\sigma}}{E} \tag{2.6}$$

$$Ke' = \{1 + (q - 1)(1 - \frac{2\sigma_y}{\overline{\Delta\sigma}})\}, \tag{2.7}$$

where q is an elastic follow-up parameter and can be adjusted to $q = 5/3$, when stress is generated by temperature gradient across wall thickness[8]. In Eq.(2.7), Ke' factor has the simier meaning to Kν factor in RCC-MR.

The evaluated strain range $\overline{\Delta\varepsilon_{tot}}$ predicts an allowable cycle number $N_f\left(\overline{\Delta\varepsilon_{tot}}\right)$ from fatigue curves of material at the maximum temperature. Here, JNC procedure takes strain rate effect into account. *Miner's* rule evaluates fatigue damage factor D_f as

$$D_f = \sum \frac{N\left(\overline{\Delta\varepsilon_{tot}}\right)}{N_f\left(\overline{\Delta\varepsilon_{tot}}\right)} \tag{2.8}$$

where, $N\left(\overline{\Delta\varepsilon_{tot}}\right)$ is the applied cycle number of strain range $\overline{\Delta\varepsilon_{tot}}$.

2.3. FATIGUE STRENGTH ANALYSIS PROCEDURE IN FREQUENCY DOMAIN

This section examines a possibility to apply stress analysis results in frequency domain directly to fatigue strength evaluation.

When introducing service period, frequencies can be converted into cycle numbers and it enables direct comparison of frequency response diagrams with fatigue curves of materials as in the next figures. From this figure, we can understand damageable frequency region immediately.

In this section, let us discuss about ideas of fatigue analysis in frequency domain and its possibility.

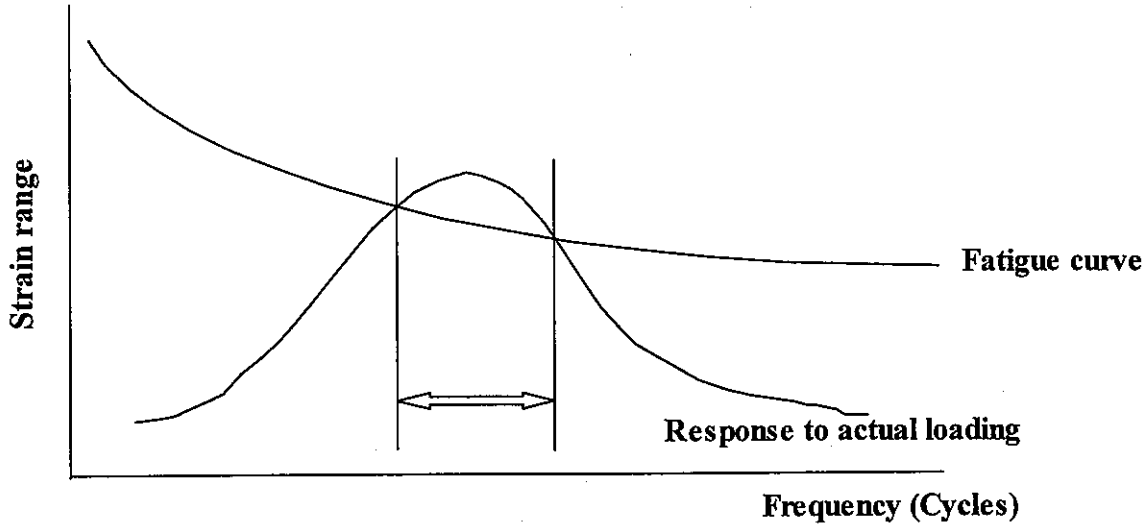

Fig.2.7 Fatigue analysis with the frequency response function

(1) Method 1

One of ideas to consider summation of frequency components is integration of components. Amplitude of low frequency components are enhanced by high frequency components, since there are more that one high frequency cycles during one cycle of low frequency cycle. So that, when ignoring phase delay that is conservative assumption, effective gains for frequency f can be calculated by integration of gains from frequency f to infinitive frequency as

$$\overline{|G(B_i, jf^*)|} = \int_{f^*}^{\infty} |G(B_i, jf)| df \,. \tag{2.9}$$

By using the stress range that corresponds to each frequency, the next equation can evaluate the total fatigue damage with the strain concentration procedure.

$$D_f = \int \frac{N(f)}{N_f(f)} df \qquad (2.10)$$

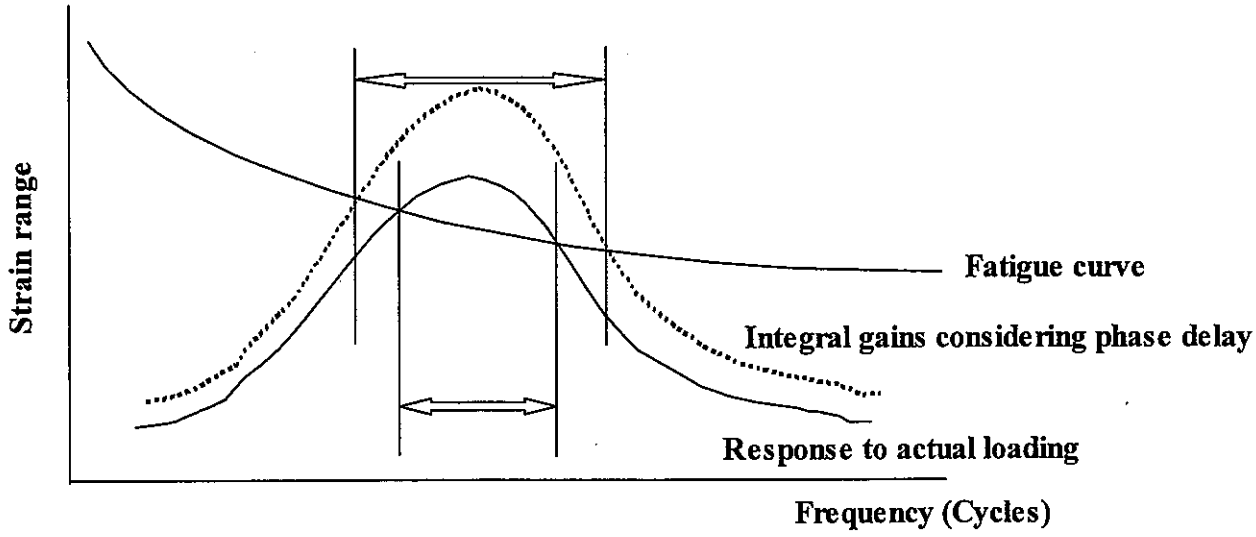

Fig.2.8 Fatigue analysis with integrated gains

(2) Method 2

The next idea is an assumption of average stress at the same level as the maximum stress as the next figure. Modified fatigue curves considering average stresses are utilized instead of normal curves. This method is for considering influence from low frequency components to high frequency components and ignores phase delay among frequency components.

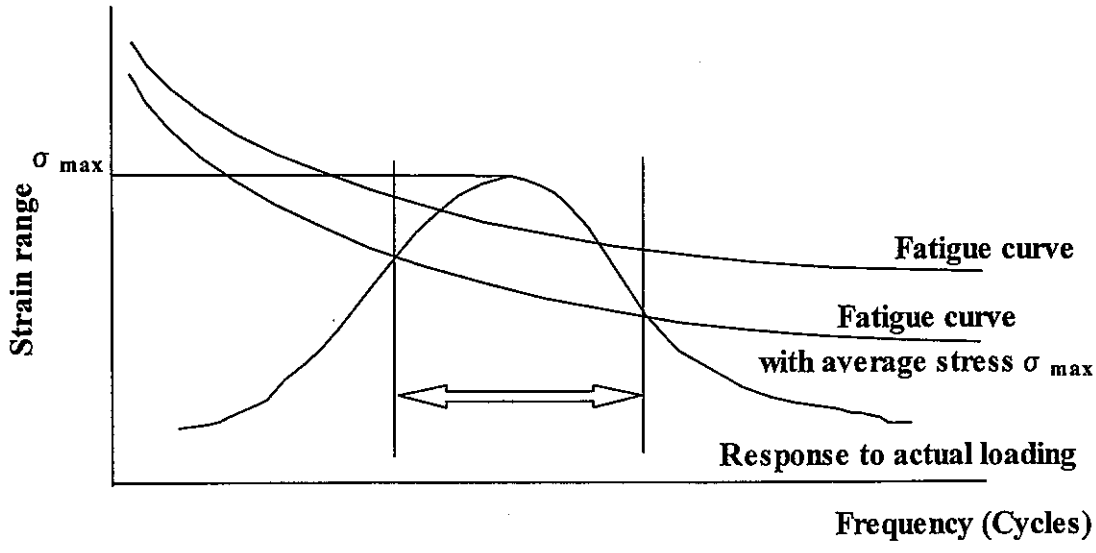

Fig.2.9 Fatigue analysis with assumption of average stress

3. VALIDATION BY SIMPLE PROBLEMS

3.1. DEFINITION OF PROBLEMS

The frequency response function method is examined through application to such simple problems as a plate model subjected to linear summation of sinusoidal temperature fluctuations (Fig.3.1). Loading conditions are summarized in Table 3.1.

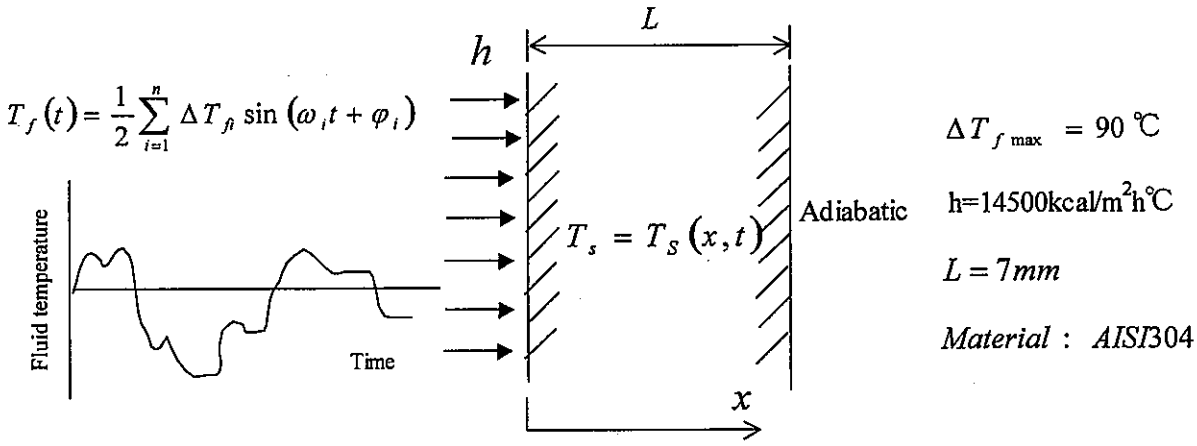

Fig.3.1 Plate model subjected to summation of sinusoidal temperature fluctuation

Table 3.1 Analysis cases

Case	n	ΔT_{f1}	ω_1	ϕ_1	ΔT_{f2}	ω_2	ϕ_2
S1	1	90*	0.085*2π	0			
S1-0.1	2	60*	0.085*2π	0	30*	0.0085*2π	0
S1-10	2	60*	0.085*2π	0	30*	0.85*2π	0
S1-0.01	2	60*	0.085*2π	0	30*	0.00085*2π	0
S1-100	2	60*	0.085*2π	0	30*	8.5*2π	0
S1-2(0.25)	2	60*	0.085*2π	0	30*	0.17*2π	−0.25*2π
R1	∞	90*	0.085*2π	0	rectangular		

* Average temperature = 385℃

Time histories of fluid temperature of above analysis cases are shown in Fig.3.2.

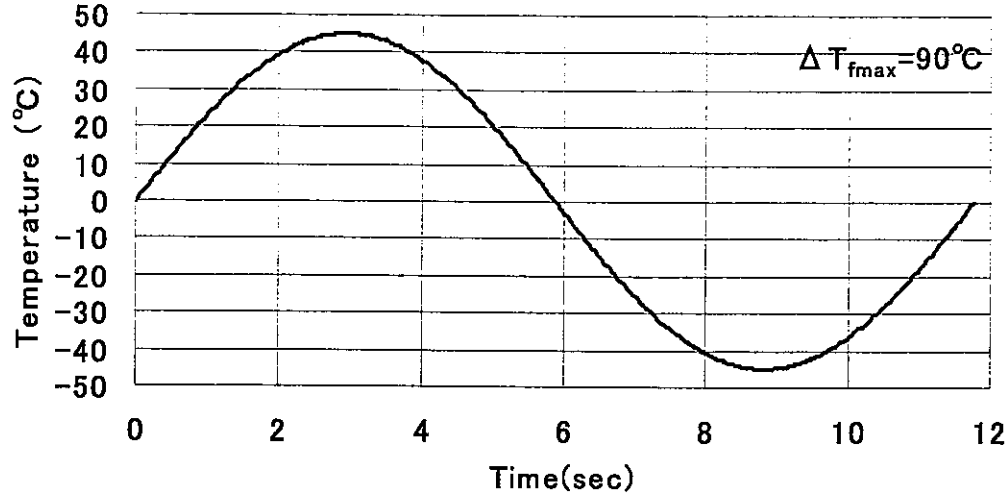

Temperature history of fluid (s1)

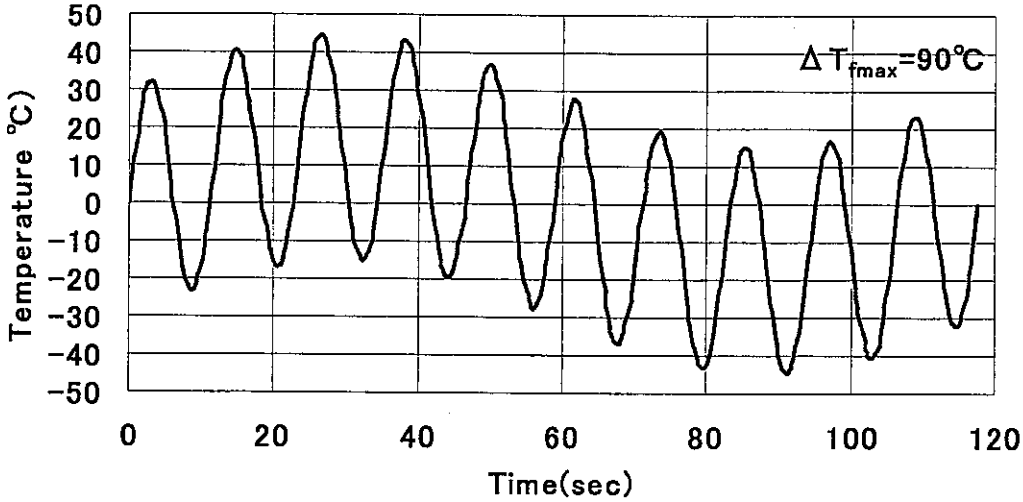

Temperature history of fluid (s1-0.1)

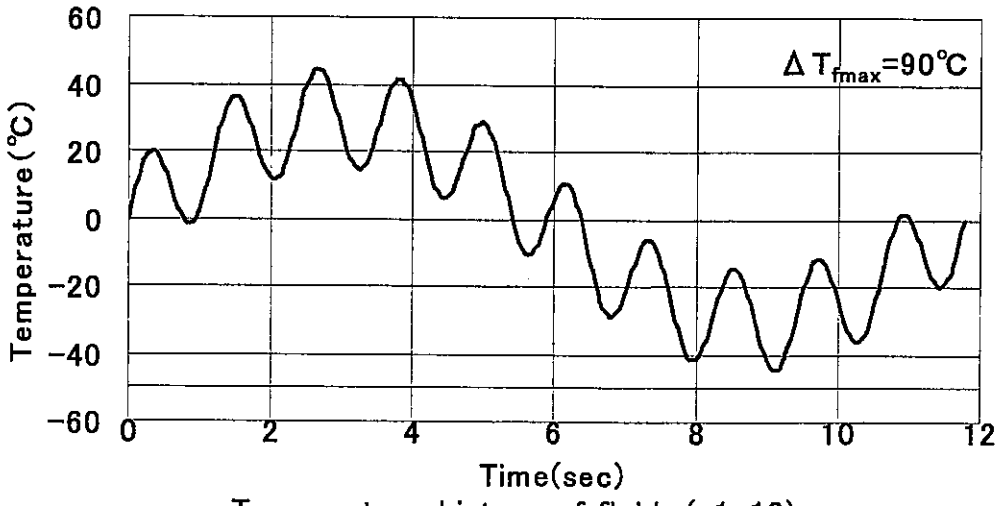

Temperature history of fluid (s1-10)

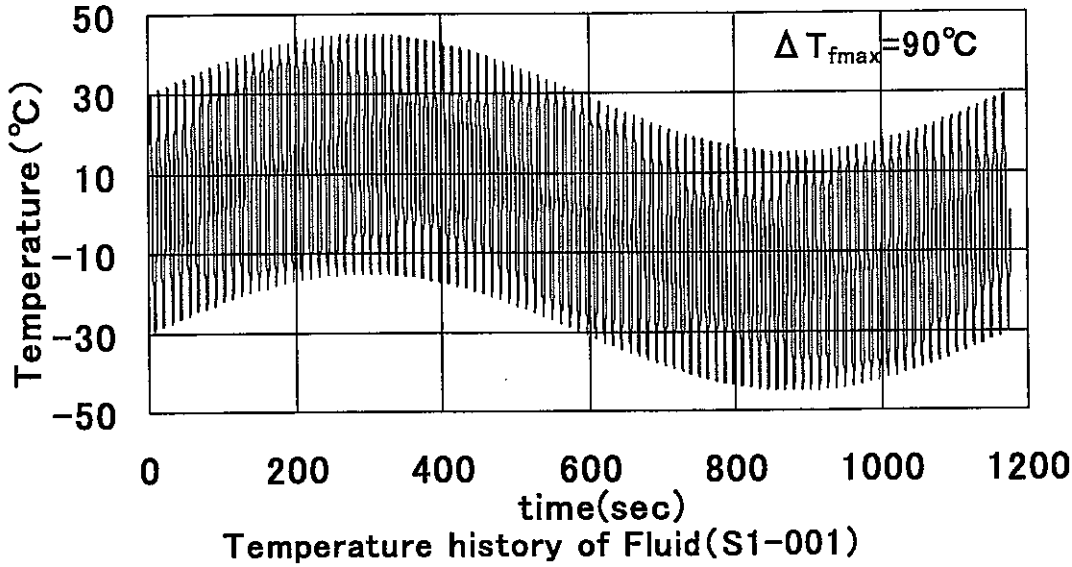

Temperature history of Fluid(S1-001)

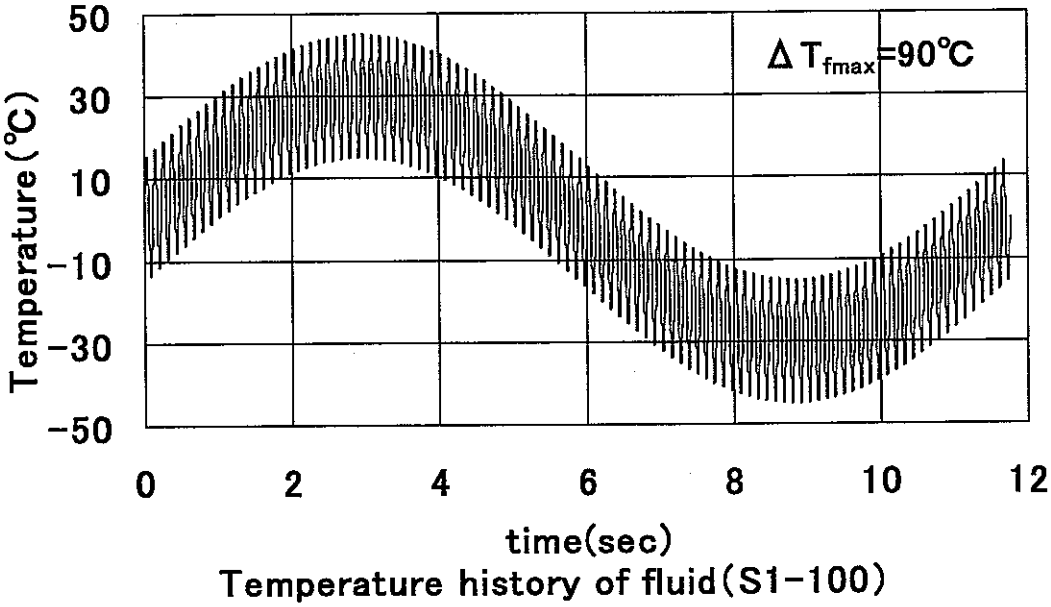

Temperature history of fluid(S1-100)

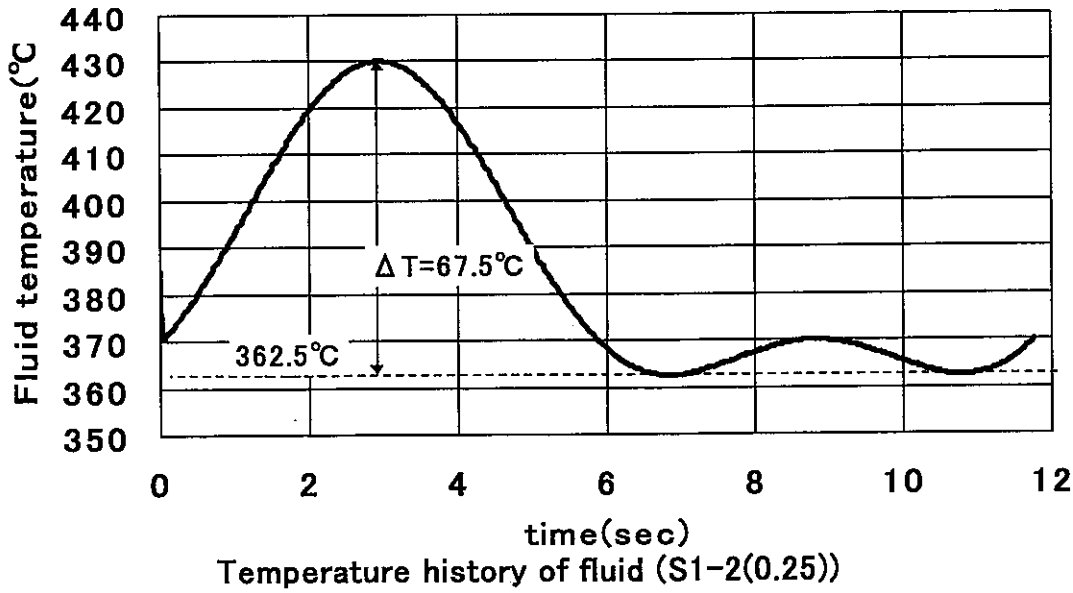

Temperature history of fluid (S1-2(0.25))

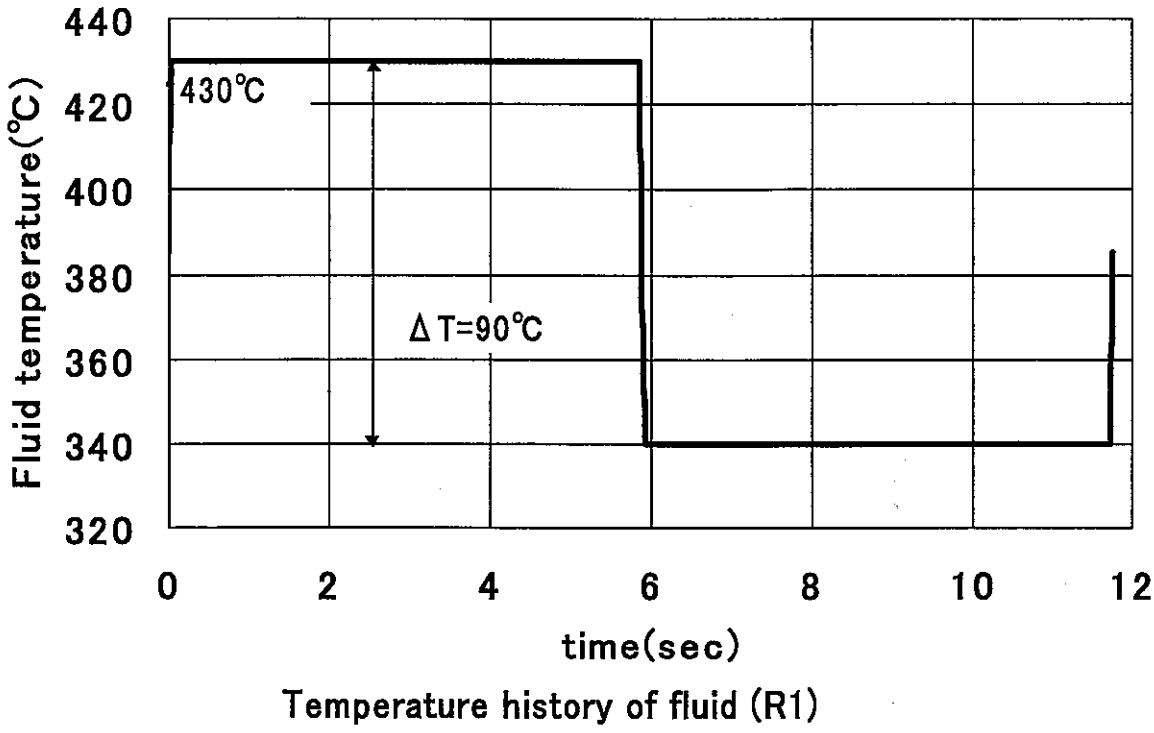

Fig.3.2 Time histories of fluid temperature on the surface

3.2 PREDICTION OF STRESS RESPONSE

(1) Finite element analysis for validation

To obtain reference data for validation of the frequency response method, finite element analyses have been conducted with mesh models shown in Fig.3.3.

Fig.3.4 are time histories of calculated thermal stress on the inner surface. When observing results of FFT analysis of F.E. calculated stress as in Fig.3.5, we can understand frequencies of stress were modulated from fluid ones by structural response characteristics.

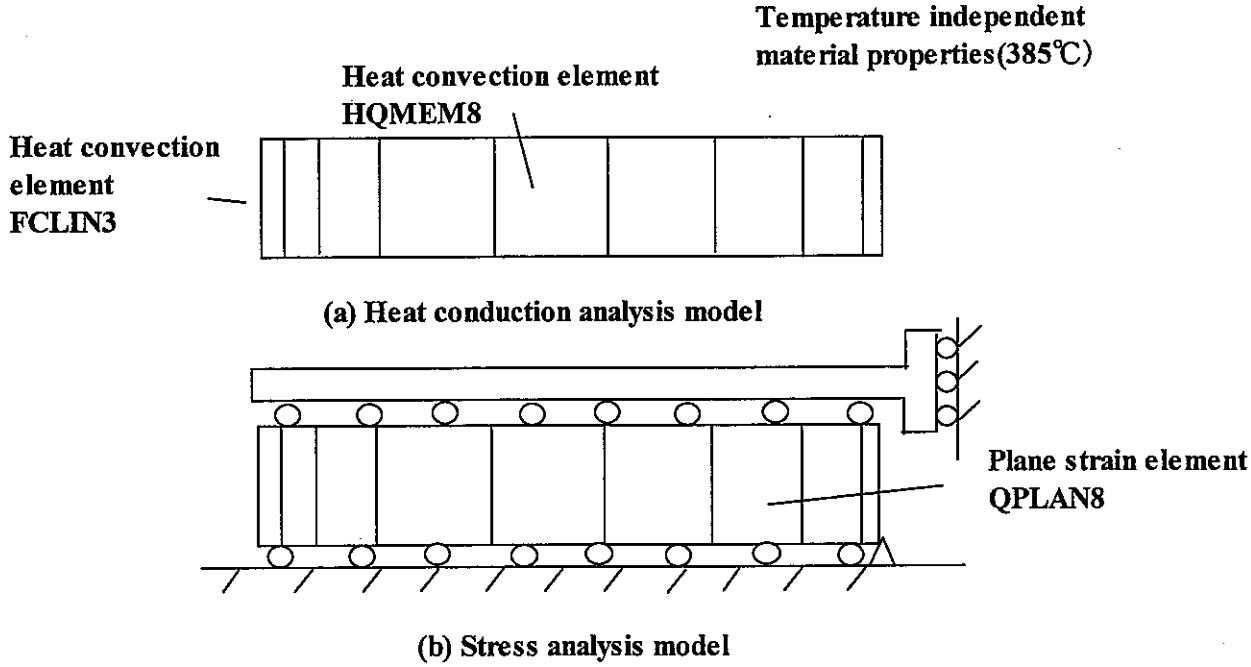

Fig.3.3 Finite element models for validation

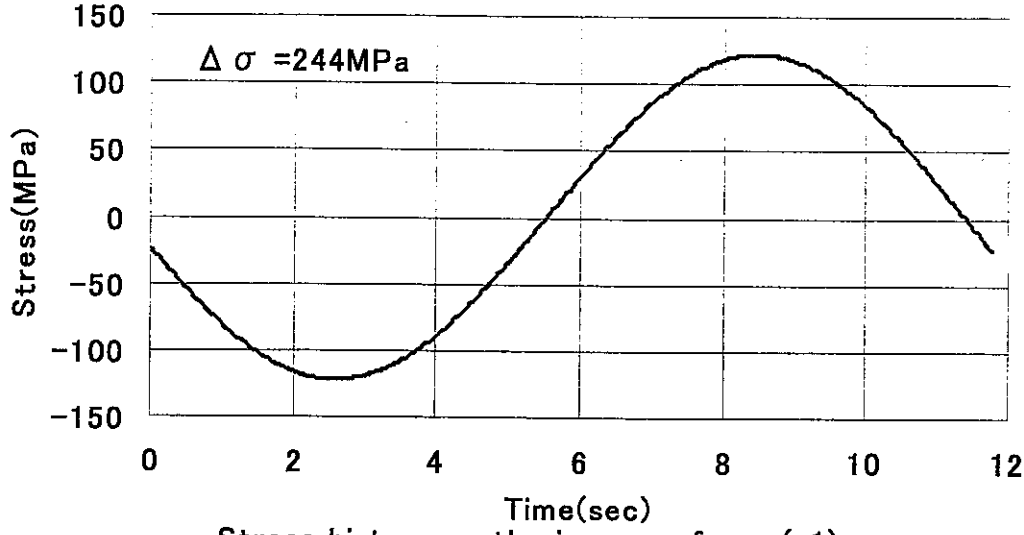

Stress history on the inner surface (s1)

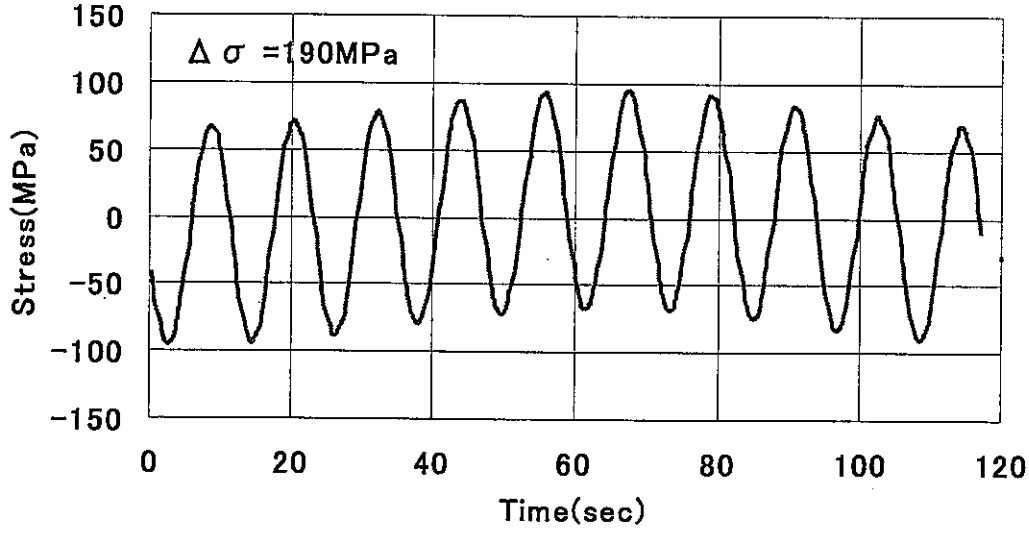

Stress history on the inner surface (s1-0.1)

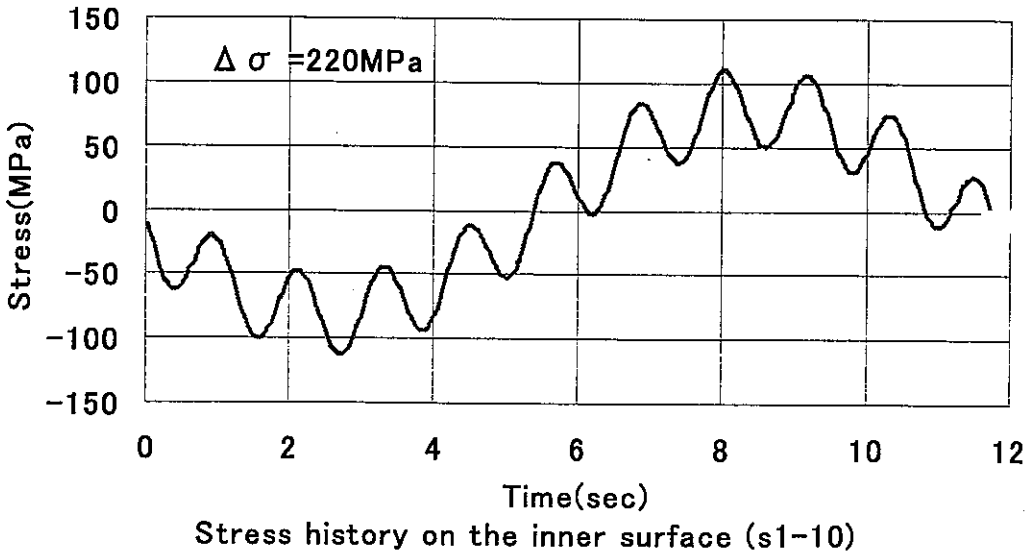

Stress history on the inner surface (s1-10)

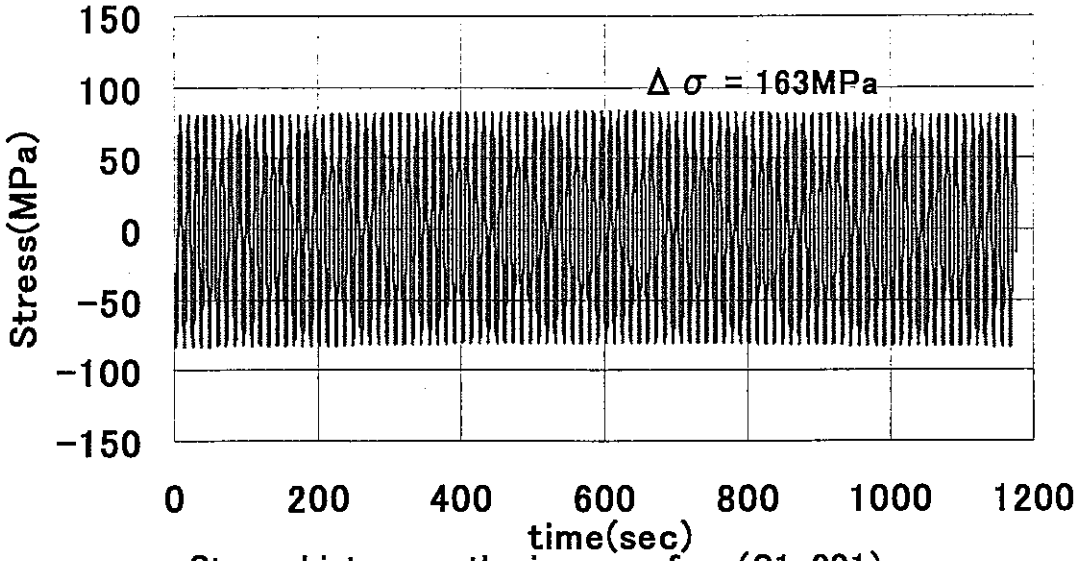

Stress history on the inner surface(S1−001)

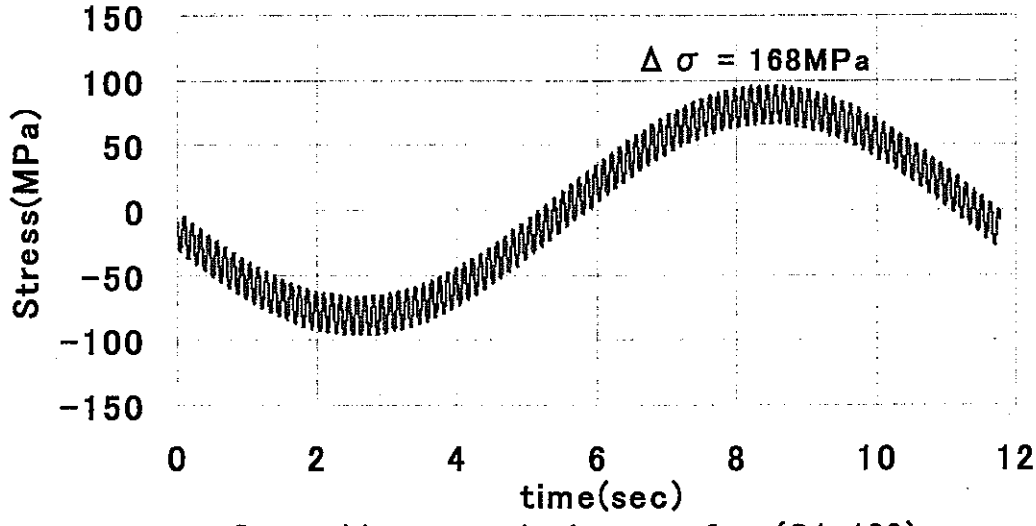

Stress history on the inner surface(S1−100)

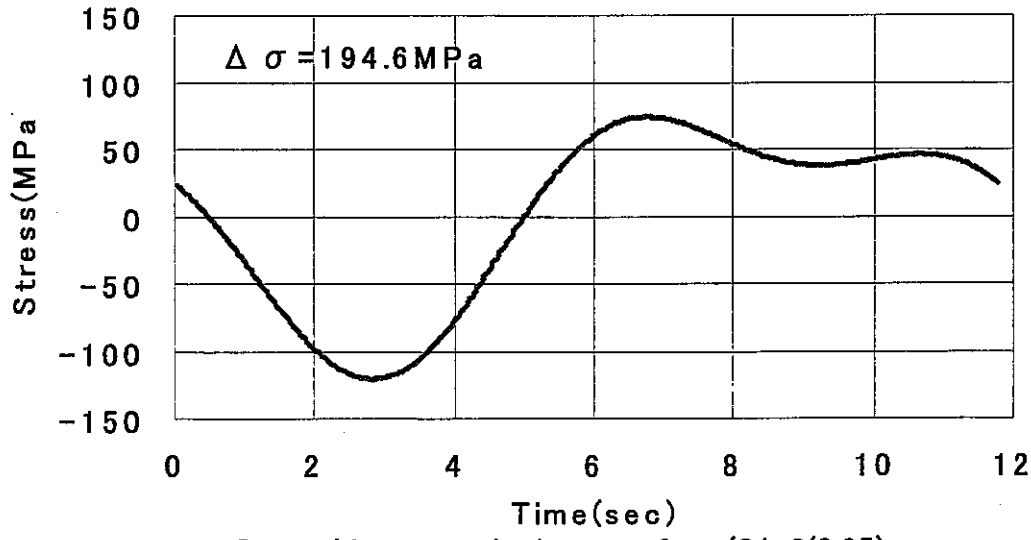

Stress history on the inner surface (S1−2(0.25)

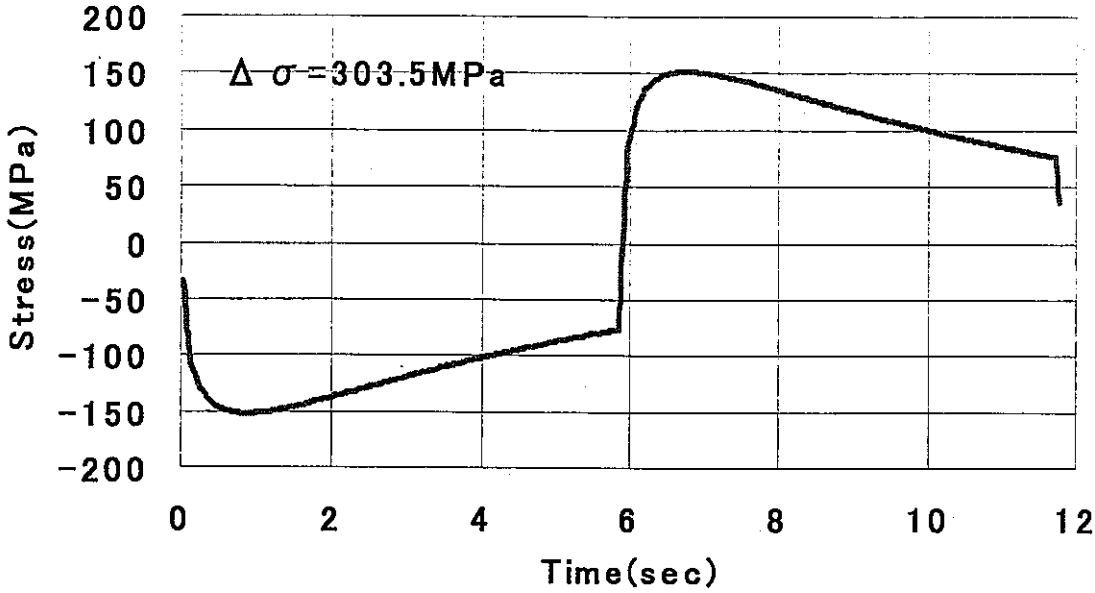

Stress history on the inner surface (R1)

Fig.3.4 Histories of calculated thermal stress on the surface

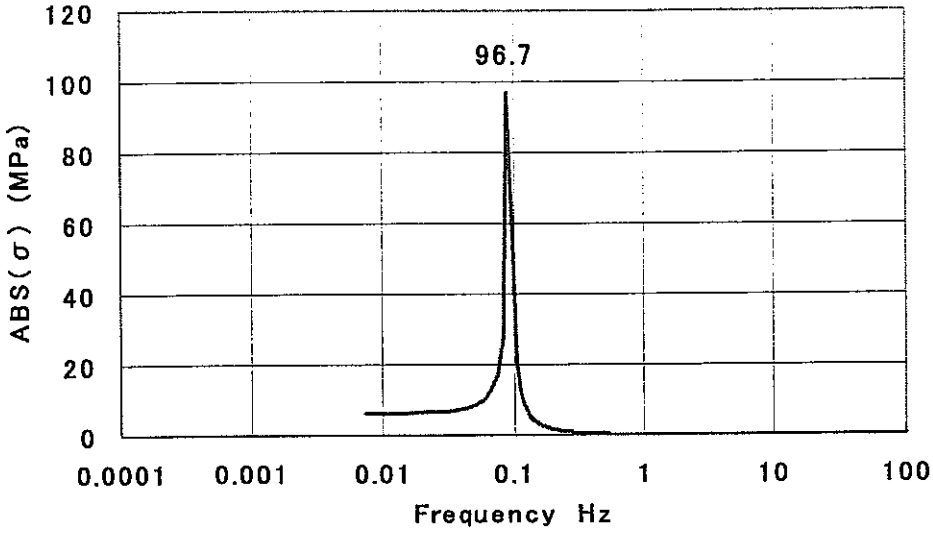

Square root of power spectrum of stress (S1)

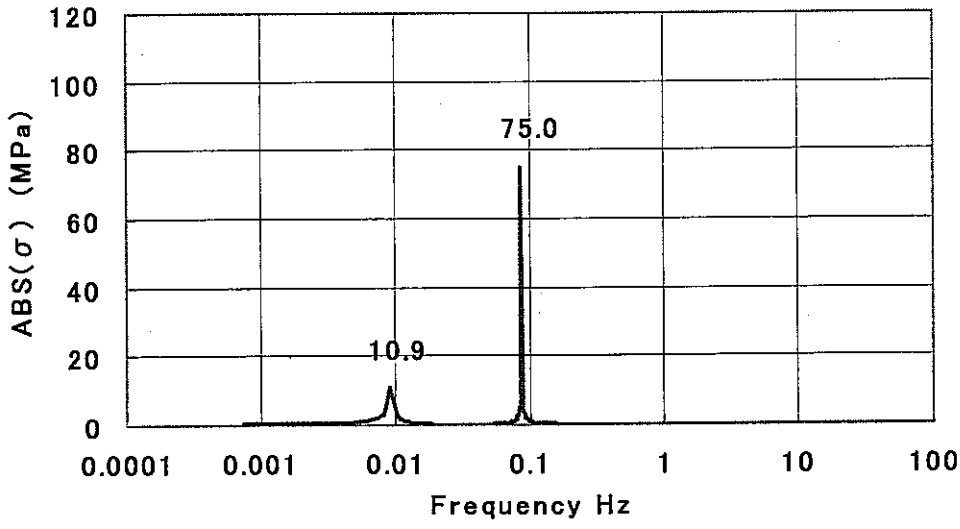

Square root of power spectrum of stress (S1-0.1)

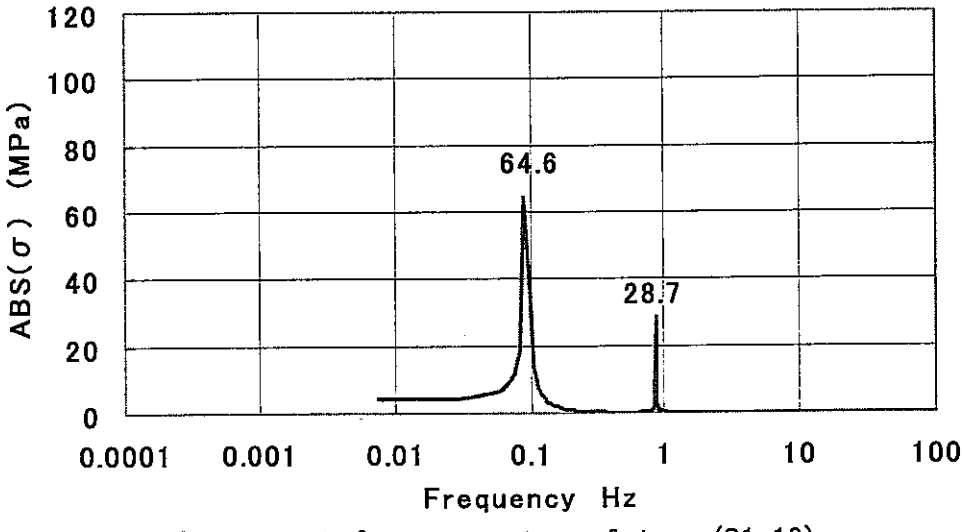

Square root of power spectrum of stress (S1-10)

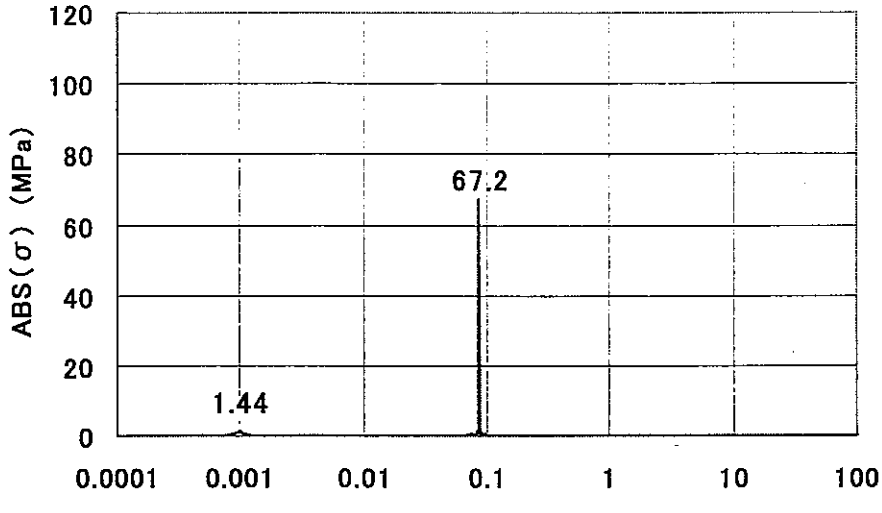

Square root of power spectrum of stress (S1-0.01)

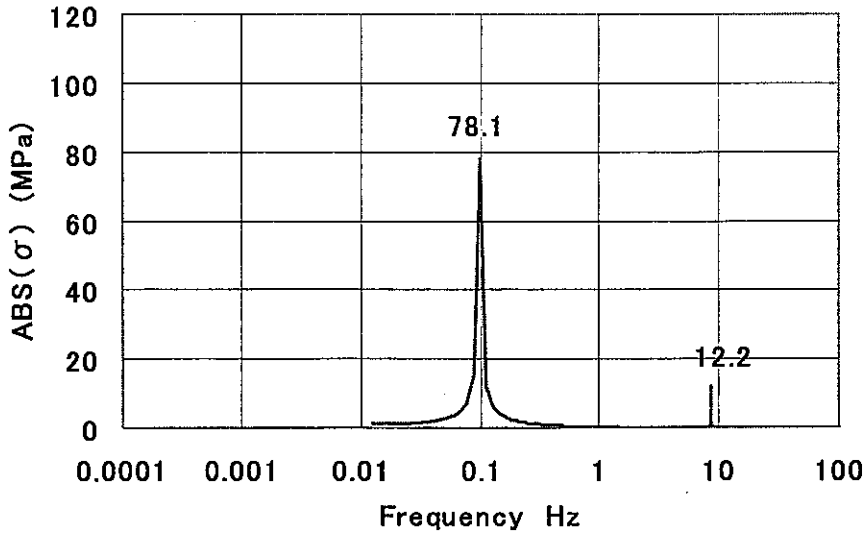

Square root of power spectrum of stress (S1-100)

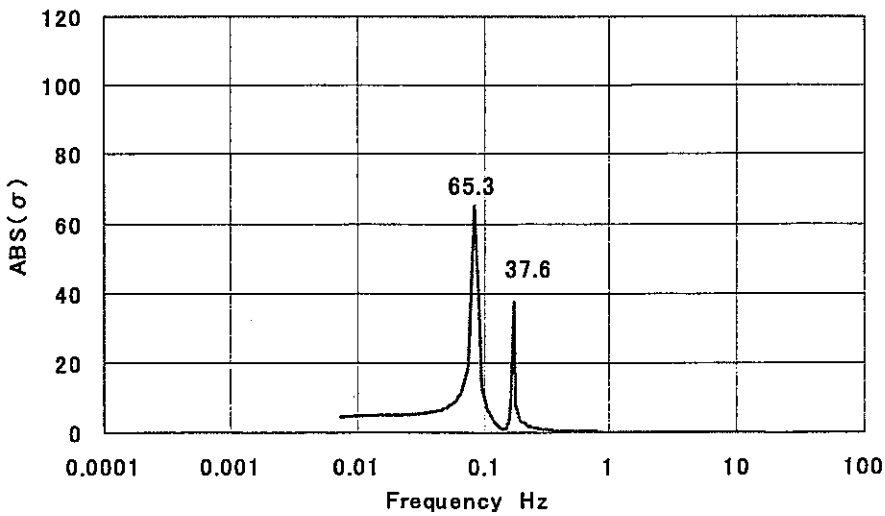

Square root of power spectrum of stress (S1-2(0.25))

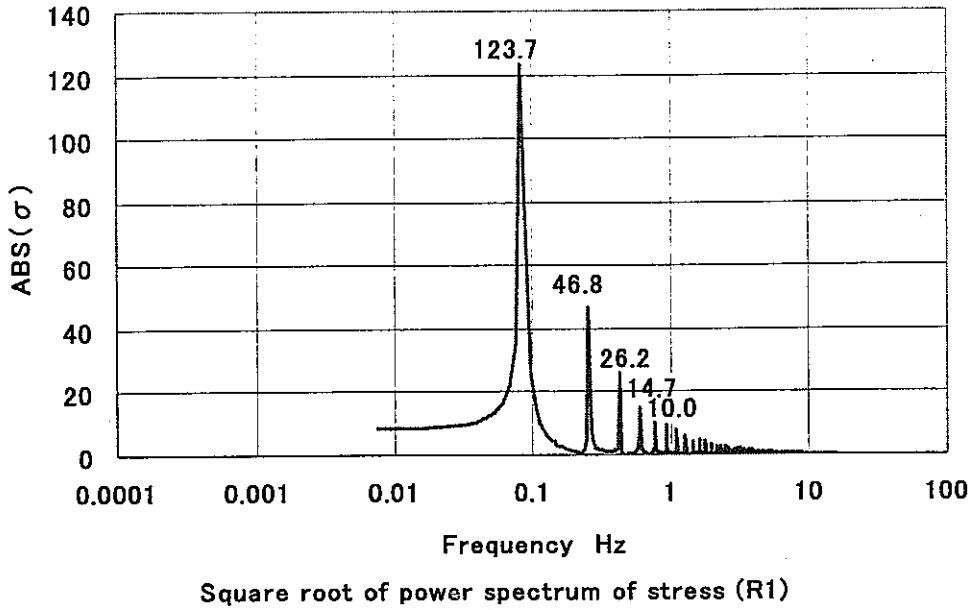

Fig.3.5 FFT analysis results of F.E. calculated stress

(2) Analysis with frequency response functions

Average of fluid temperature of the problem shown in Fig.3.1 is 385 ℃. By using material properties of 304SS at 385℃ and wall thickness 7mm, non-dimensional frequencies were calculated from actual ones.

Heat transfer coefficient 14500 kcal/m^2/h/℃ [5] was also translated to Biot number.

Results are described in the next table.

Table 3.2 Non-dimensional parameters of FAENA 3rd

Frequency f (Hz)	Non-dimensional frequency f*	Biot number Bi
0.085	0.927	6.07
0.170	1.85	

From above two parameters, frequency response function of thermal stress was determined and its gain and phase delay are shown in the next diagrams.

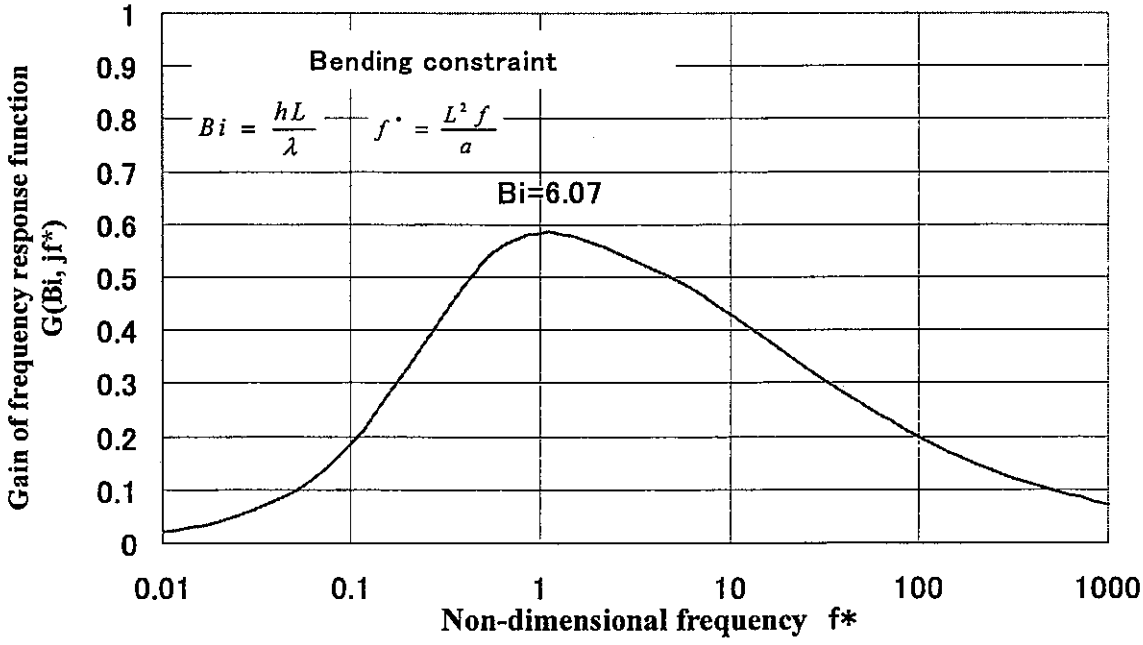

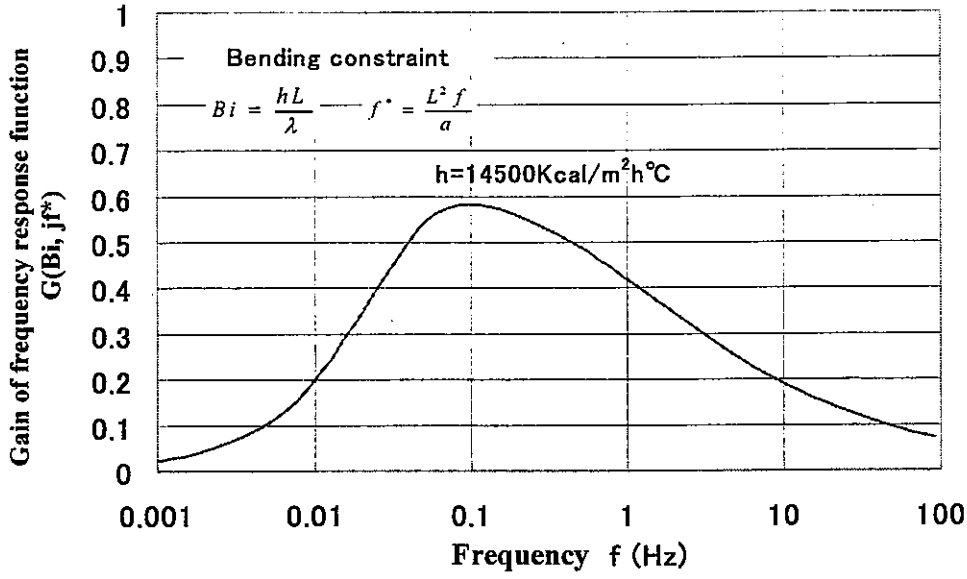

Fig.3.6 Gain of frequency response function

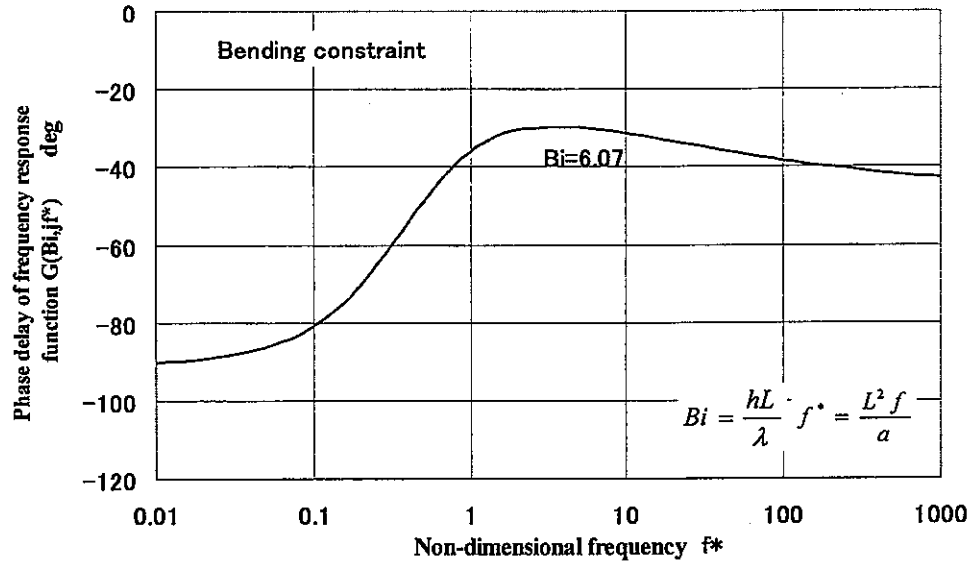

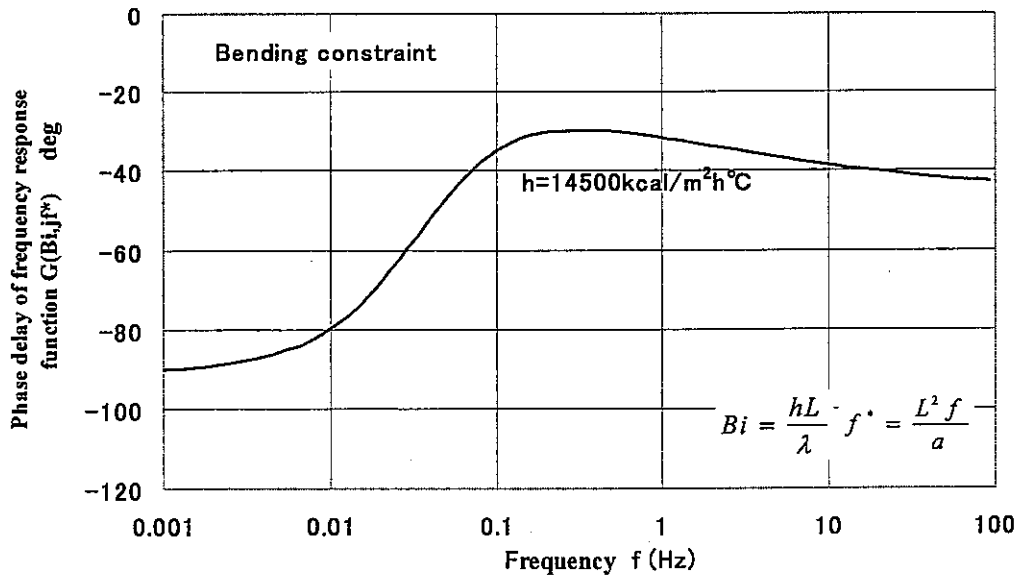

Fig.3.7 Phase delay of frequency response function

In order to apply frequency response function, FFT analysis was conducted on fluid temperature fluctuations. Next figures show these results.

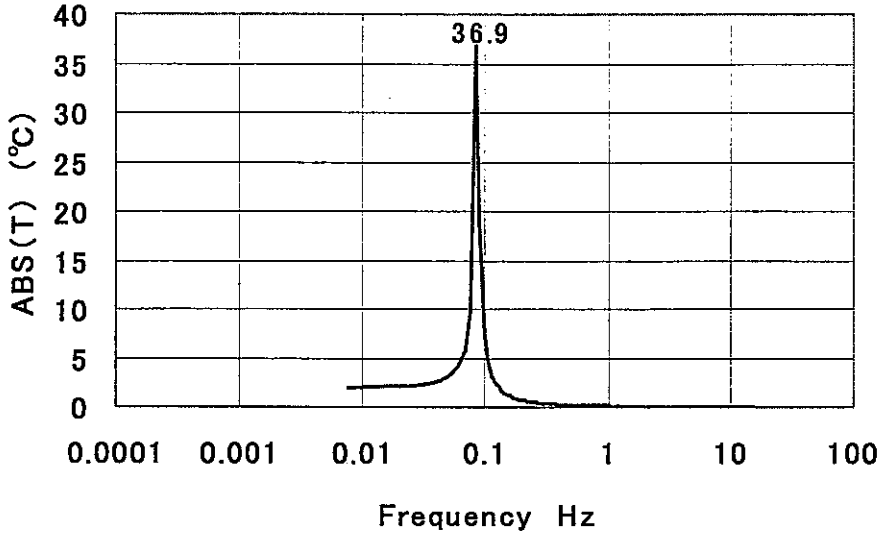

Square root of power spectrum of fluid temperature (S1)

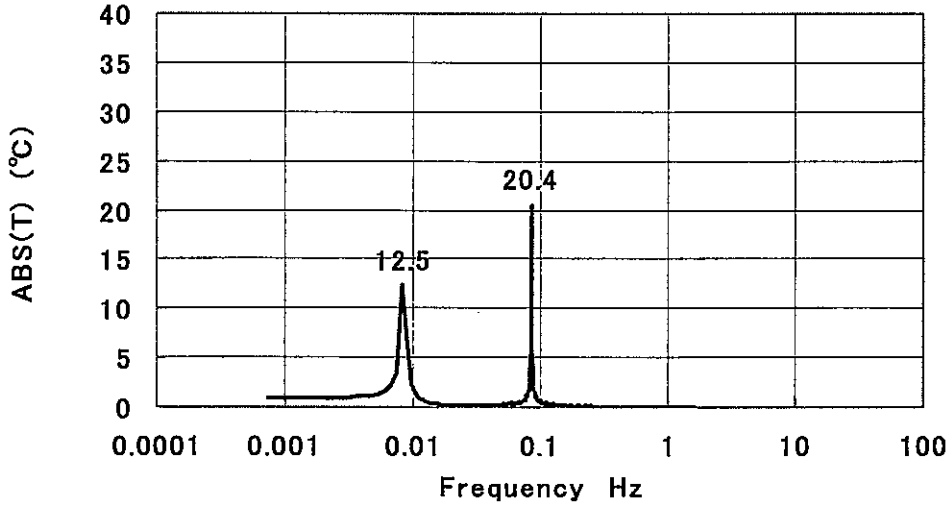

Square root of power spectrum of fluid temperature (S1-0.1)

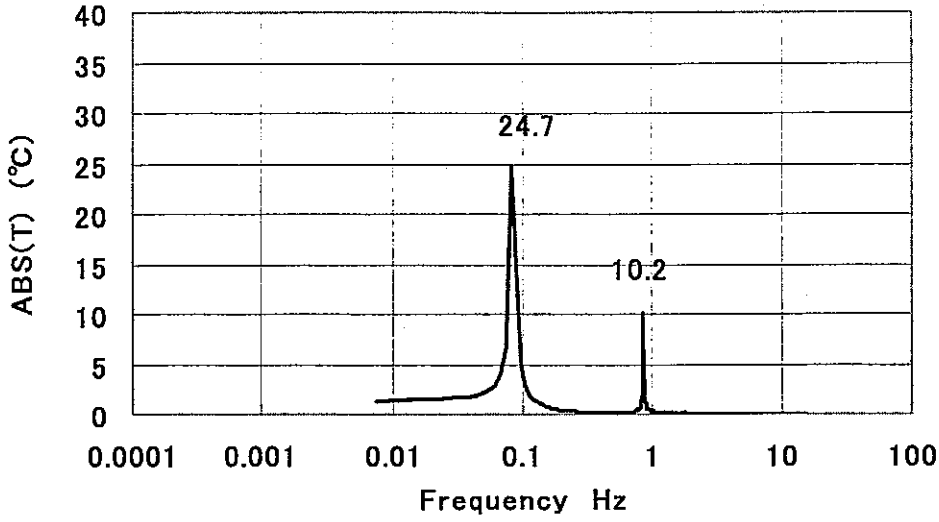

Square root of power spectrum of fluid temperature (S1-10)

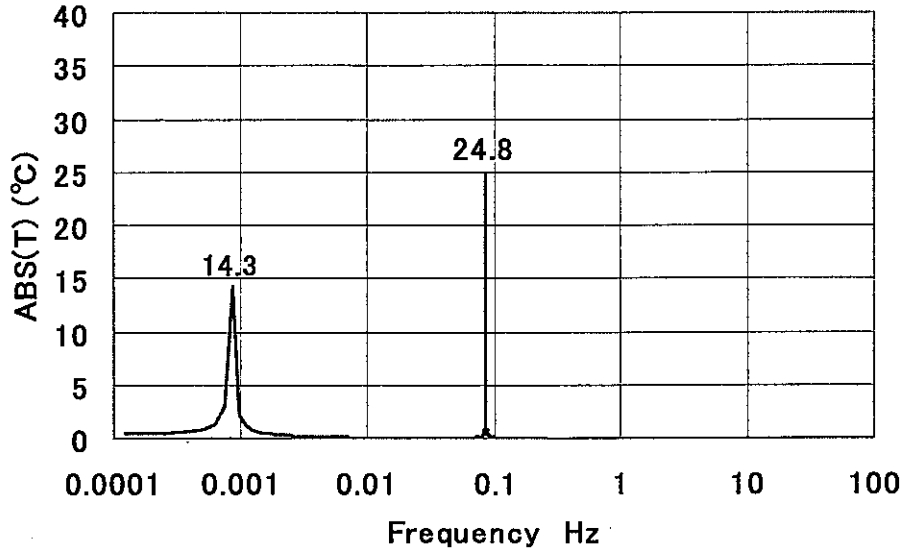

Square root of power spectrum of fluid temp (S1-0.01)

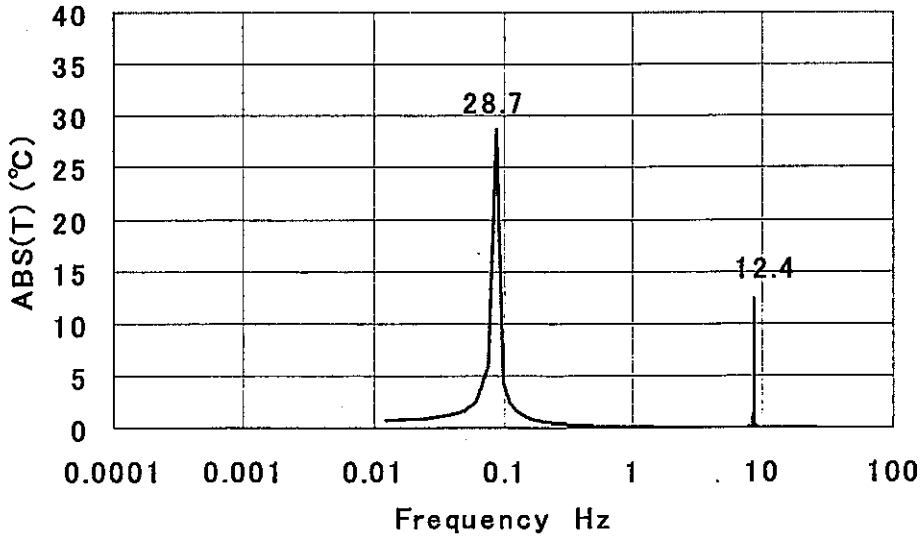

Square root of power spectrum of fluid temp.(S1-100)

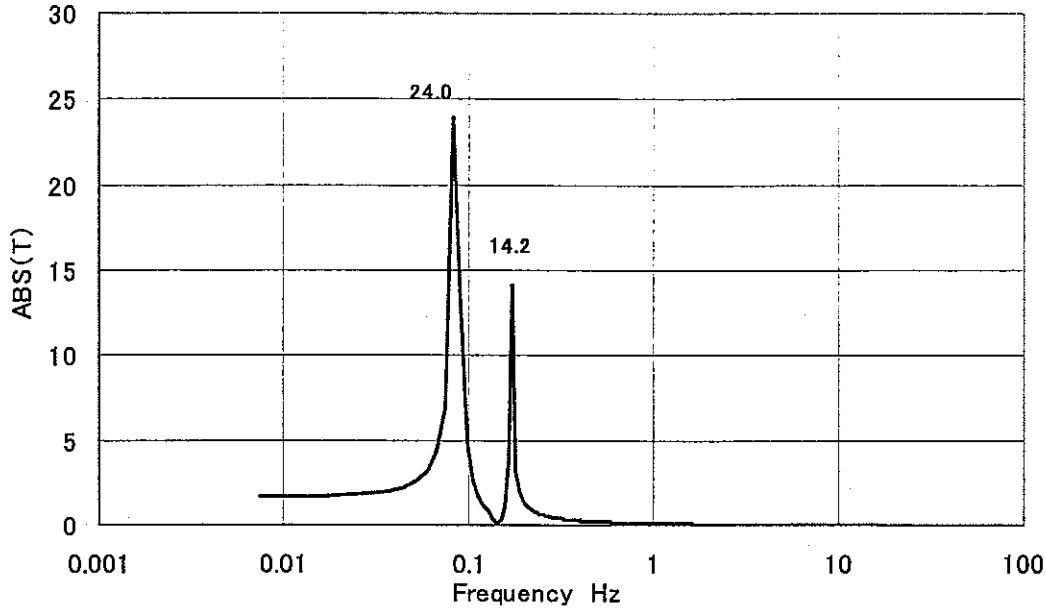

Square root of power spectrum of fluid temperature (S1-2(0.25))

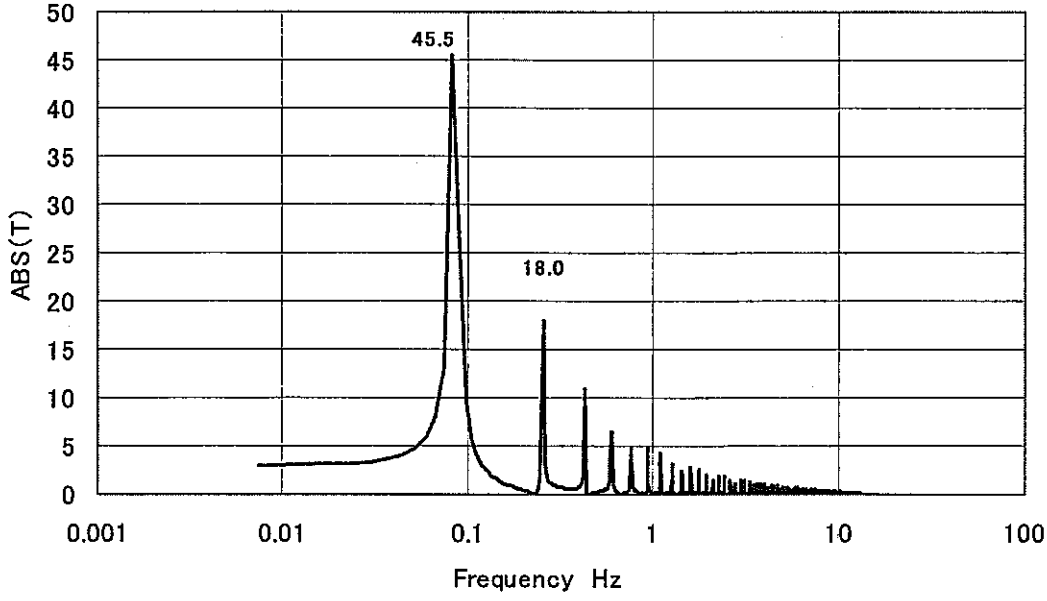

Square root of power spectrum of fluid temperature (R1)

Fig.3.8 Gain of fluid temperature fluctuation

By using Eq.(2.2) induced thermal stress was evaluated from Figs 3.6 –3.8 in frequency domain. Gains of evaluated stress are as in the next figures.

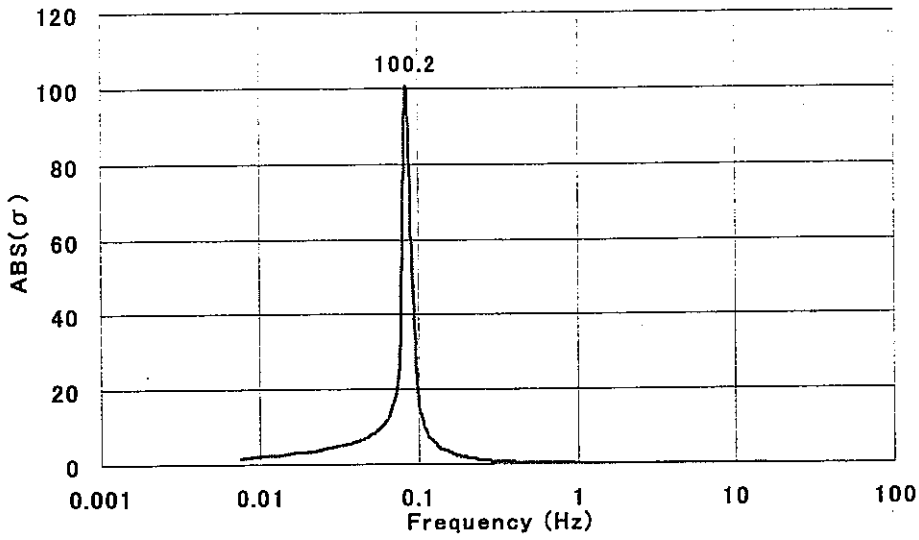

Evaluated stress by frequency response function (S1)

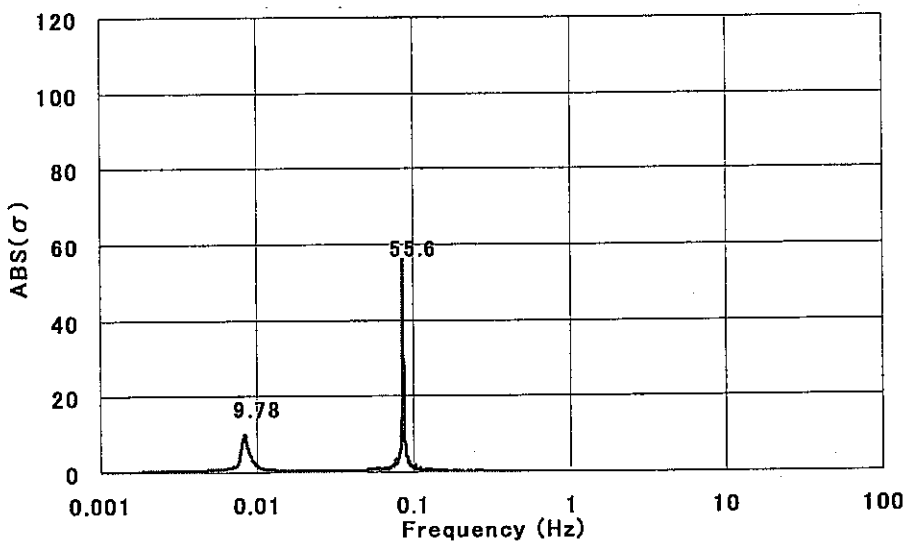

Evaluated stress by frequency response function (S1-0.1)

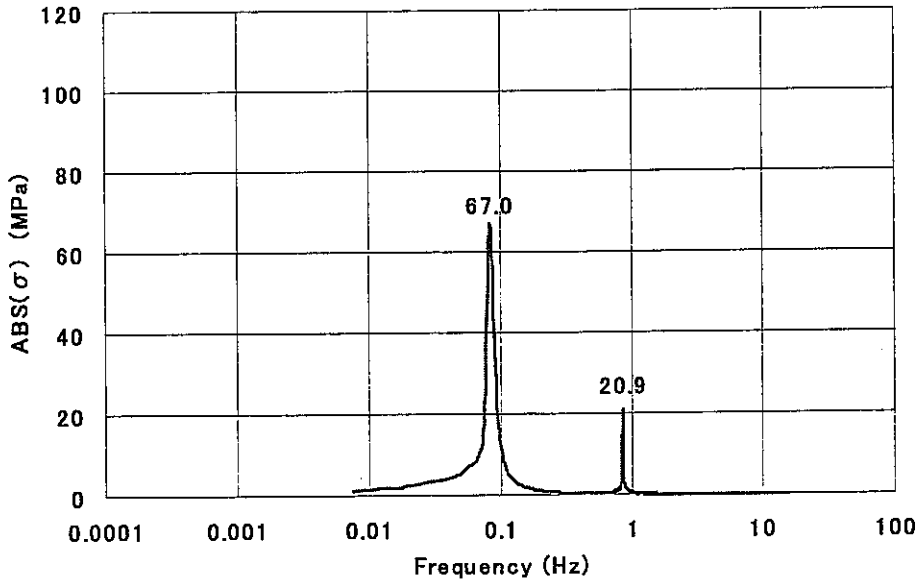

Evaluated stress by frequency response function (S1-10)

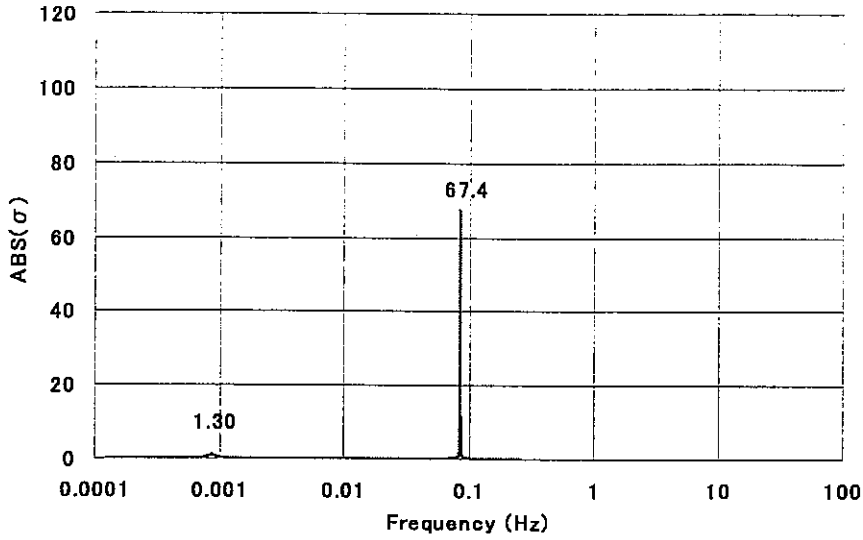

Evaluated stress by frequency response function (S1-0.01)

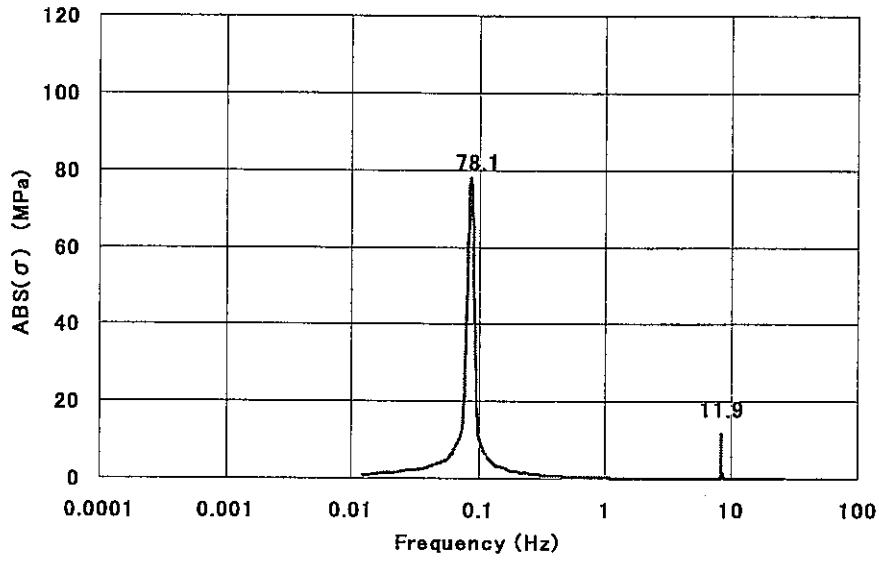

Evaluated stress by frequency response function (S1-100)

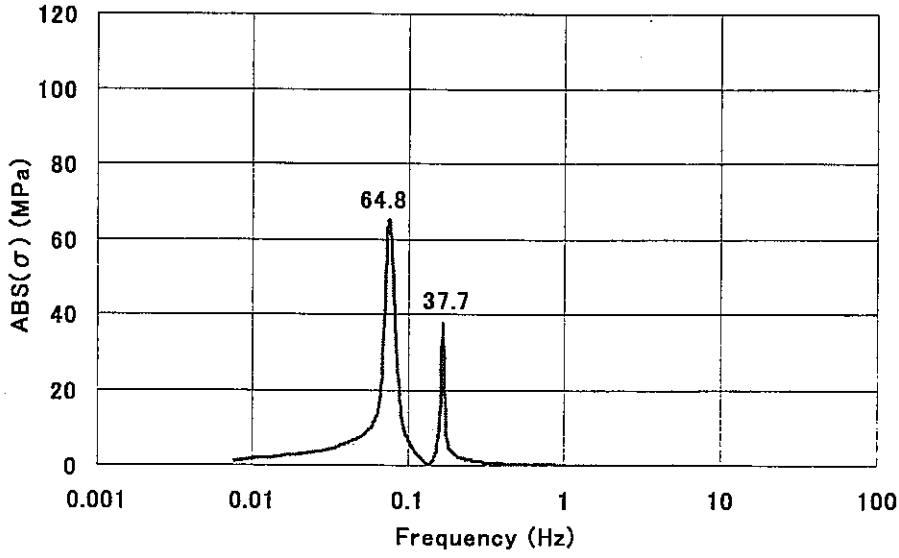

Evaluated stress by frequency response function (S1-2(0.25)

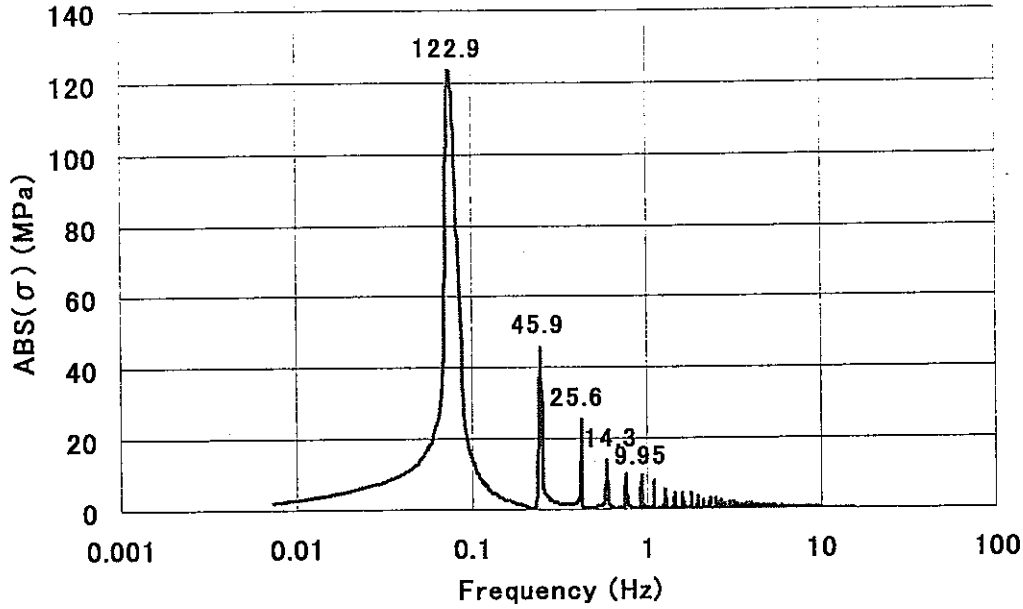

Fig.3.9 Gain of stress fluctuation

When comparing above results with F.E. calculated results shown in Fig.3.4, frequency response function was proved to be adequate except low frequency region. The reason why low frequency fluctuation has errors is limitation of sampling points of FFT as 4096.

By inverse FFT analysis of Fig.3.9 considering phase delay, time history of stress can be evaluated as in next figures. These results are approximately the same as F.E. calculated ones except the case R1.

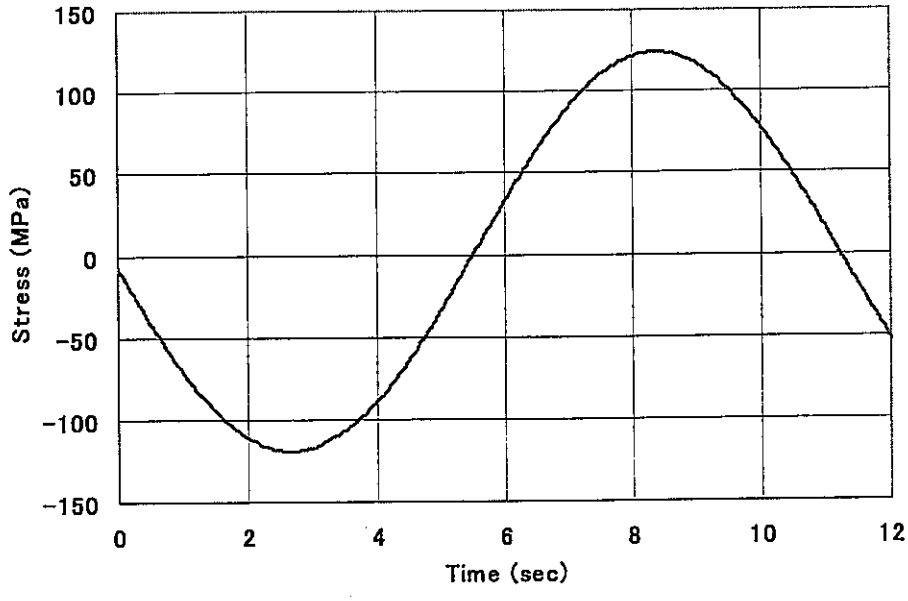

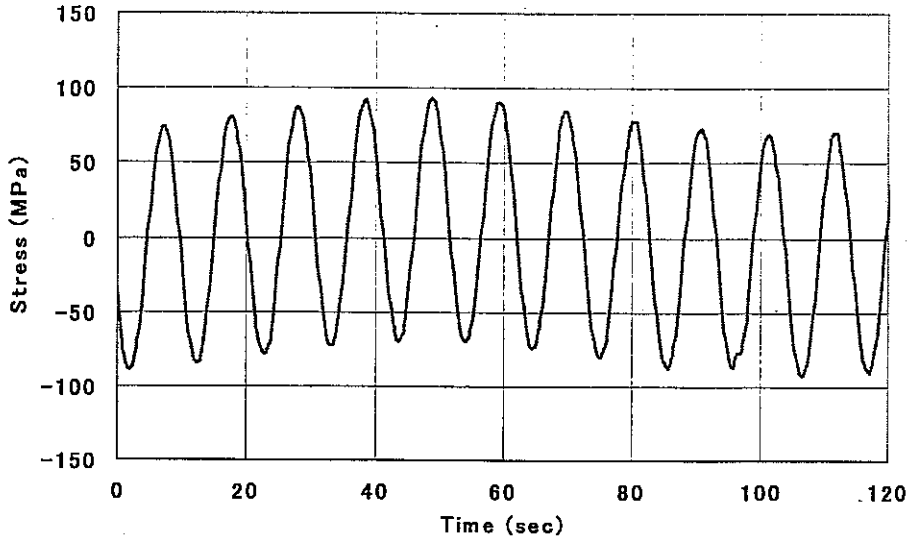

Evaluated stress by frequency response function and inverse FFT (S1-0.1)

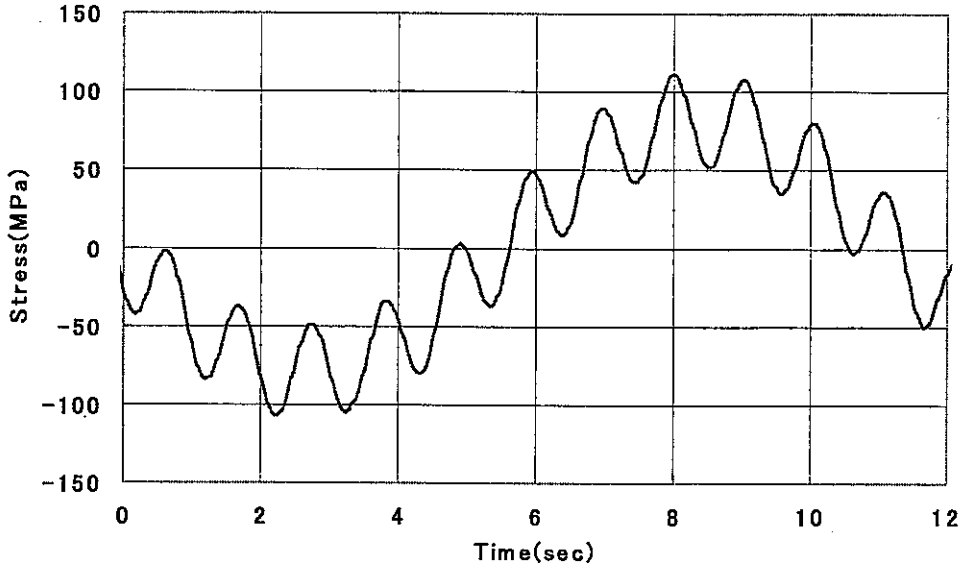

Evaluated stress by frequency response function and inverse FFT (S1-10)

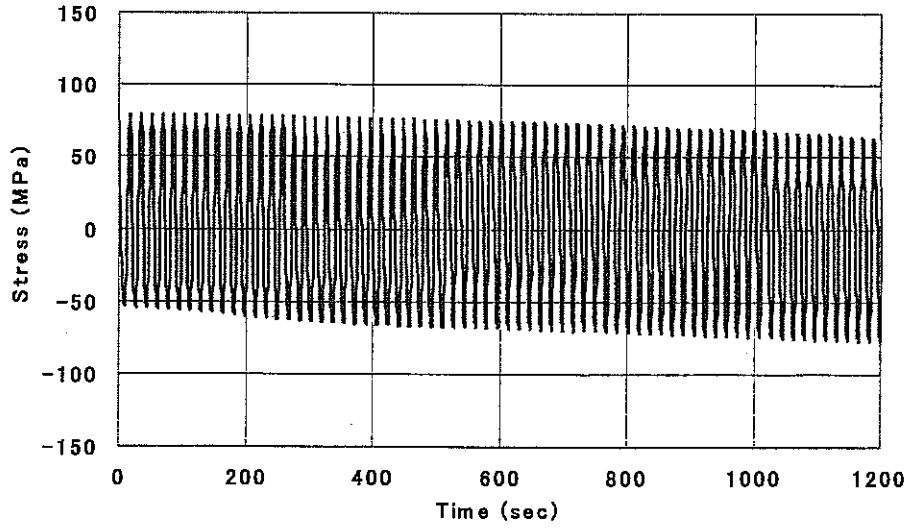

Evaluated stress by frequency response function and inverse FFT (S1-0.01)

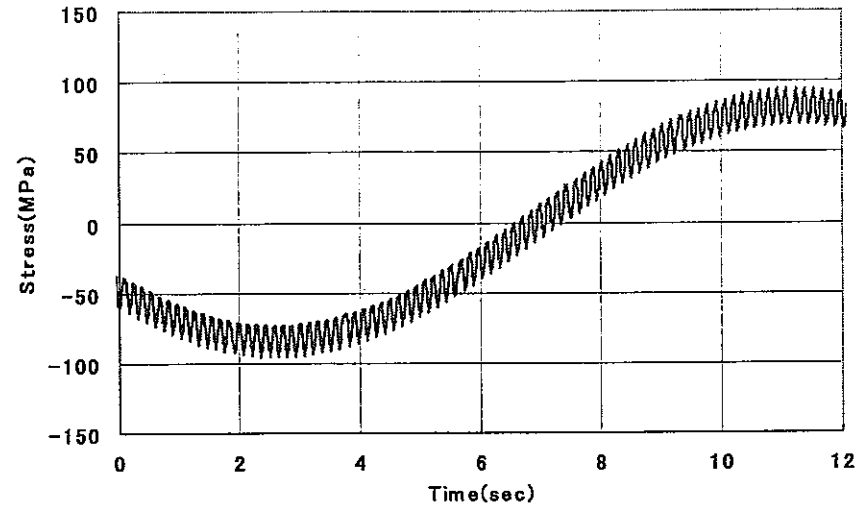

Evaluated stress by frequency response function and inverse FFT (S1-100)

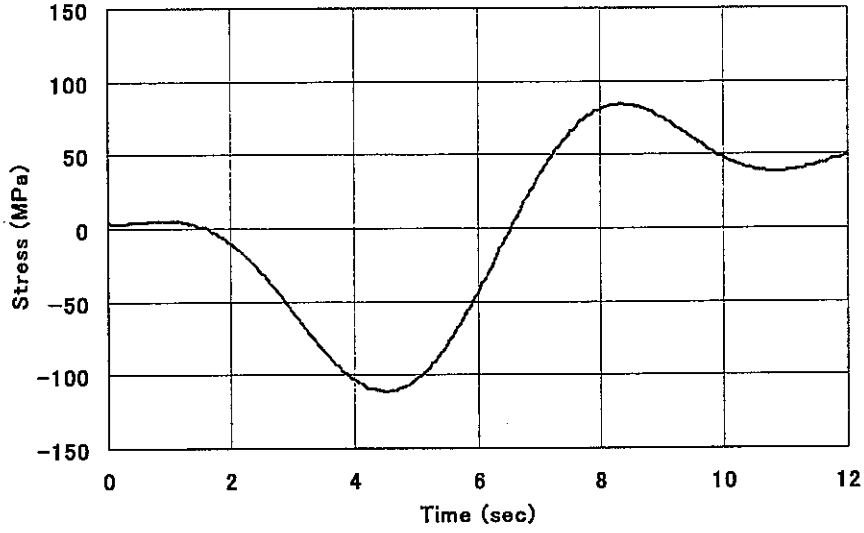

Evaluated stress by frequency response function and inverse FFT (S1-2(0.25)

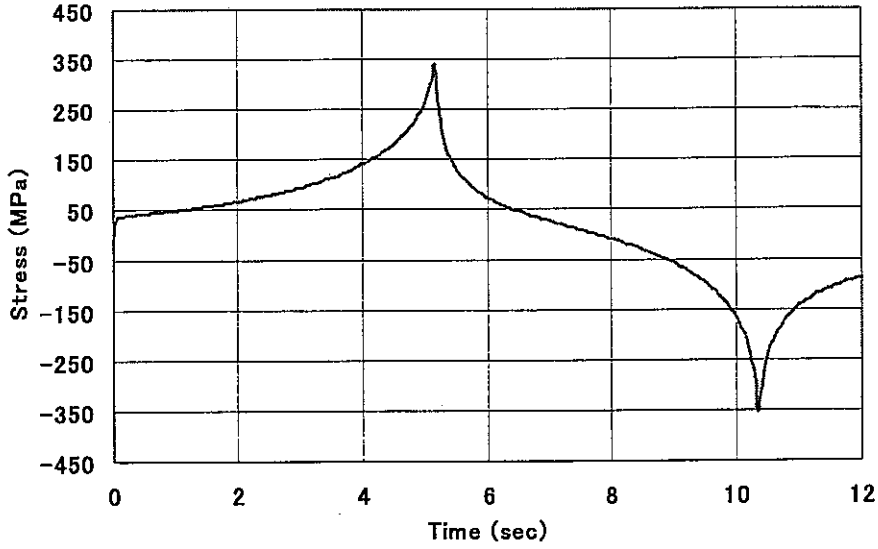

Evaluated stress by frequency response function and inverse FFT (R1)

Fig.3.10 Time history of stress evaluated by inverse FFT

3.3 FATIGUE STRENGTH ANALYSIS IN TIME DOMAIN

Using stress analysis results by FEM and the frequency response function with inverse FFT, fatigue strength analyses were conducted according to the procedure explained in the section 2.2.

Rain flow counting results of 120sec stress analysis and evaluated fatigue damage for 30 years period were shown in the next figures.

(1) Stress analysis results by FEM

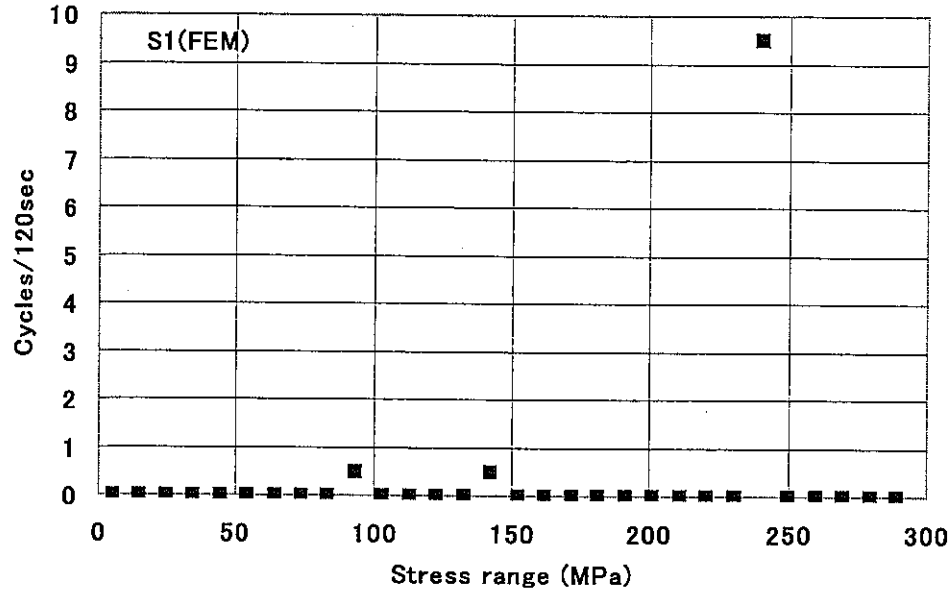

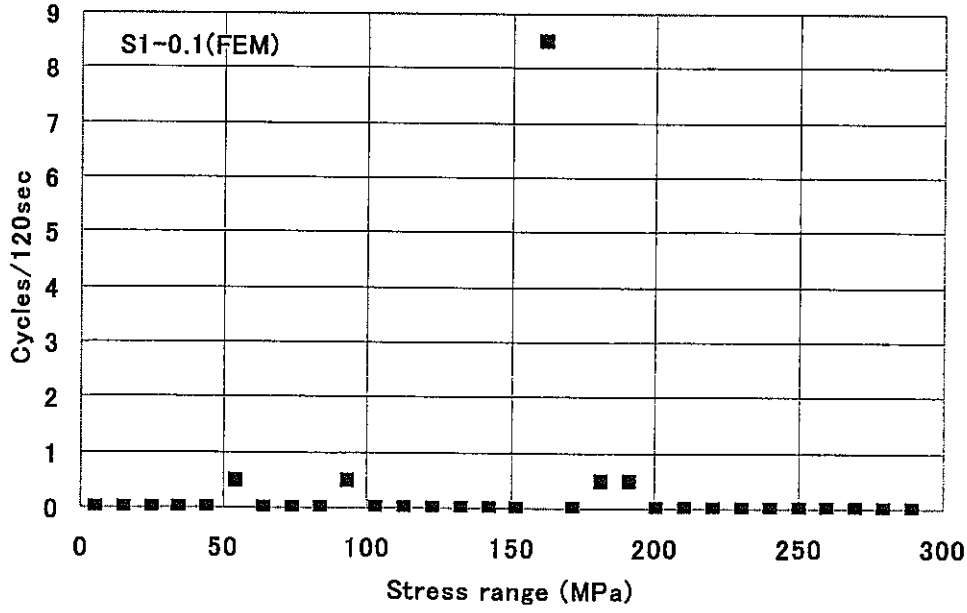

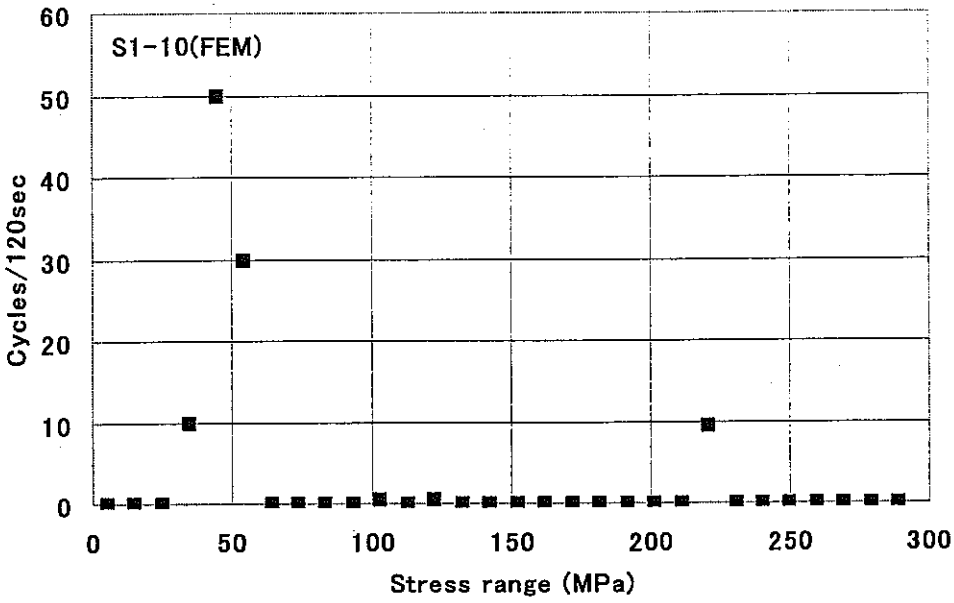
S1-10(FEM)
Cycles/120sec
0
10
20
30
40
50
60
0
50
100
150
200
250
300
Stress range (MPa)

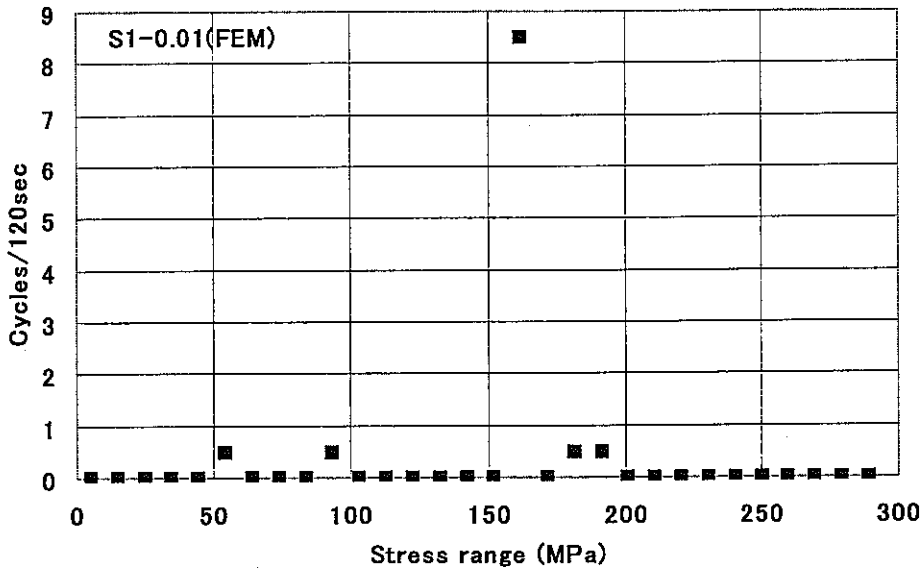
S1-0.01(FEM)
Cycles/120sec
0
1
2
3
4
5
6
7
8
9
0
50
100
150
200
250
300
Stress range (MPa)

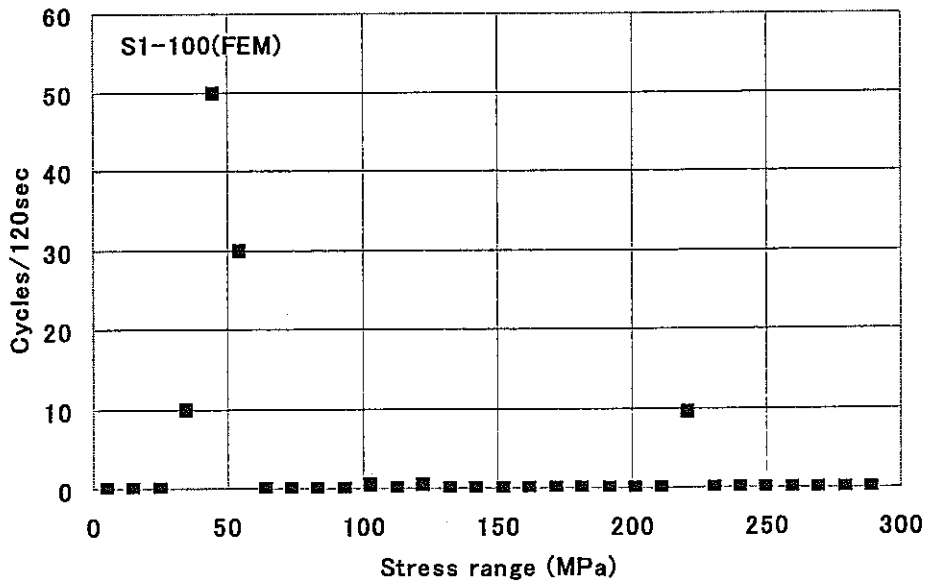
S1-100(FEM)
Cycles/120sec
0
10
20
30
40
50
60
0
50
100
150
200
250
300
Stress range (MPa)

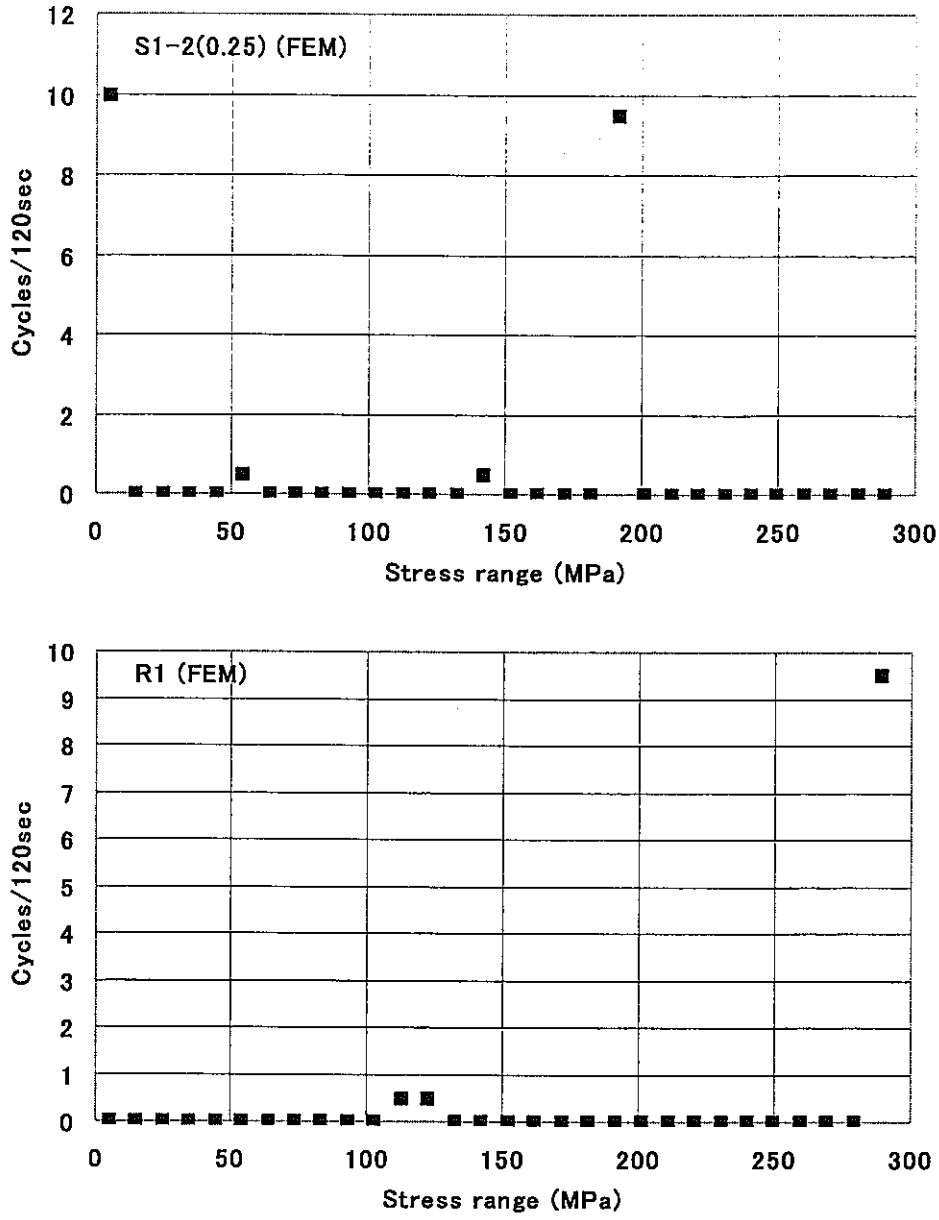

Fig.3.11 Rain flow counting results during 120 sec (FEM)

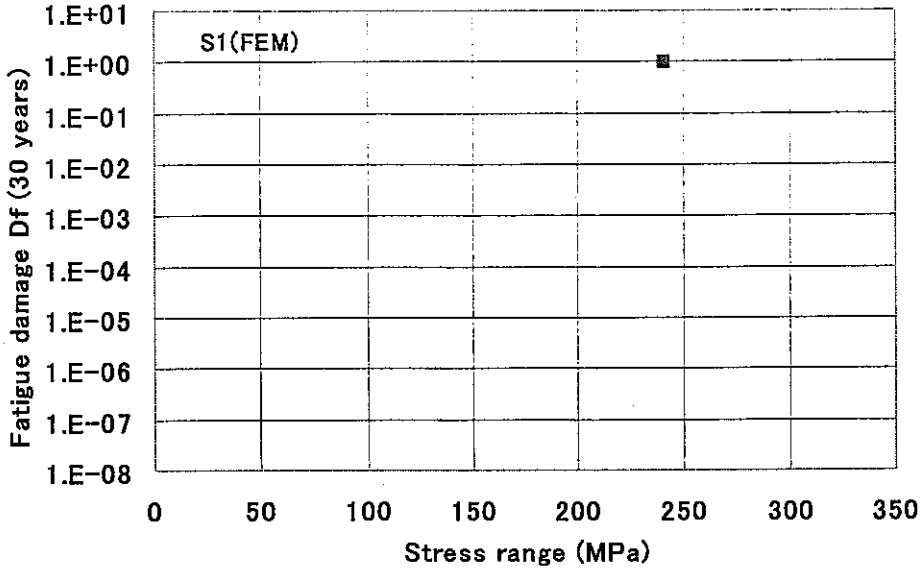
S1(FEM)
Fatigue damage Df (30 years)
1.E+01
1.E+00
1.E-01
1.E-02
1.E-03
1.E-04
1.E-05
1.E-06
1.E-07
1.E-08
0
50
100
150
200
250
300
350
Stress range (MPa)

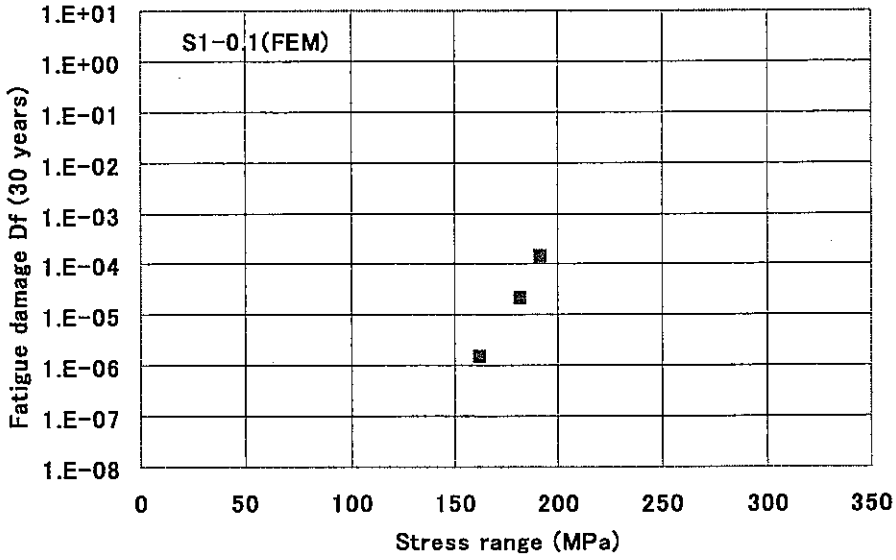
S1-0.1(FEM)
Fatigue damage Df (30 years)
1.E+01
1.E+00
1.E-01
1.E-02
1.E-03
1.E-04
1.E-05
1.E-06
1.E-07
1.E-08
0
50
100
150
200
250
300
350
Stress range (MPa)

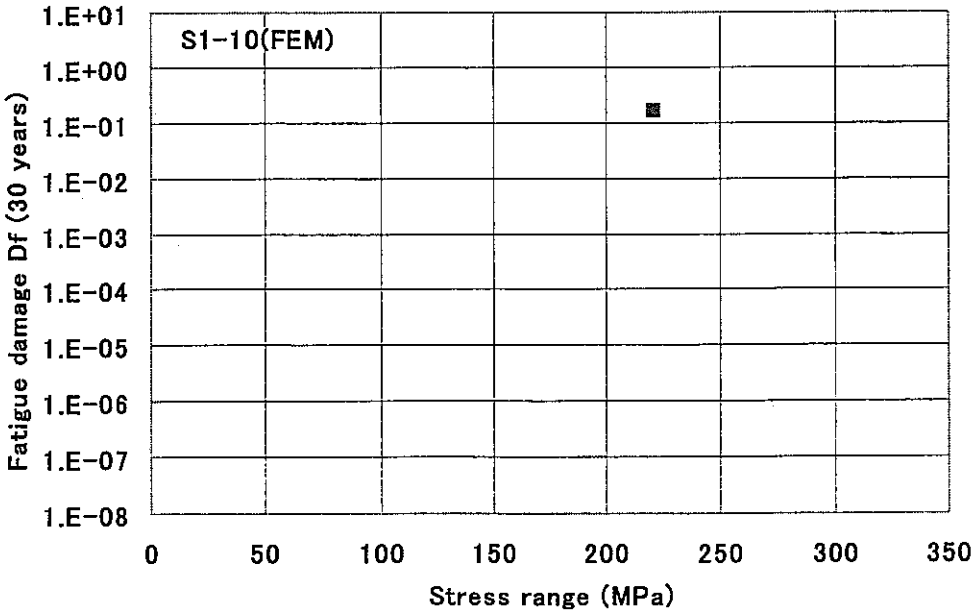
S1-10(FEM)
Fatigue damage Df (30 years)
1.E+01
1.E+00
1.E-01
1.E-02
1.E-03
1.E-04
1.E-05
1.E-06
1.E-07
1.E-08
0
50
100
150
200
250
300
350
Stress range (MPa)

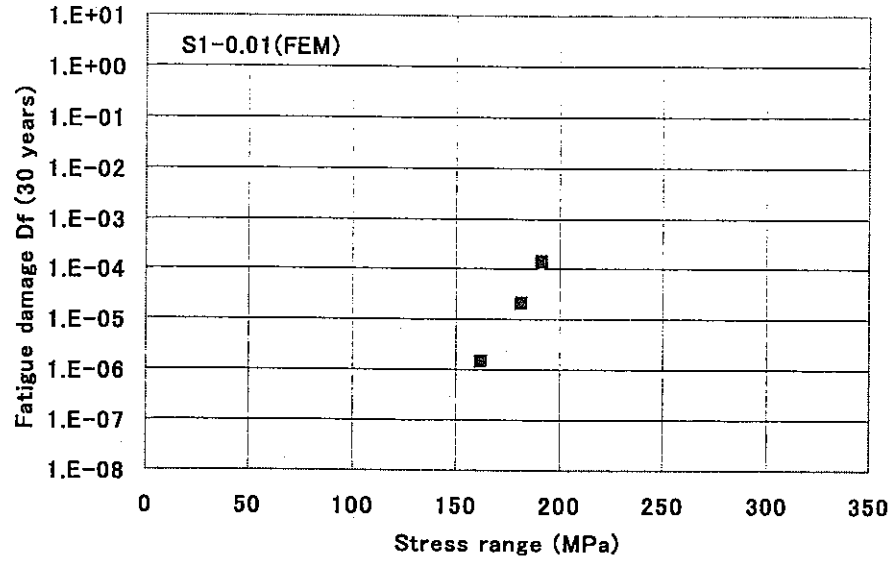
S1-0.01(FEM)
Fatigue damage Df (30 years)
1.E+01
1.E+00
1.E-01
1.E-02
1.E-03
1.E-04
1.E-05
1.E-06
1.E-07
1.E-08
0
50
100
150
200
250
300
350
Stress range (MPa)

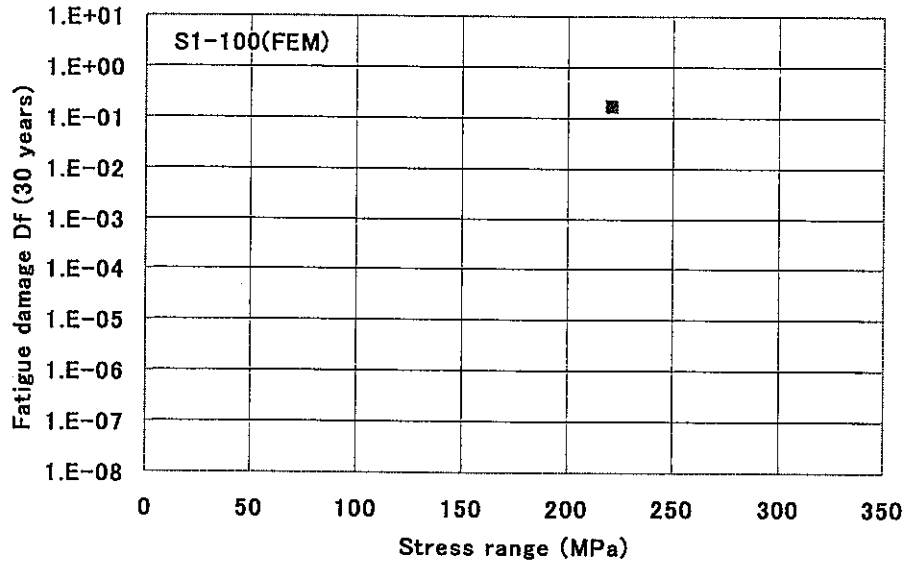
S1-100(FEM)
Fatigue damage Df (30 years)
1.E+01
1.E+00
1.E-01
1.E-02
1.E-03
1.E-04
1.E-05
1.E-06
1.E-07
1.E-08
0
50
100
150
200
250
300
350
Stress range (MPa)

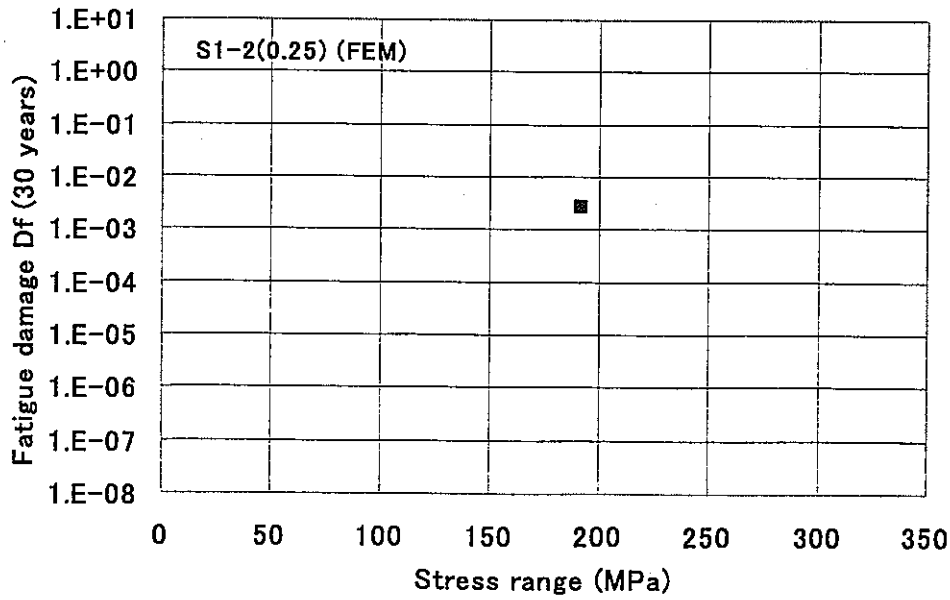
S1-2(0.25) (FEM)
Fatigue damage Df (30 years)
1.E+01
1.E+00
1.E-01
1.E-02
1.E-03
1.E-04
1.E-05
1.E-06
1.E-07
1.E-08
0
50
100
150
200
250
300
350
Stress range (MPa)

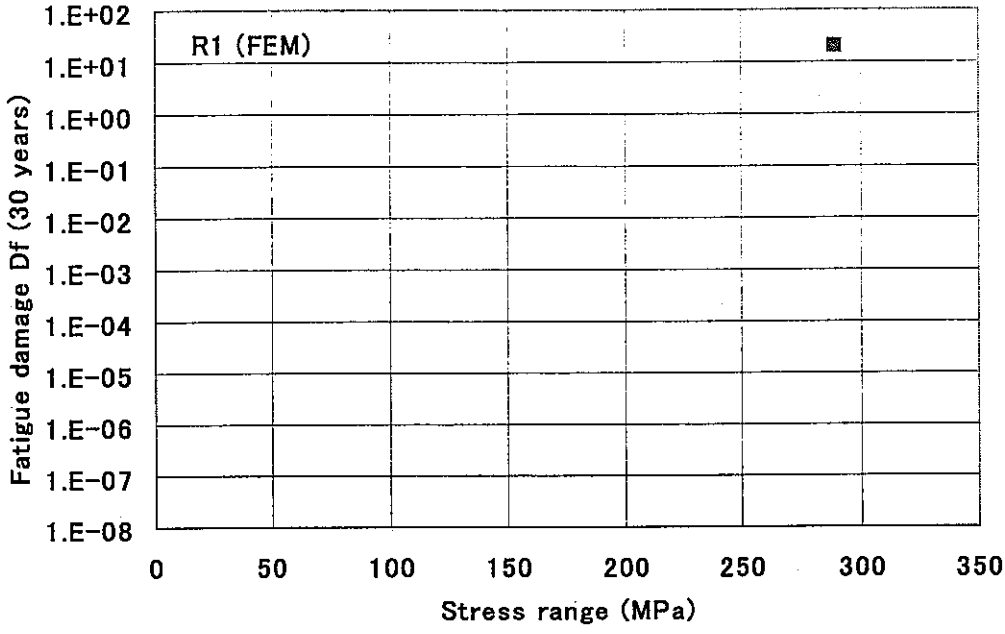

Fig.3.12 Calculated fatigue damage after 30years (FEM)

(2) Stress analysis results by the frequency response function with inverse FFT

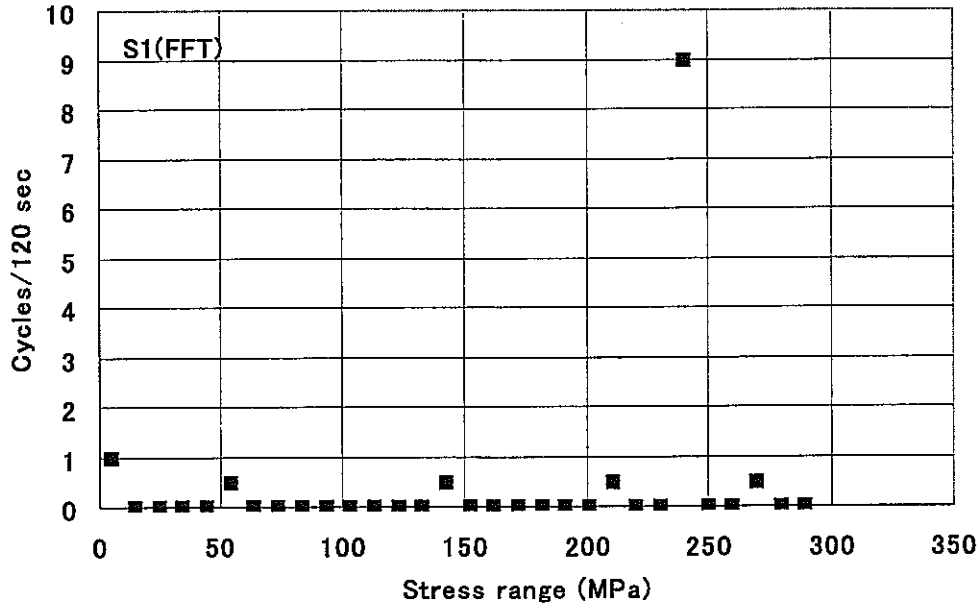

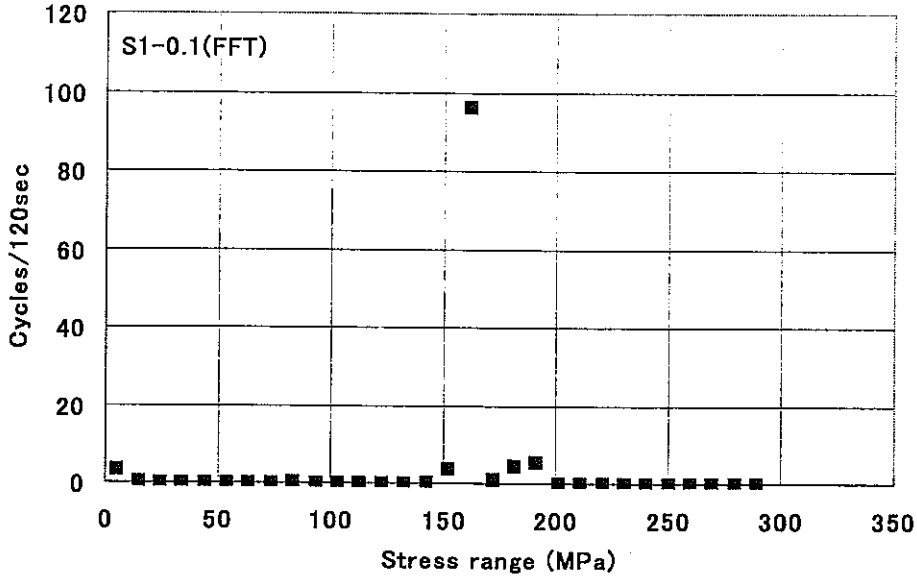
S1-0.1(FFT)
Cycles/120sec
Stress range (MPa)
0
20
40
60
80
100
120
0
50
100
150
200
250
300
350

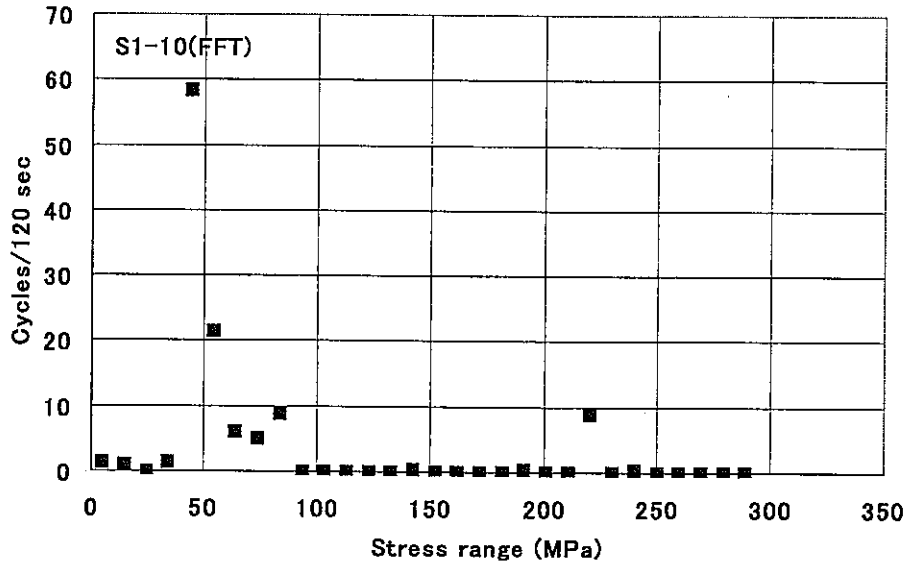
S1-10(FFT)
Cycles/120 sec
Stress range (MPa)
0
10
20
30
40
50
60
70
0
50
100
150
200
250
300
350

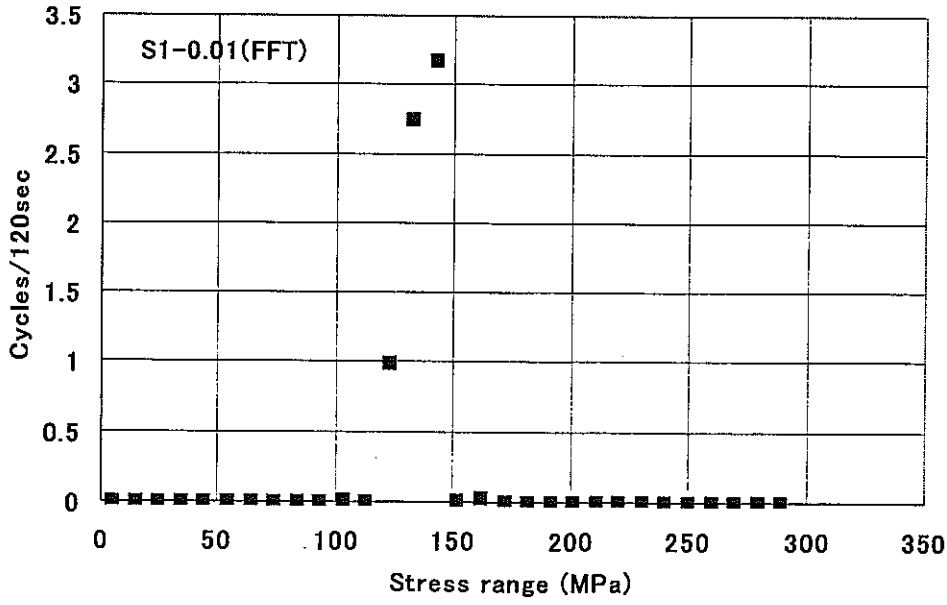
S1-0.01(FFT)
Cycles/120sec
Stress range (MPa)
0
0.5
1
1.5
2
2.5
3
3.5
0
50
100
150
200
250
300
350

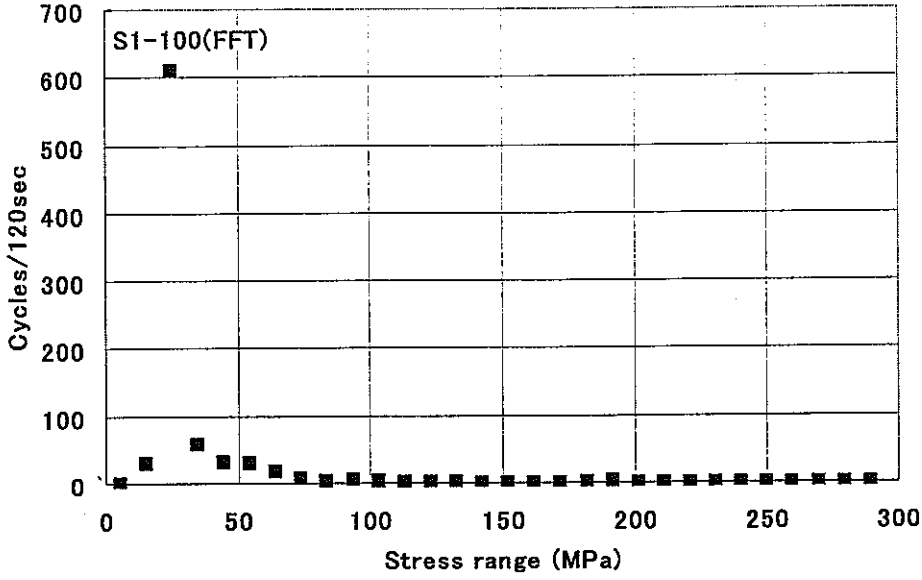

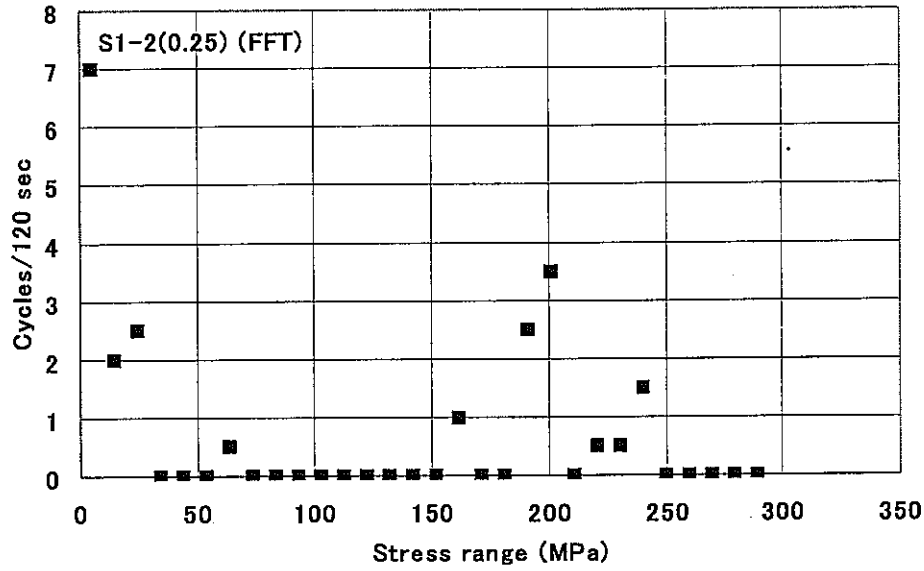

Fig.3.13 Rain flow counting results during 120 sec (FFT)

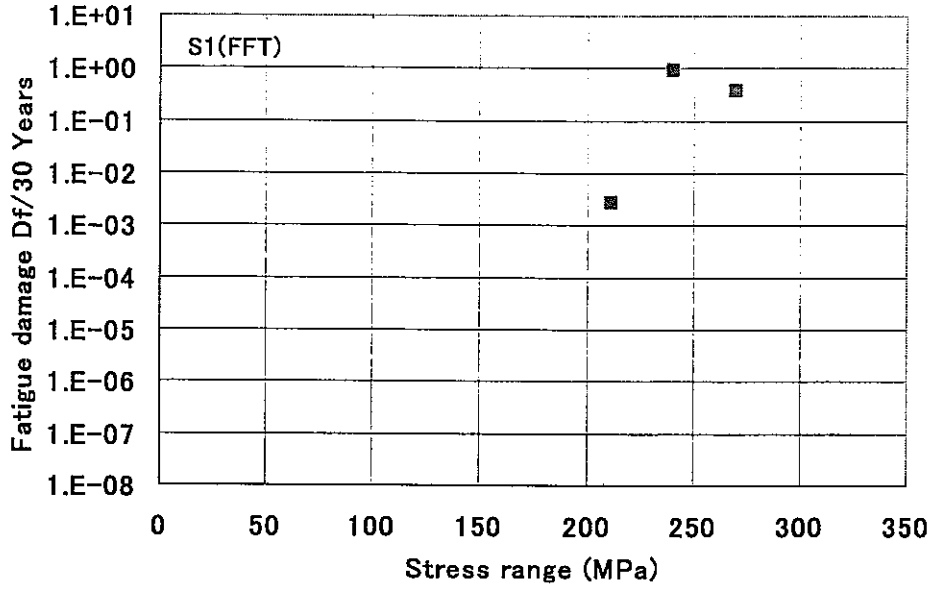
S1(FFT)
Fatigue damage Df/30 Years
1.E+01
1.E+00
1.E-01
1.E-02
1.E-03
1.E-04
1.E-05
1.E-06
1.E-07
1.E-08
0
50
100
150
200
250
300
350
Stress range (MPa)

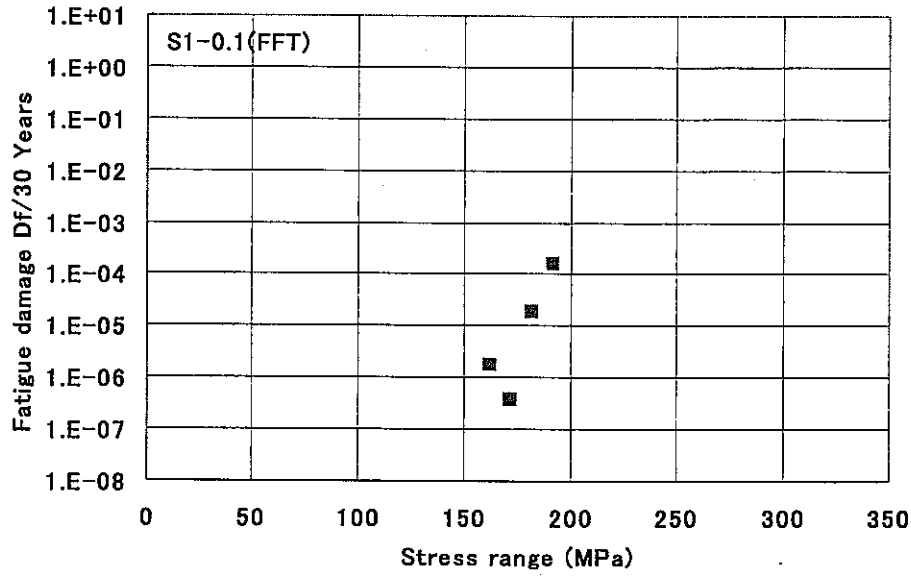
S1-0.1(FFT)
Fatigue damage Df/30 Years
1.E+01
1.E+00
1.E-01
1.E-02
1.E-03
1.E-04
1.E-05
1.E-06
1.E-07
1.E-08
0
50
100
150
200
250
300
350
Stress range (MPa)

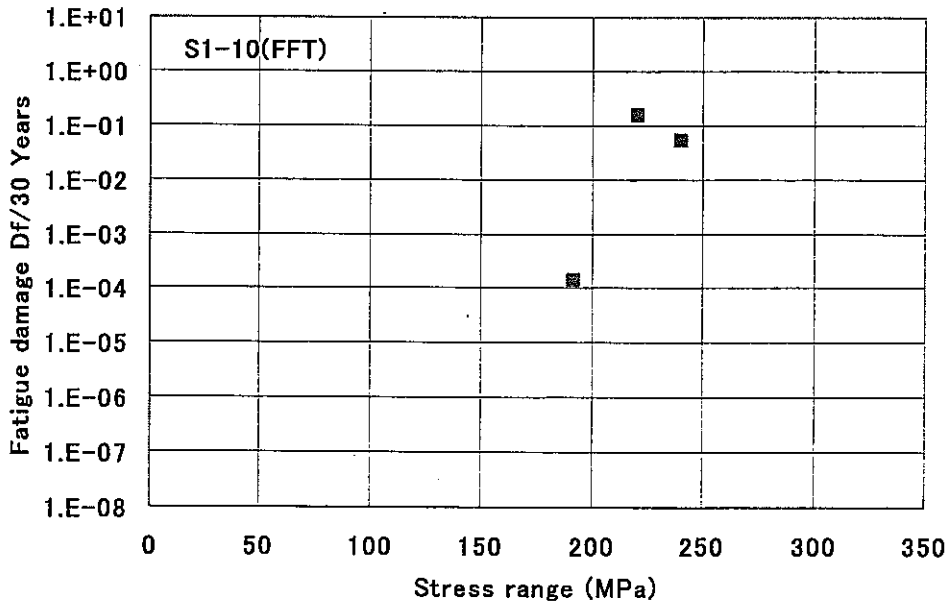
S1-10(FFT)
Fatigue damage Df/30 Years
1.E+01
1.E+00
1.E-01
1.E-02
1.E-03
1.E-04
1.E-05
1.E-06
1.E-07
1.E-08
0
50
100
150
200
250
300
350
Stress range (MPa)

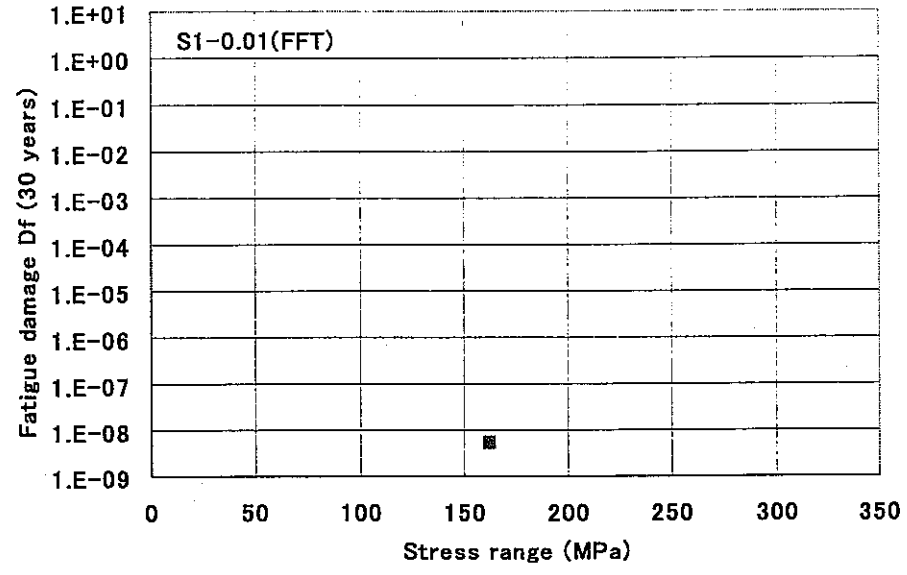

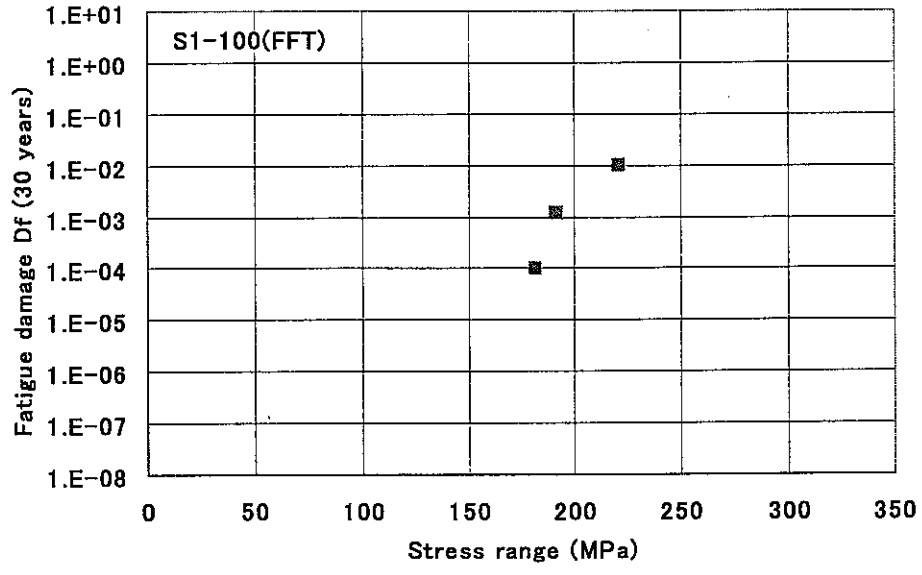

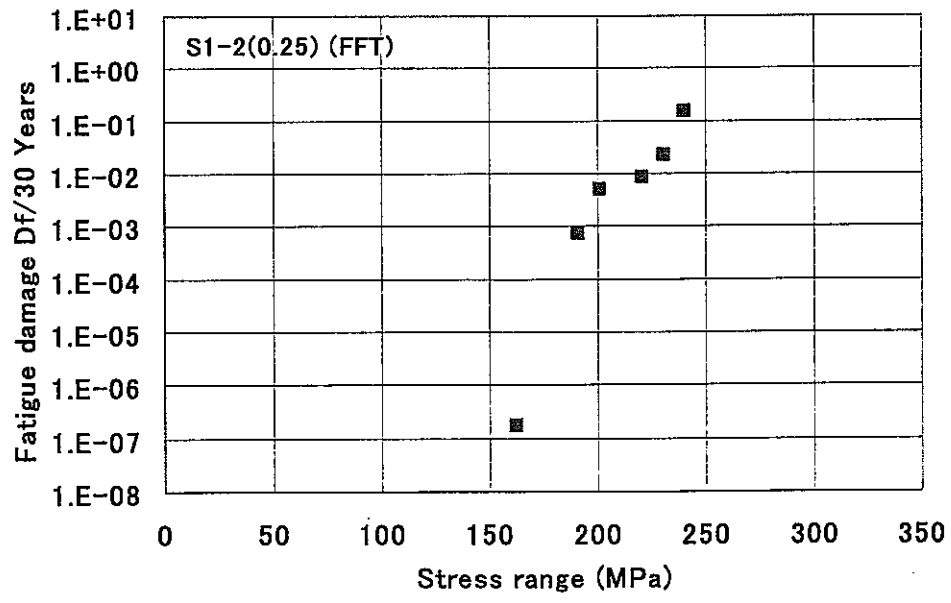

Fig.3.14 Calculated fatigue damage after 30years (FFT)

The next table shows total fatigue damages after 30 years calculated by FEM and Inverse FFT. In the high cycle fatigue regime, small differences of stress range lead to large different fatigue damages. These results clarified that frequency response approach with inverse FFT is adequate.

Table 3.3 Comparison of calculated fatigue damage after 30years

Case	Df (FEM + Rainflow)	Df (Inverse FFT + Rainflow)
S1	1.03E+00	1.37E+00
S1-0.1	1.73E-04	1.90E-04
S1-10	1.67E-01	2.13E-01
S1-0.01	1.73E-04	5.67E-09
S1-100	1.67E-01	1.19E-02
S1-2(0.25)	2.84E-03	2.01E-01
R1	2.00E+01	NA

3.4 FATIGUE STRENGTH ANALYSIS IN FREQUENCY DOMAIN

The next table shows the summary of Fourier analysis results shown in the former section. ΔT_f means temperature amplitudes of original problems. ΔT_{fFFT} means ones calculated by FFT analysis from time history data. There are some differences among original temperature range ΔT_f and estimated one ΔT_{fFFT} due to errors of FFT analysis. In order to distinguish FFT analysis errors from ones by fatigue analysis method, fatigue damages were calculated based on both original temperature range ΔT_f and estimated one ΔT_{fFFT}

In this table, evaluated stresses by the frequency response function have good agreements with F.E. analysis results in frequency domain. However it seems to be better to take care about errors between original temperature ranges and Fourier analyzed ones.

Table 3.4 Summary of Fourier analysis results

Case	frequency(Hz)	ΔT_f(°C)	ΔT_f(°C)$_{FFT}$	| G |	K | G | ΔT_f(°C)	K | G | ΔT_f(°C)$_{FFT}$	$\Delta\sigma_{FFT}$(FEM)
S1	0.085	90	73.8	0.580	244.1	200.2	193.4
S1-0.1	0.085	60	40.8	0.580	162.7	110.7	150.0
	0.0085	30	25	0.185	26.0	21.6	21.8
S1-10	0.085	60	49.4	0.580	162.7	134.0	129.2
	0.85	30	20.4	0.429	60.2	40.9	57.4
S1-0.01	0.085	60	49.6	0.580	162.7	134.5	134.4
	0.00085	30	28.6	0.020	2.8	2.7	2.9
S1-100	0.085	60	57.4	0.580	162.7	155.7	156.2
	8.5	30	24.8	0.199	27.9	23.1	24.4
S1-2(0.25)	0.085	60	48	0.580	162.7	130.2	130.6
	0.17	30	28.4	0.566	79.4	75.2	75.2
R1	0.085	127.27922	91	0.580	345.2	246.8	247.4
	0.17	45	36	0.566	119.1	95.3	93.6
	0.255	18	21.6	0.543	45.7	54.8	52.4
	0.34	22.5	9.48	0.521	54.8	23.1	29.4

In order to apply the Method 1 explained in the section 2.3 to calculate fatigue damages after 30 years, stress ranges $\Delta\sigma|_{x=o}$ were evaluated with integral gains as

$$\Delta\sigma|_{x=o} = \sum K|G|\Delta T_f \quad \text{(From temperature amplitude of original problem)} \quad (3.1)$$

and

$$\Delta\sigma|_{x=o} = \sum K|G|\Delta T_{fFFT} \quad \text{(From FFT analized temperature amplitude).} \quad (3.2)$$

Both stress calculated from original temperature ranges and Fourier analyzed ones were shown in the next table.

Table 3.5 Evaluation of stress from integral gains

Case	frequency(Hz)	ΔTf(℃)	K｜G｜ΔTf(℃)	K｜G｜$\Delta Tf(℃)_{FFT}$	ΣK｜G｜ΔTf(℃)	Σ K｜G｜$\Delta Tf(℃)_{FFT}$
S1	0.085	90	244.1	200.2	244.1	200.2
S1-0.1	0.085	60	162.7	110.7	162.7	110.7
	0.0085	30	26.0	21.6	188.7	132.3
S1-10	0.085	60	162.7	134.0	222.9	174.9
	0.85	30	60.2	40.9	60.2	40.9
S1-0.01	0.085	60	162.7	134.5	162.7	134.5
	0.00085	30	2.8	2.7	165.5	137.2
S1-100	0.085	60	162.7	155.7	190.6	178.8
	8.5	30	27.9	23.1	27.9	23.1
S1-2(0.25)	0.085	60	162.7	130.2	242.1	205.3
	0.17	30	79.4	75.2	79.4	75.2
R1	0.085	127.27922	345.2	246.8	564.8	420.0
	0.17	45	119.1	95.3	219.6	173.2
	0.255	18	45.7	54.8	100.5	77.9
	0.34	22.5	54.8	23.1	54.8	23.1

The next table shows Fatigue damages from stress ranges of Table 3.5. These results are well correlated with results of the Table 3.3, and fatigue damage evaluation is possible in frequency domain.

Table 3.6 Fatigue damage after 30years calculated in frequency domain

Case	frequency(Hz)	ΔTf(℃)	ΣK｜G｜ΔTf(℃)	Σ K｜G｜$\Delta Tf(℃)_{FFT}$	Df	Df_{FFT}
S1	0.085	90	244.1	200.2	1.09E+00	1.48E-02
S1-0.1	0.085	60	0.1	60.0	3.07E-05	8.19E-16
	0.0085	30	0.1	90.0		
S1-10	0.085	60	0.9	90.0	1.76E-01	3.86E-05
	0.85	30	0.9	30.0		
S1-0.01	0.085	60	0.1	60.0	2.22E-06	2.40E-13
	0.00085	30	0.1	90.0		
S1-100	0.085	60	8.6	90.0	2.99E-03	4.28E-04
	8.5	30	8.5	30.0		
S1-2(0.25)	0.085	60	0.3	90.0	1.11E-01	5.65E-02
	0.17	30	0.2	30.0		
R1	0.085	127.27922	0.9	212.8	N.A.	N.A.
	0.17	45	0.8	85.5		
	0.255	18	0.6	40.5		
	0.34	22.5	0.3	22.5		

4. APPLICATION TO PHENIX SECONDARY CIRCUIT

4.1. PROBLEM DEFINITION

An actual thermal striping problem at a tee junction of the PHENIX secondary circuit (Fig.4.1) was studied in the framework of the IAEA coordinated research program on "Harmonization and validation of Fast Reactor thermomechanical and thermohydraulic codes and relations using experimental data" [1]. A small pipe is attached to a main pipe of the PHENIX secondary circuit containing cold sodium at 340℃, and discharges hot sodium at 430℃ into the main pipe. The two convergent flows with different temperatures (ΔT=90℃) are therefore mixed at the tee junction area. At the circumferential welded joint that locates at 160mm down stream from the tee junction, through wall cracks have been observed during the course of a campaign of inspection after operation of 90,000 hours.

Temperature histories were measured at several portions on the outer surface of Phenix secondary piping system during operative conditions. Among them, TC-2 and TC-5 (Fig.4.2) indicated the large temperature amplitudes as Fig.4.3 and Fig.4.4. By using this data, temperature and stress histories were estimated by using the frequency response approach.

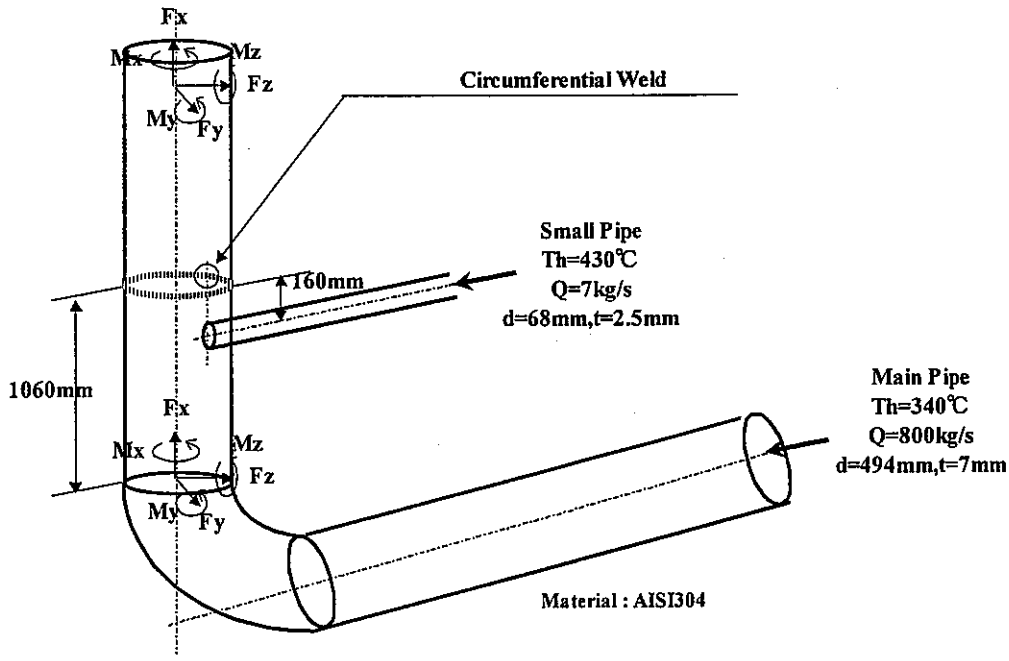

Fig.4.1 Geometrical Characteristics of the Phenix Secondary Piping System

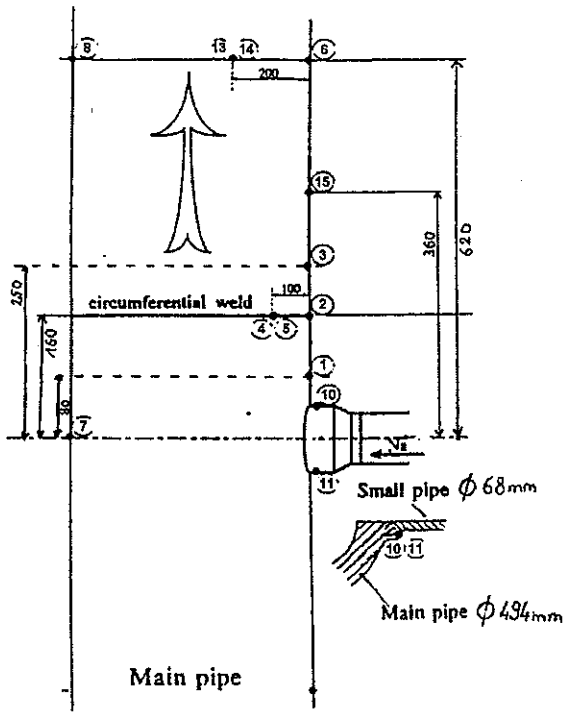

Fig.4.2 Location of thermocouples on the Phenix piping system

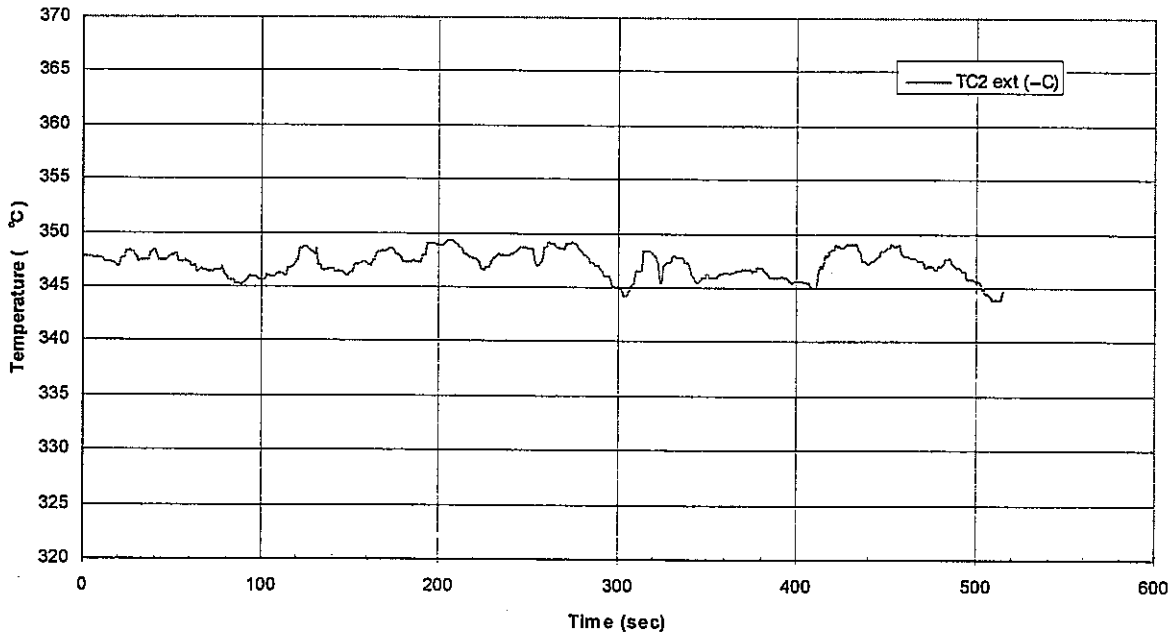

Fig.4.3 Measured temperature history by TC2

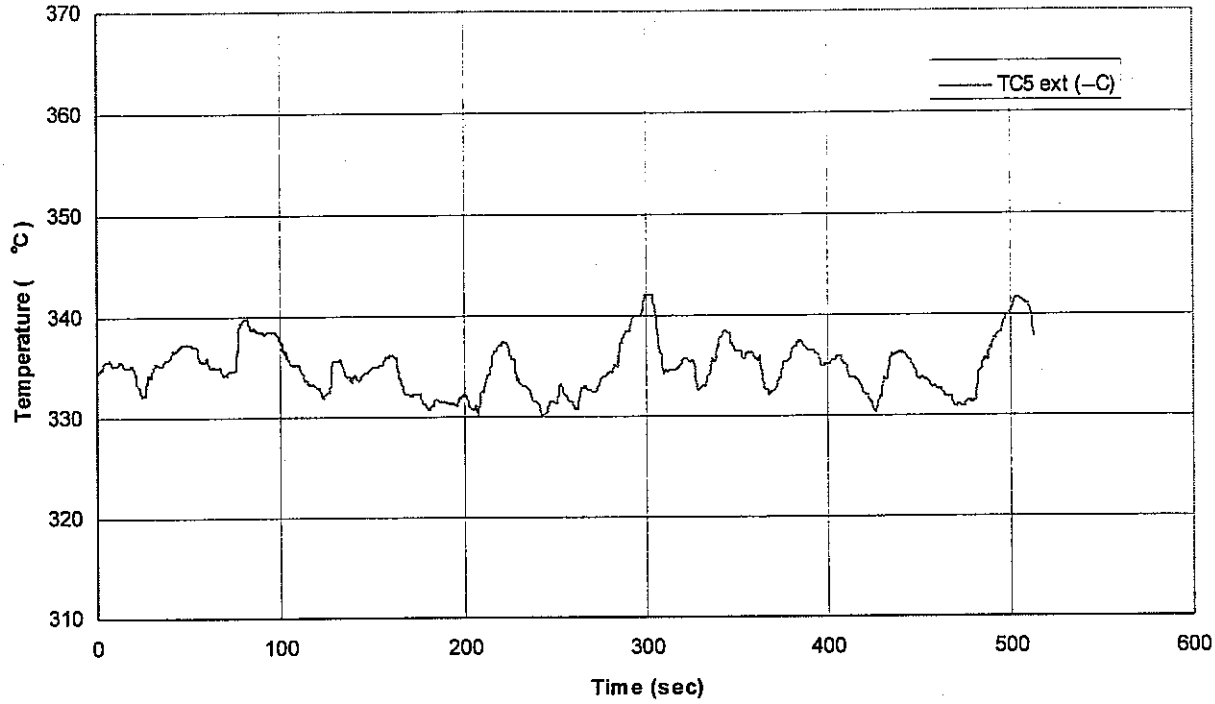

Fig.4.4 Measured temperature history by TC5

4.2. PREDICTION OF TEMPERATURE RESPONSE

From temperature measurements on the outer surface of the pipe, temperatures on the inner surface and fluid were predicted by the frequency response approach with the CEA program[4]. A heat transfer coefficient was assumed as 15000W/m^2℃ to evaluate fluid temperature that can be considered as bulk flow.

In order to apply frequency response function, FFT analysis was conducted on fluid temperature fluctuation and these results were converted to frequency characteristics on the inner surface by the inverse frequency response functions. Time histories of temperature were also calculated by inverse FFT analyses as in the next figures.

(1) TC-2

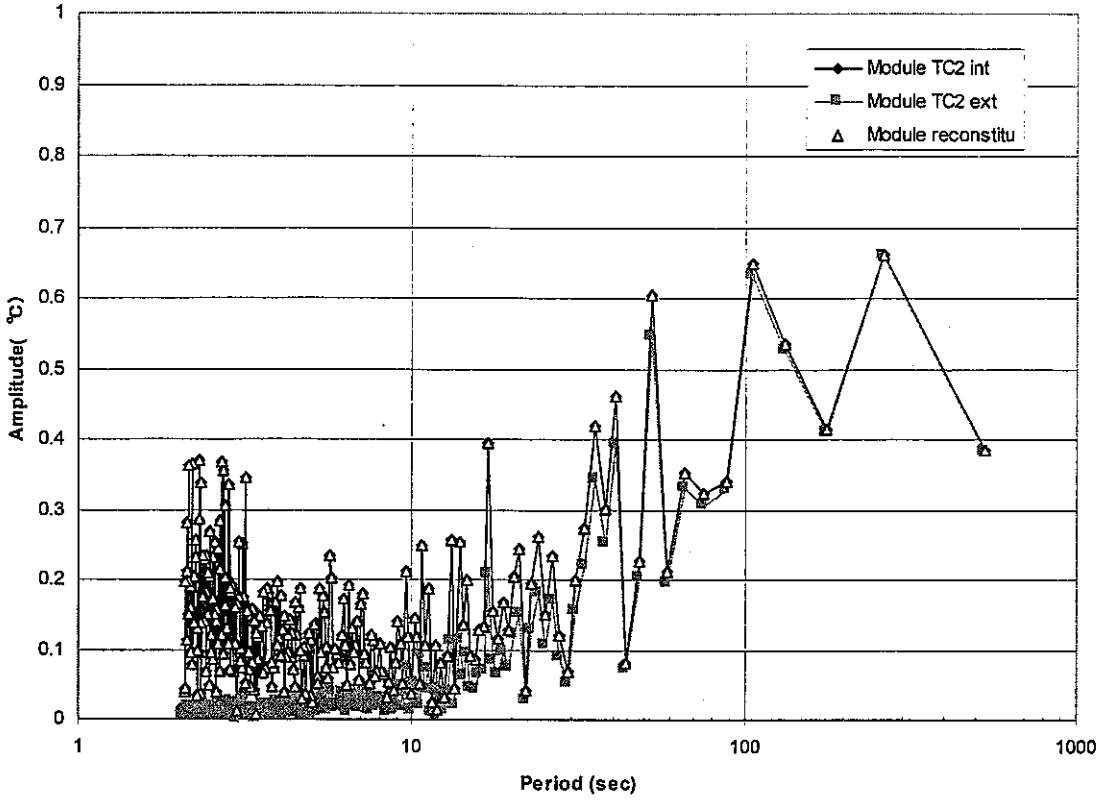

Fig.4.5 Frequency characteristics of measured temperature by TC2

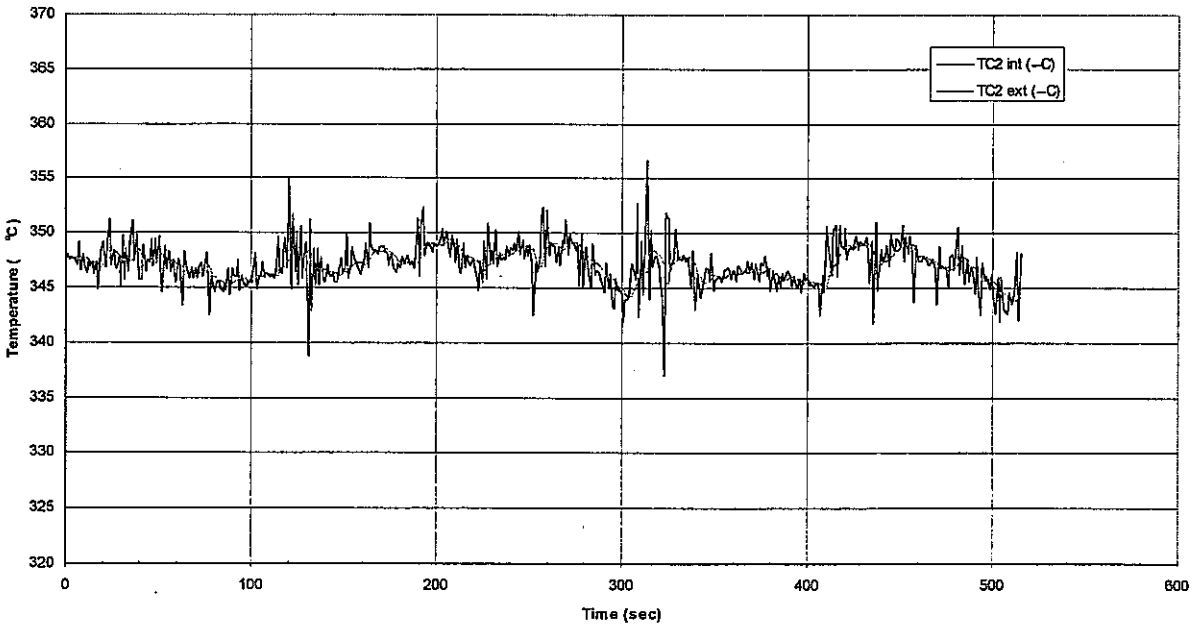

Fig.4.6 Evaluated time history of inner surface temperature at TC2

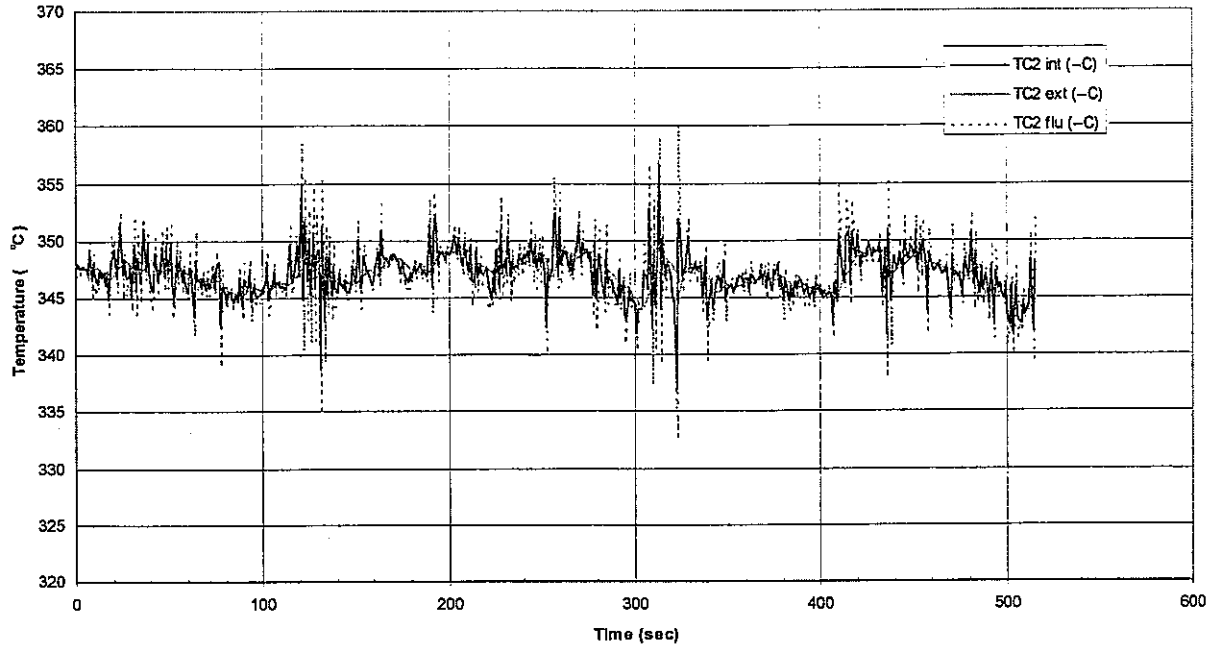

Fig.4.7 Evaluated time history of fluid temperature at TC2

(2) TC-5

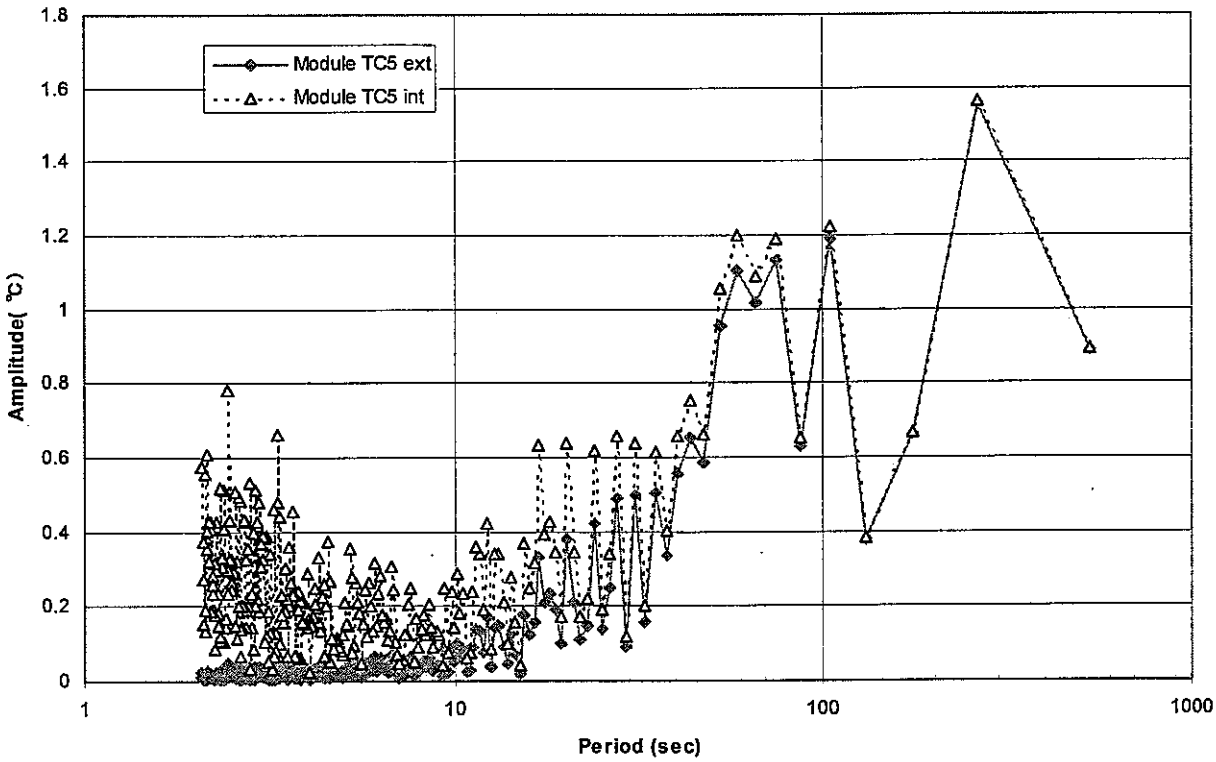

Fig.4.8 Frequency characteristics of measured temperature by TC5

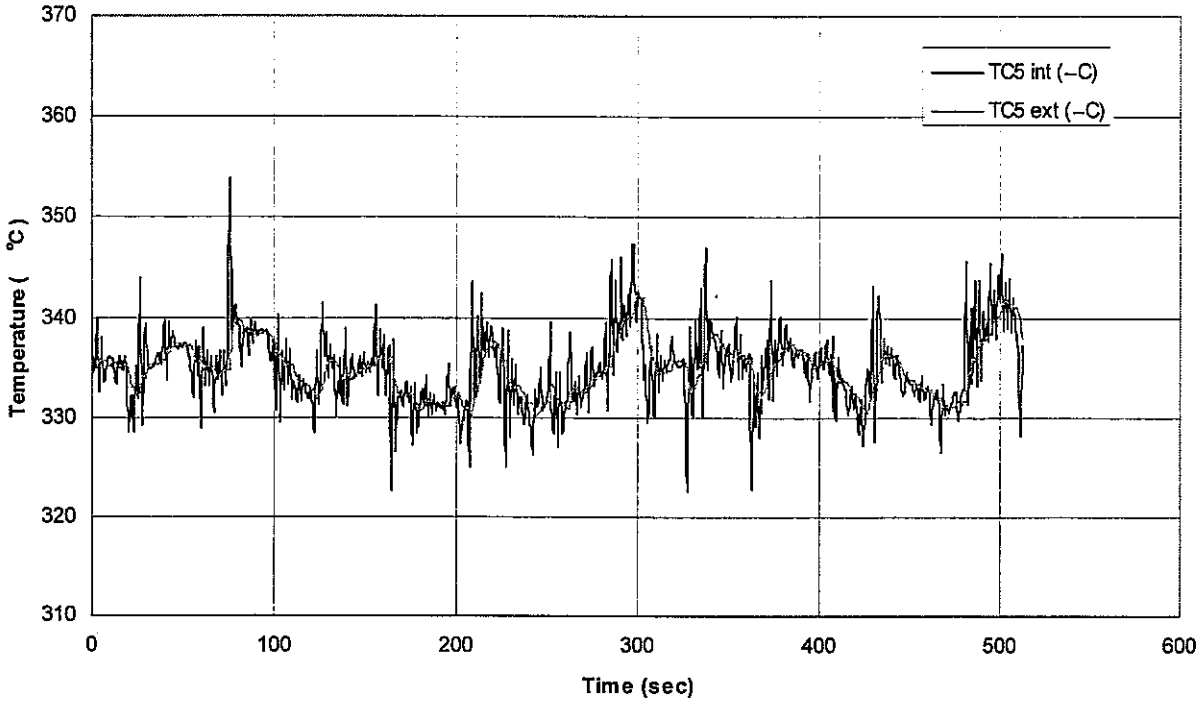

Fig.4.9 Evaluated time history of inner surface temperature at TC5

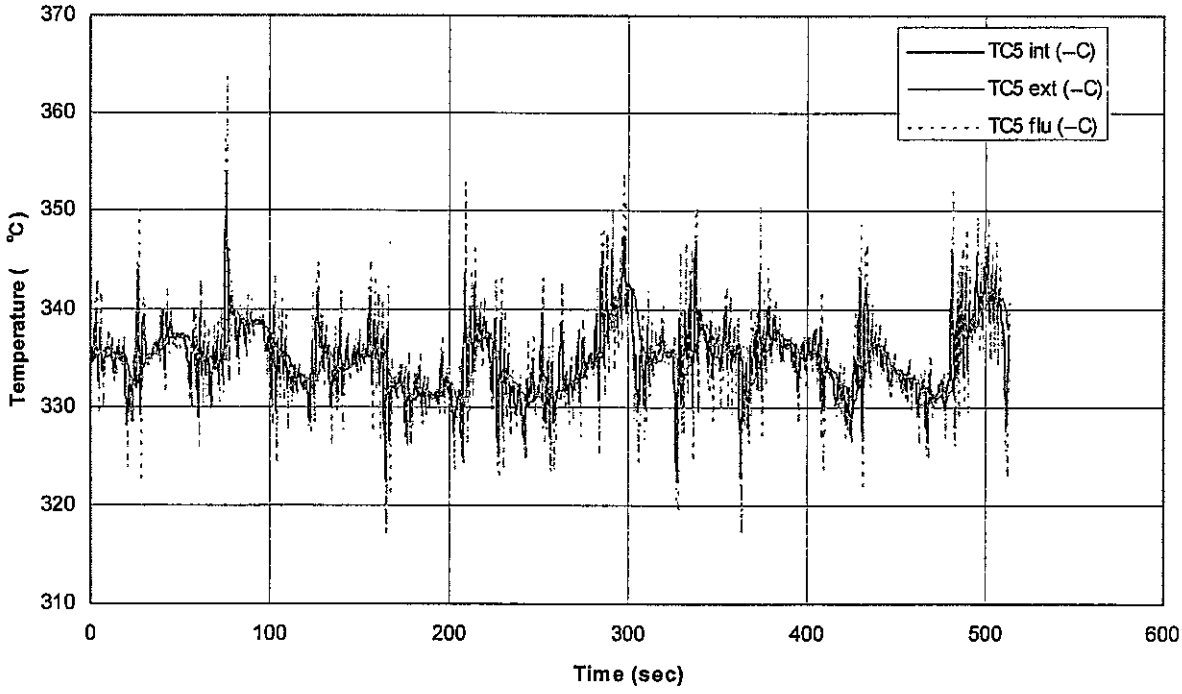

Fig.4.10 Evaluated time history of fluid temperature at TC5

4.3. PREDICTION OF STRESS RESPONSE

Inverse function of stress response to fluid temperature can predict stresses on the inner surface from external temperature. Since the frequency response function of stress depends on constraint conditions[2], stresses were evaluated for peak constraint, bending constraint and membrane plus bending constraint conditions.

(1) TC-2

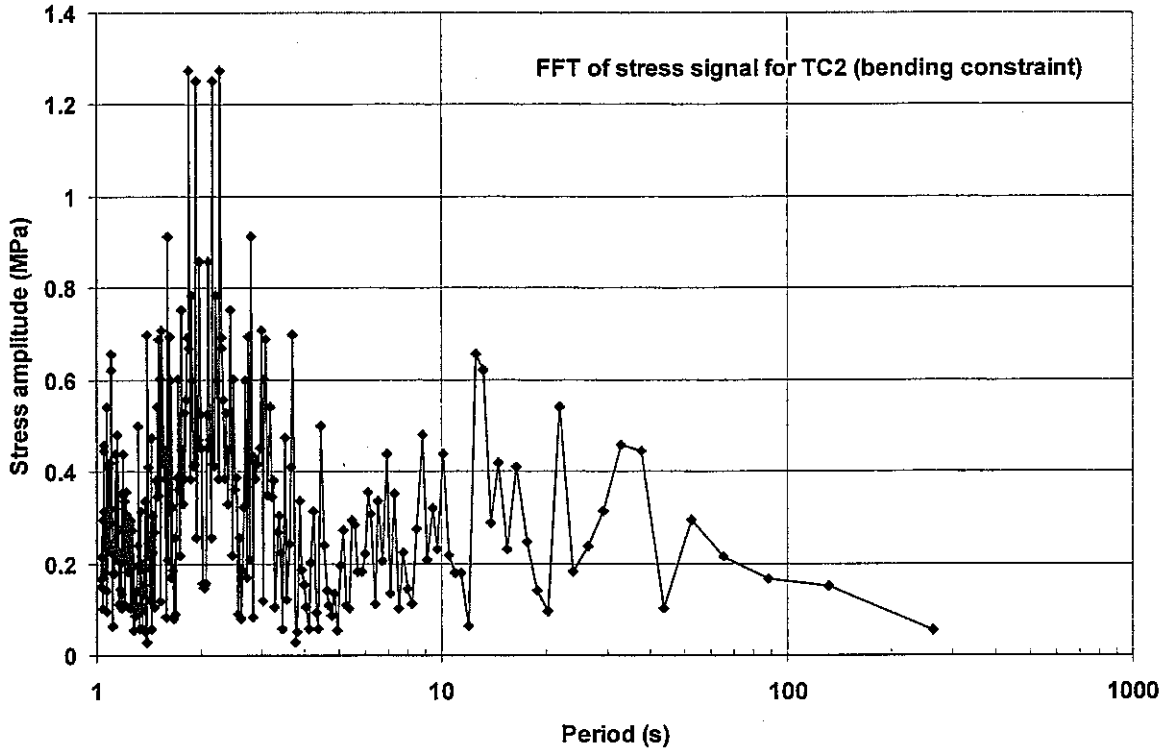

Fig.4.11 Frequency characteristics of inner stress at TC2

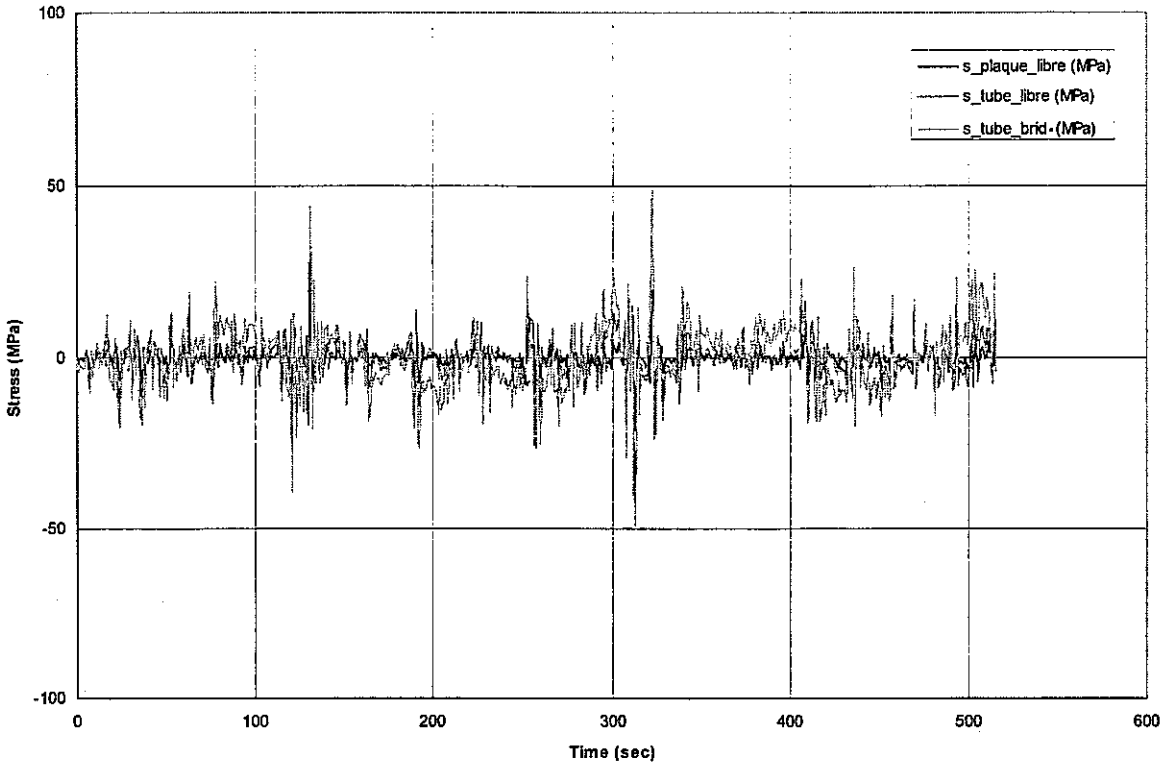

Fig.4.12 Evaluated time history of inner stress at TC2

(2) TC-5

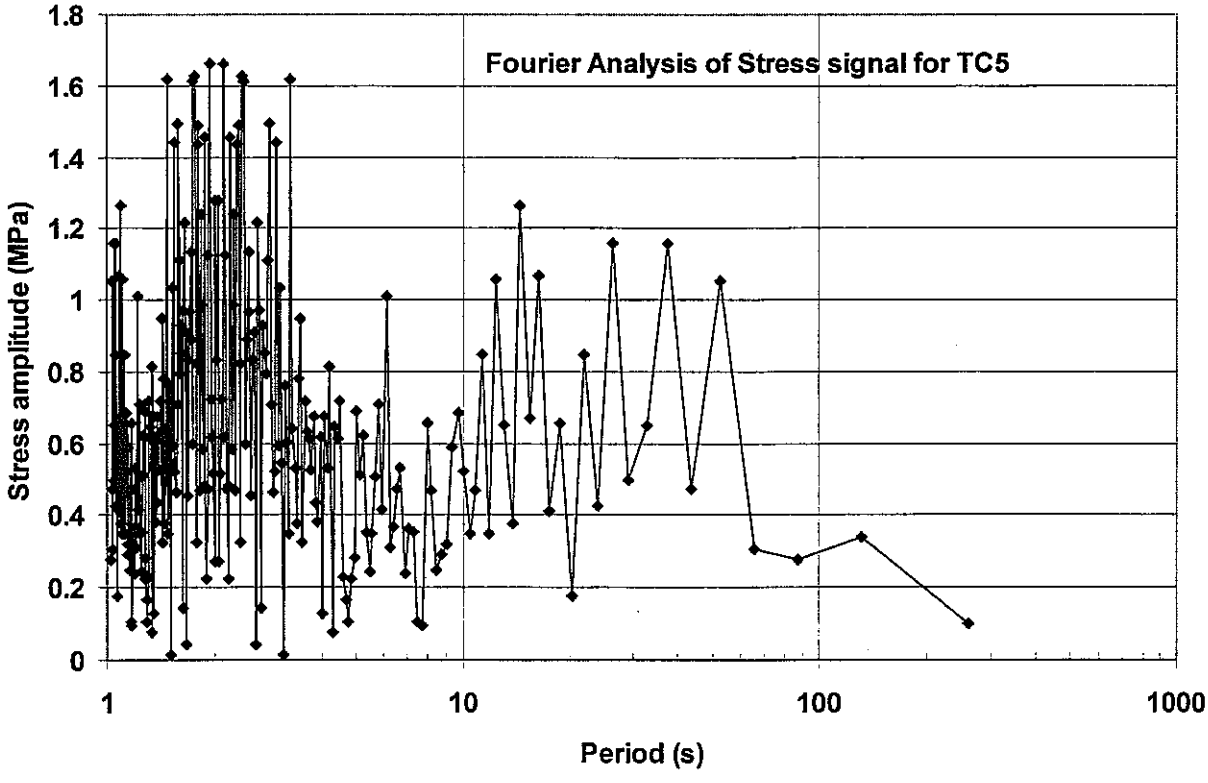

Fig.4.13 Frequency characteristics of inner stress at TC5

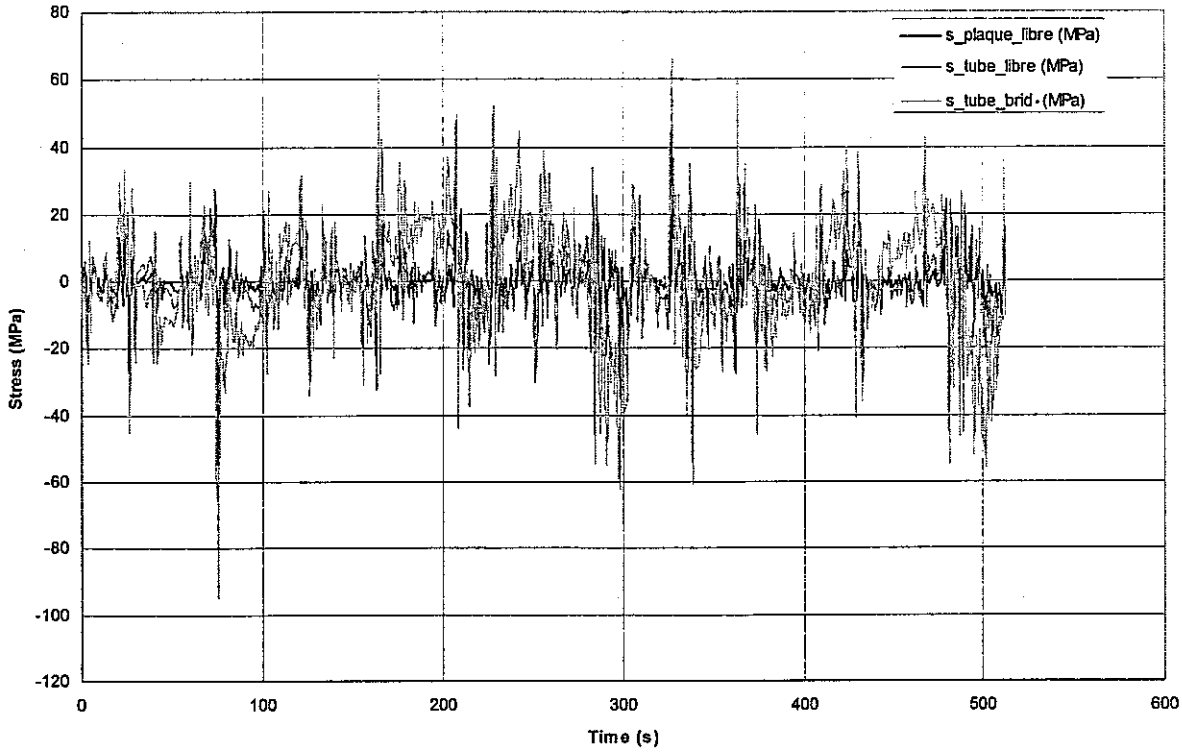

Fig.4.14 Evaluated time history of inner stress at TC5

4.4 FATIGUE STRENGTH ANALYSIS

Using stress analysis results by the frequency response function with inverse FFT, fatigue strength analyses were conducted with the rain flow wave counting method and Miner's rule [5].

Rainflow counting results of 550 sec stress analysis and evaluated fatigue damage for 90,000 hours period were shown in the next figures.

(1) TC-2

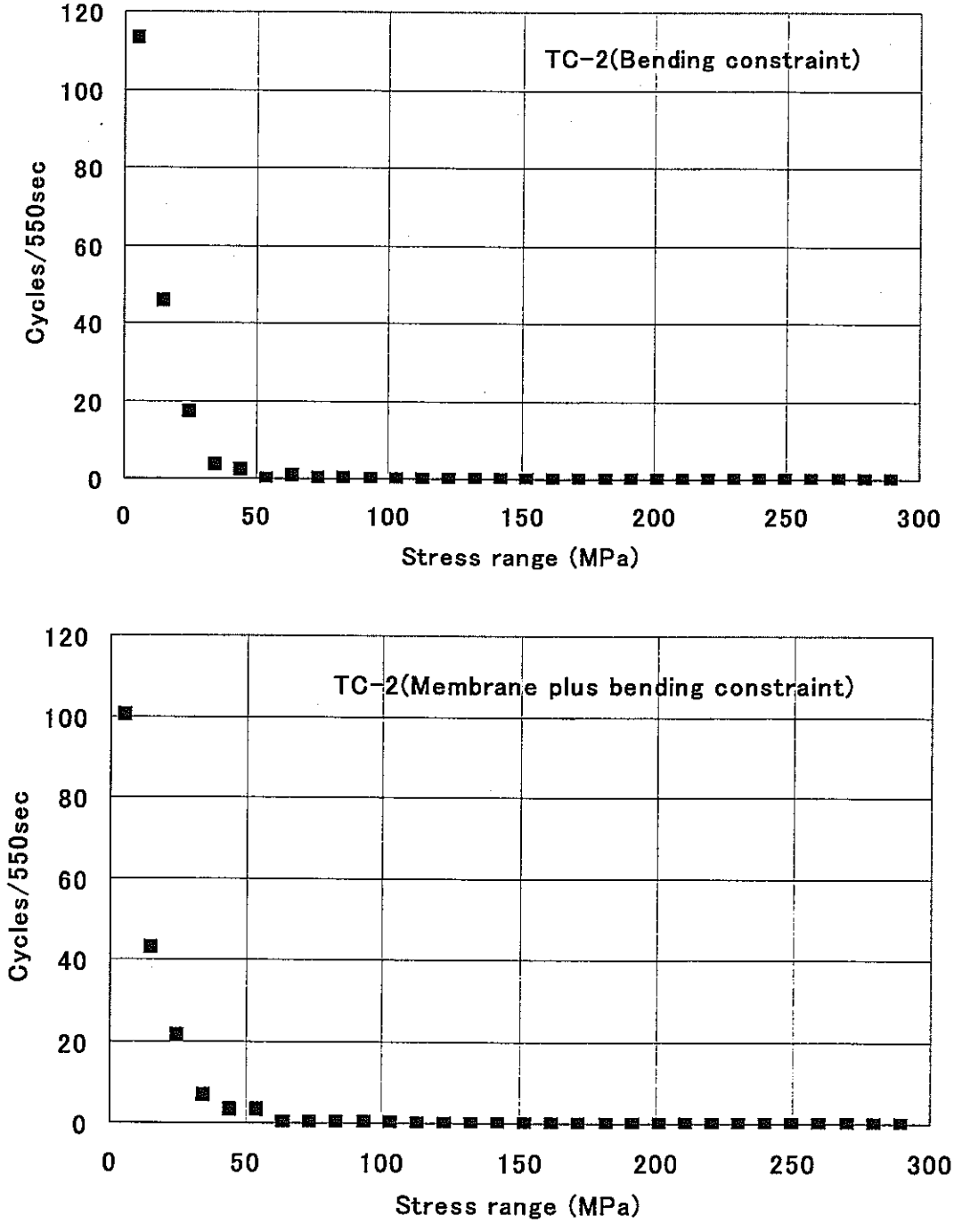

Fig.4.15 Rain flow counting results during 550 sec (TC-2)

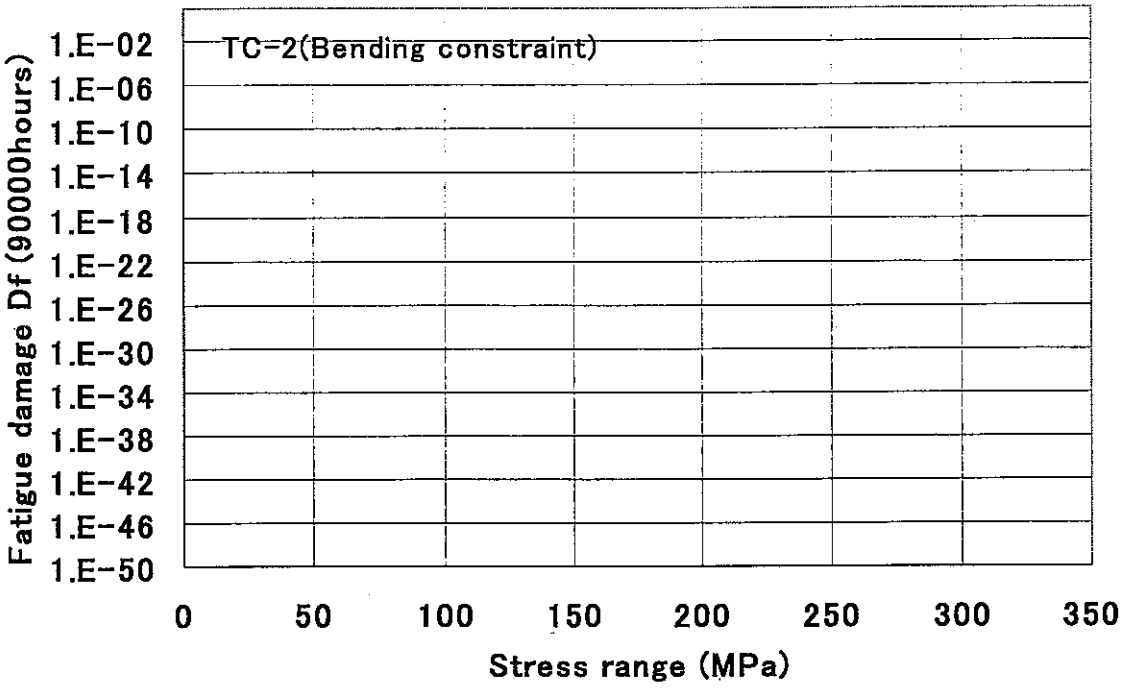

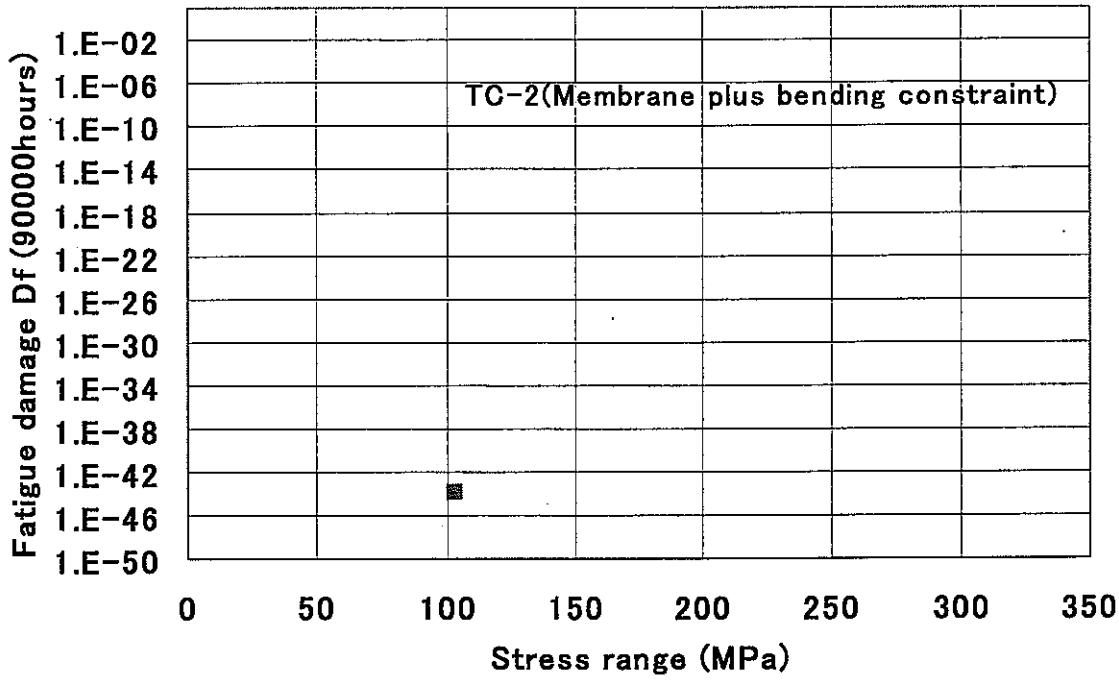

Fig.4.16 Calculated fatigue damage after 90,000 hours (TC-2)

(2) TC-5

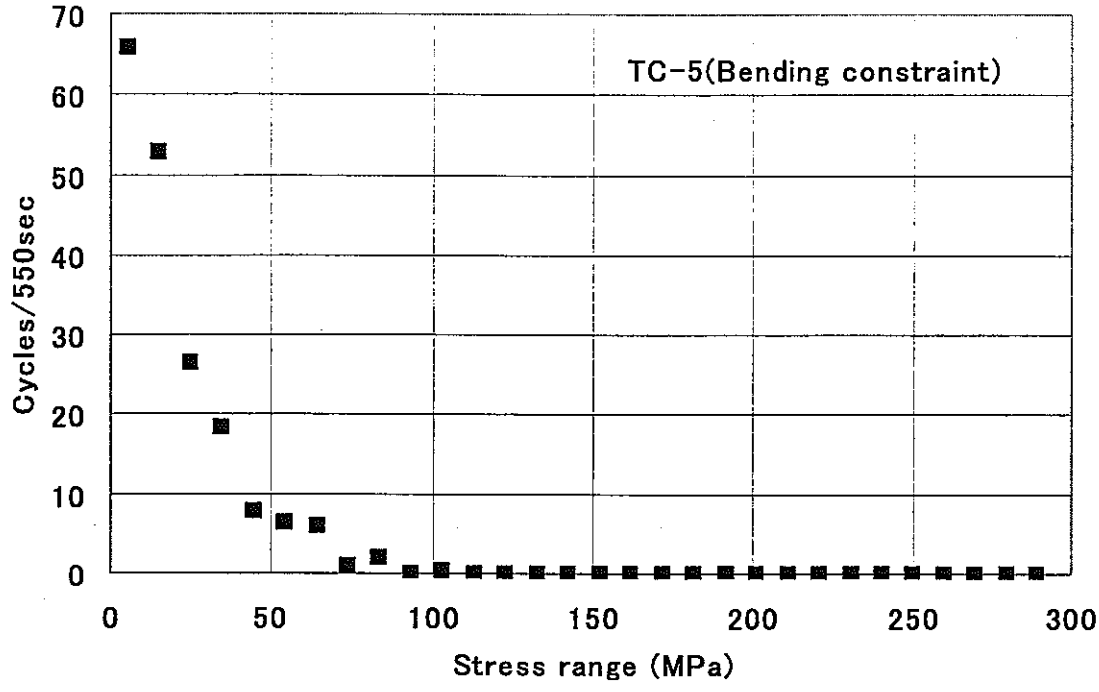

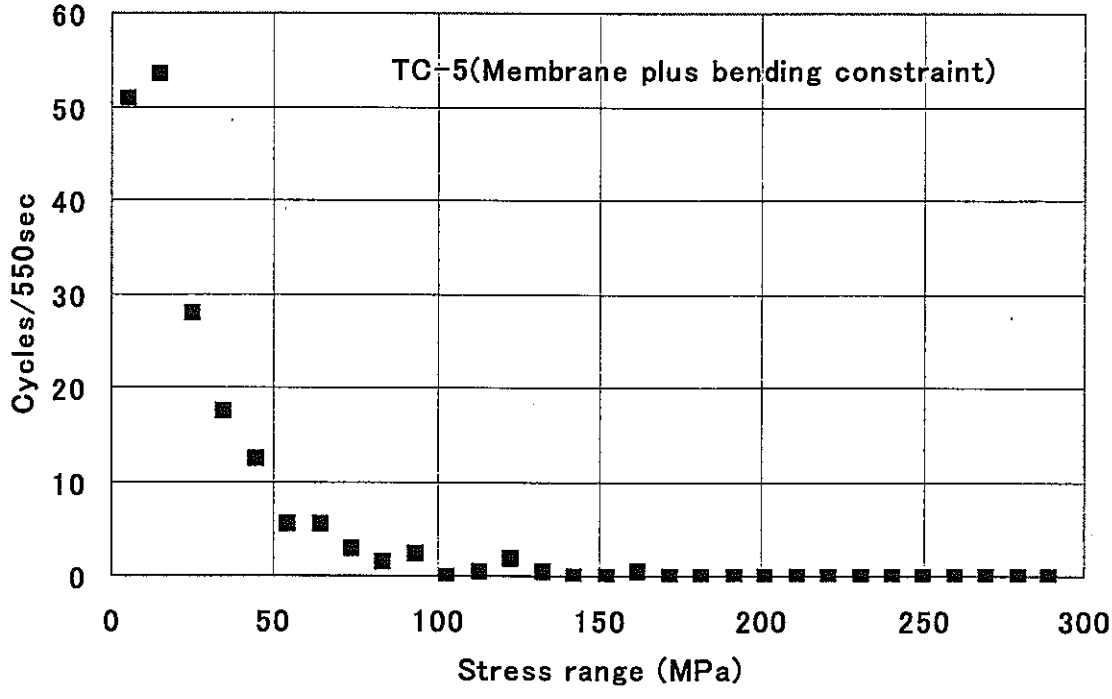

Fig.4.17 Rain flow counting results during 550 sec (TC-5)

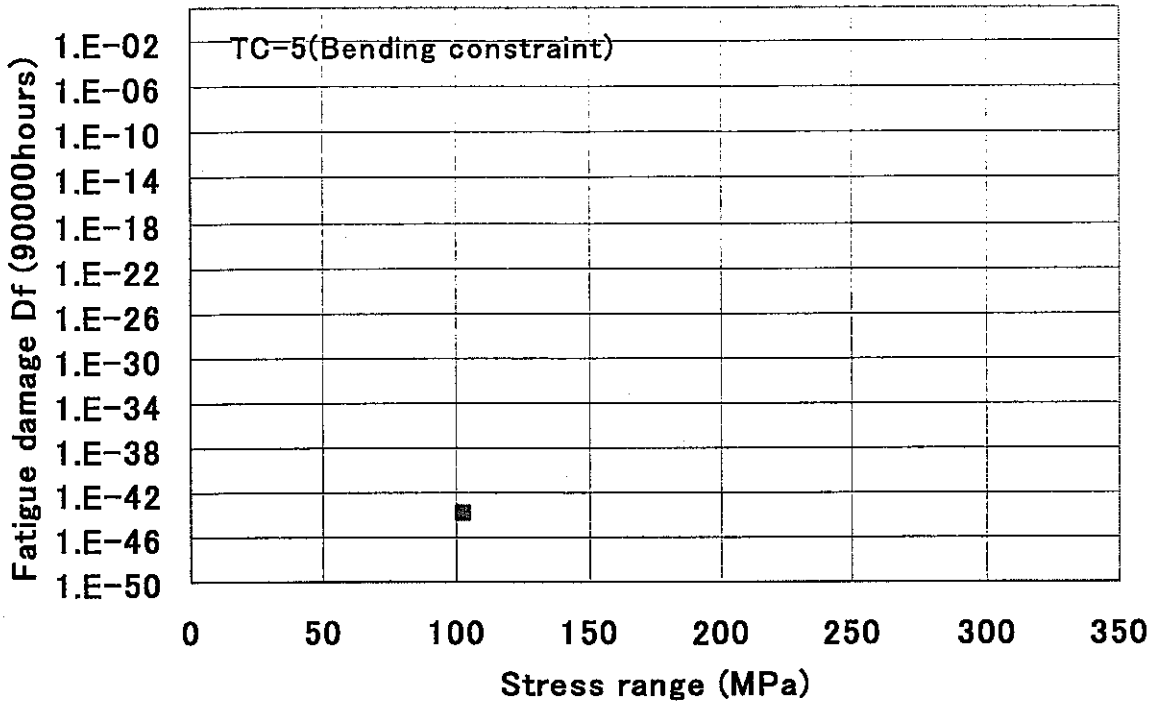

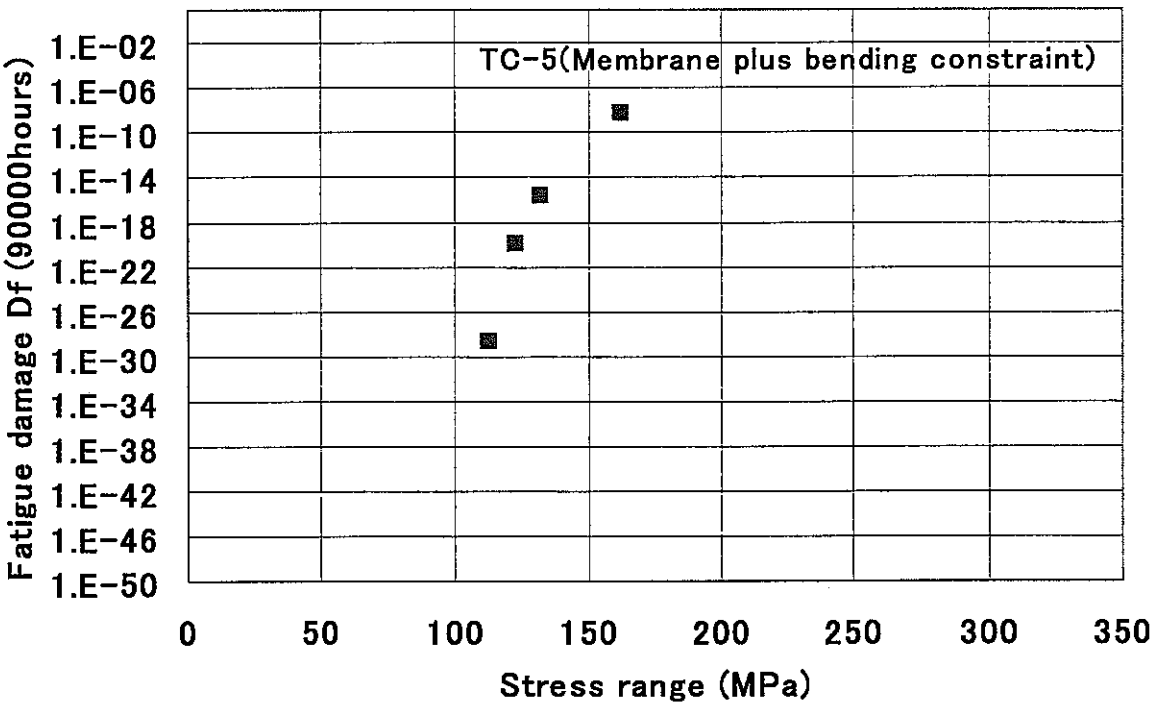

Fig.4.18 Calculated fatigue damage after 90,000 hours (TC-5)

Table 4.1 Summary of calculated fatigue damages during 90000 hours

Case	Df (Inverse FFT + Rainflow)
TC-2 (Bending constraint)	0.0E+00
TC-2 (Membrane plus bending constraint)	1.8E-44
TC-5 (Bending constraint)	1.8E-44
TC-5 (Membrane plus bending constraint)	6.8E-09

5. EXTRAPOLATION OF SIGNALS TO LONG TIME DURATIONS

Thermal striping is so complex to compute by thermalhydraulics codes that several months of CPU time are often required to obtain a few seconds of temperature histories for industrial problems (as for example for Phenix Tee Junction). Signals obtained are not enough long in duration to perform an accurate fatigue analysis, with the determination of histograms of cycles and fatigue damage inside structures. This is the reason why a bibliographic study was decided in 1999 concerning the possibilities to extrapolate Rainflow counting to sample of long durations (time durations). Moreover, a particular paper was chosen to start this study since it was used in Interatom and UKAEA thermal striping analyses : this paper has been written by E.J. Gumbel in 1954 [9] (entitled «Statistical Theory of Extreme Values and some Practical applications»). The main lines of this paper are summarized thereafter.

5.1. GENERAL PURPOSE

In his introduction, Gumbel says that the aim of a statistical theory of extreme values is to explain the extreme arrising in a statistical sample of a given length, and to extrapolate them to a longer sample length. But to be applicable, the observed variables must have three important properties :

- they must be statistical variables. That means they do not obey to a simple physical law. In general, the assumption is made since the proof is difficult to establish
- initial distribution of results of observations must remain the same if an other sample is chosen. This point should have important implies for the case of thermal striping, which requires constant results in case of repeatedly Rainflow cycles histograms. Does it mean that statistics of extreme values could not be applied for the extrapolation of very small samples ?
- different samples have to be independent. The result of one event is not dependent on the precedent, which seems to be a criteria similar to the first.

A history of theory of extreme values is then given. According to Gumbel, the oldest theories considered that the maximal possible value for any statistical variate was equal to 3 times the standard deviation. But it was established that this maximum value depends on the number of observations that are made : longer is the size of the observed samples, higher is the maximum value. The theory of extreme value was first studied by Bortkiewicz (1922) and R. Von Mises (1923).

It is interesting to list the applications of theory of extreme values that have been made by Gumbel. These applications are detailed and discussed in the article, with a description of the problems coming from the application. The applications were mainly related with meteorological phenomena like floods (annual maxima of daily rain discharges, interesting for industrial applications), droughts (annual mimima of daily rain discharges, for pollution predictions), gusts (largest strength of winds, for aeronautic domains), rupture strengh of materials, quality control, oldest age of a human population,...

5.2. DISTRIBUTION OF NUMBER OF EXCEEDANCES. LAW OF RARE EXCEEDANCES.

Main theory of extreme values is then described for the case of a continuous variable called □. A better understanding should be achieved after giving the following definitions :

- n is the number of past observations (also called sample size)
- N is the number of future observations
- m is an index corresponding to one of the n past observations (m =1,2,...,n . m = 1 correspond to the present state and m = n correspond to the oldest trial. We should understand that for m = 1 we know the largest observation among the sample size, for m = 2 we know only the second largest observation among the whole sample size, for m = 3 we know the third largest result,...)
- x is the number of trials with a result larger than or equal to the mth observation , for the N future trials

The probability of x is given by a simple equation, called distribution-free :

$$w(n,m,N,x) = \frac{n!\ N!\ (m+x-1)!(N+n-m-x)!\ m}{m!\ (n-m)!\ x!\ (N-x)!\ (N+n)!} \tag{5.1}$$

This function decreases with x, and the mean number of exceedance is equal to

$$\bar{x}_m = \frac{m\,N}{n+1} \tag{5.2}$$

, the standard deviation being

$$\sigma_m = \sqrt{\frac{m\,(n-m+1)\,N\,(N+n+1)}{(n+1)^2\,(n+2)}} \tag{5.3}$$

A law of practical importance is the law of rare exceedances, which can be obtained with assumptions that n and N are large, and m and x are small. In that case, the probability of x becomes :

$$w(x) = \frac{(x+m-1)!}{x!\,(m-1)!}\left(\frac{1}{2}\right)^{m+x} \tag{5.4}$$

with $\bar{x}_m = m$ and $\sigma_m = \sqrt{2\,m}$. This distribution is very similar to Poisson's distribution, the latter having a variance half.

5.3. APPLICATION TO EXTRAPOLATION OF SIGNALS

There are two main problems in the application of this type of model. The first is a practical one : it is not possible in Excel, even with a Stirling approximation, to evaluate factorial of large numbers which are required for thermal striping signals. So, this theory has not been applied to Phénix Tee junction temperature fluctuation signal. The second, of theoretical nature, is more important since it seems to question the validity of application of theory in case of thermal striping : the temperature fluctuations during thermal striping are within a finite range, whereas Gumbel analyses deal, strictly speaking, with unlimited distributions. This detail could lead sometimes to predictions larger than real values.

5.4. APPLICATION TO EXTRAPOLATION OF SIGNALS

The purpose of this part is to describe a possible future way to obtain an accurate signal extrapolation, based on study of random walk process. In fact it is well known that discrete random walk process describes diffusional type phenomena when it is assumed a given time duration between two successive events [10]. In the following we tried to explain what is random walk process ; then we describe how to adjust this type of simulation to an initial experimental or calculated signal, even if the method for adjustment could easily be improved. Then we show an example of application concerning Phénix Tee Junction.

5.4.1 DESCRIPTION OF RANDOM WALK PROCESS

Random walk process are very well explained in the literature [10]. They are described by means of the famous example of the gambler theory (which is not so closely related with Gumbel theory of rare exceedances). Consider a gambler who has a certain amount of money n, playing with another person to a game : at each trial, there is a probability p that the gambler wins (then q=1-p that the gambler looses). If the player looses, he must gives one unity of money to the other person ; in the other hand, the gambler receives one unity of money.

The problem is completely described if the « boudary conditions » are precised ; they must be of different types. For instance , the process is repeated until the player wins (his amount of money reaches 2n), or the player looses (amount of money is equal to zero). This type of boundary condition is called absorbing barrier (the game is finished when the condition is reached)

Another important boundary condition is the reflecting barrier : when amount of money decreases to zero (respectively increase to 2n) the other persons gives one unit of money to the gambler and the game continues (respectively the gambler gives one unit of money to the other person and the game continues). The reflecting barrier is of practical importance for us since the random walk process is then of infinite duration, as temperature fluctuations due to incomplete mixing.

Other types of boundary conditions combined the two precedent forms but are less interesting for us.

The different random walk process can be summarized by the figure below :

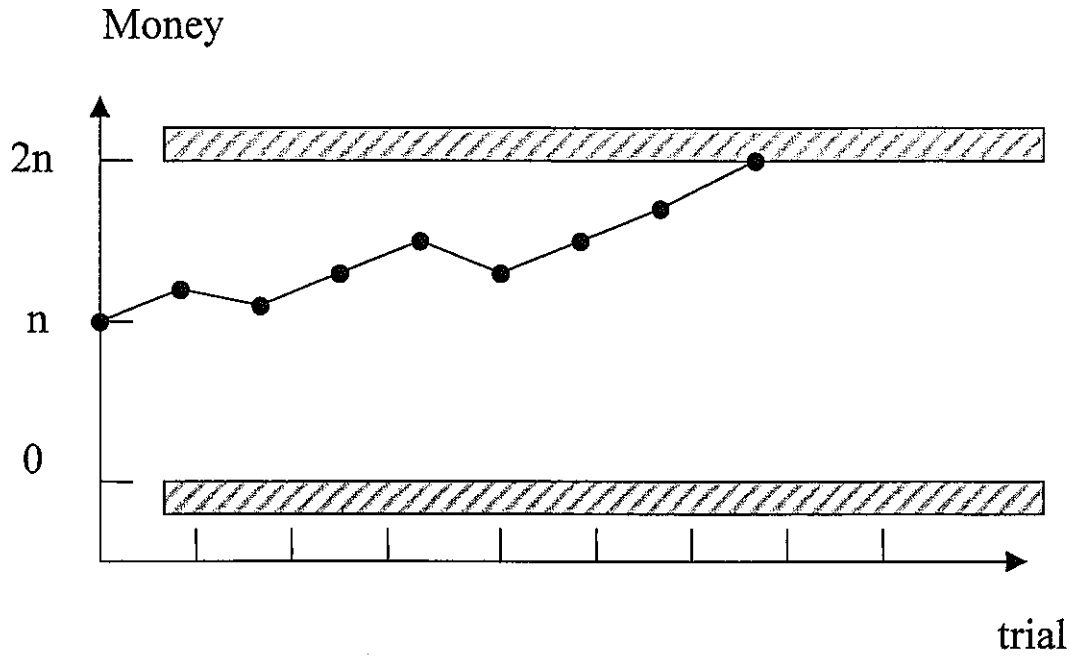

Fig. 5.1 : random walk process end example due to absorbing barrier

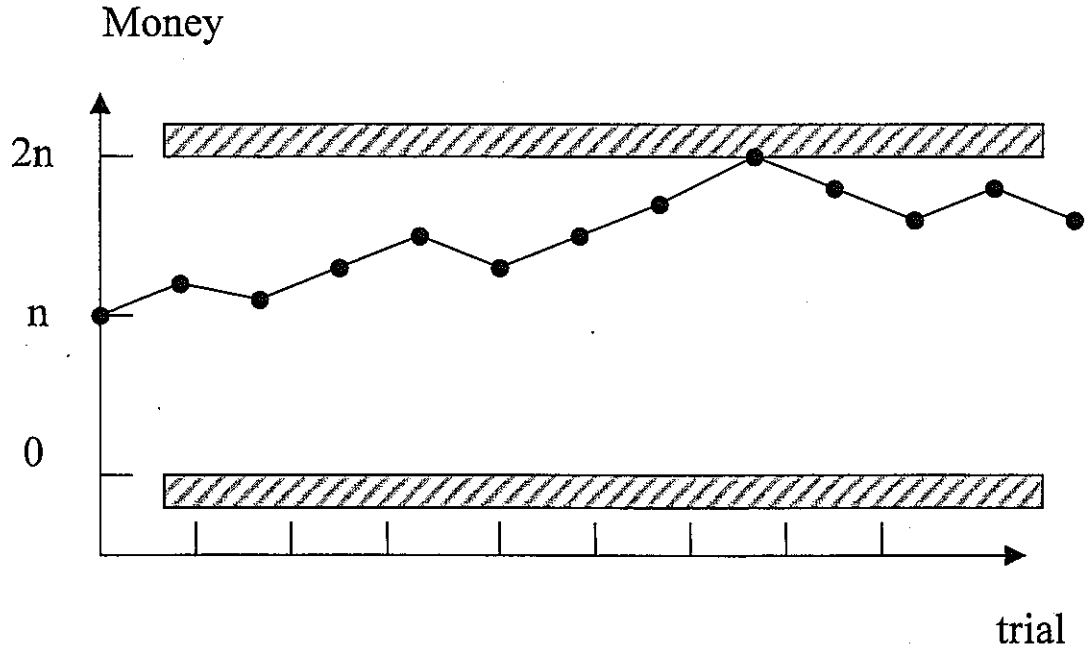

Fig. 5.2 : infinite random walk process due to reflecting barriers

An important hypothesis is that two successive events are independant : in example above, it means that the gambler gains or loss are not influenced by a previous gain or loss. In that case, combination theory apply to determine the

mean number of trials necessary to reach the boundary (0 or 2n). If probability p is equal to ½ , and if initial amount of the gambler is n, the mean number of trials to reach 2n or 0 is :

$d = n^2$

This corresponds to the mean game duration in the case of the absorbing barrier. Note that if initial amount of money is only β n with $0<\beta<1$ (β n being an integer) , the mean duration to reach 0 or 2 β n is simply $d = \beta^2 n^2$.

It is easy to define a constant time duration dt between two successive events so that mean time duration to reach 0 or 2 β n is $t_m = \beta^2 n^2 dt$

5.4.2 APPLICATION TO THERMAL STRIPING SIGNALS

We would like to transform the gambler example into a thermal fluctuation problem. ΔT being equal to Tmax-Tmin , this is obtained by changing n in $\Delta T / (2 dT)$, β in $2 (T-T_{moy}) / \Delta T$ if we consider that temperature changes are of amplitude dT during one step (that means during the time increment dt).

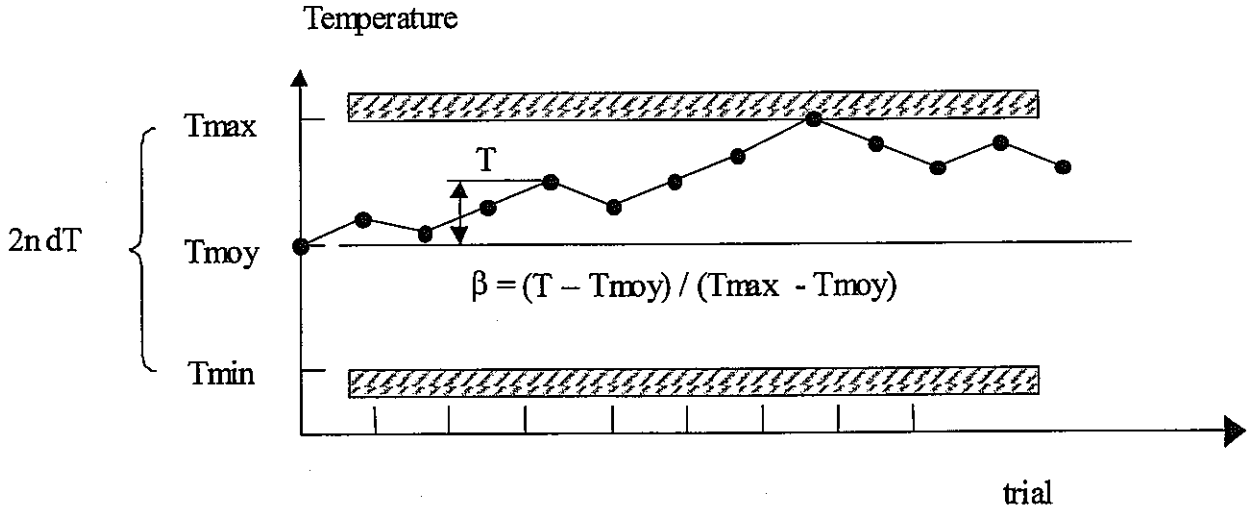

Fig. 5.3 : explanation of transformation from gambler theory to thermal striping problem

This means that at each time increment dt, we assume that a given elementary volume of liquid has probability ½ to increase or decrease his temperature of dT degree. Thus starting from the mean temperature at time zero, it's possible to know the mean duration necessary to reach temperature T, applying the equation of 5.4.1 :

$$t_m = \beta^2 n^2 dt = (2\,(T-T_{moy}) / \Delta T\,)^2\,(\,\Delta T / 2\,dT)^2 dt = [\,(T-T_{moy})/dT\,]^2\,dt \qquad (5.5)$$

All we have to do is then to select time dt, temperature increment dT, and local maximum possible ΔT which are not known in order to obtain the better agreement between simulated and measured signals; we should remark that the calculated mean temperature is imposed equal to the experimental mean temperature : it means that we suppose the experimental signal has a sufficient duration to give an accurate value for the mean temperature (consequently, we don't need to estimate the mean temperature) . This process has been programmed in Excel and applied to Phenix J1 Tee junction signals (thermocouple n°1 placed on the external surface). The two following figures show the results of two sets of 5 simulations ; figure 5.4 corresponds to dt = 0.033s, Tmax-Tmin = 1°C, n = 150. Figure 5.5 corresponds to dt=0.033s, Tmax-Tmin = 1.5°C, n = 75. It obviously appears that a ΔT of 1.5°C is better for the simulation of the process ; the example shown are just for illustration purpose and it is an evidence that it is possible to find a set of parameters giving a better "agreement" with the measurement. We discuss in the following paragraph on which criteria the agreement has to be defined, and what are the possibilities to improve this simple model.

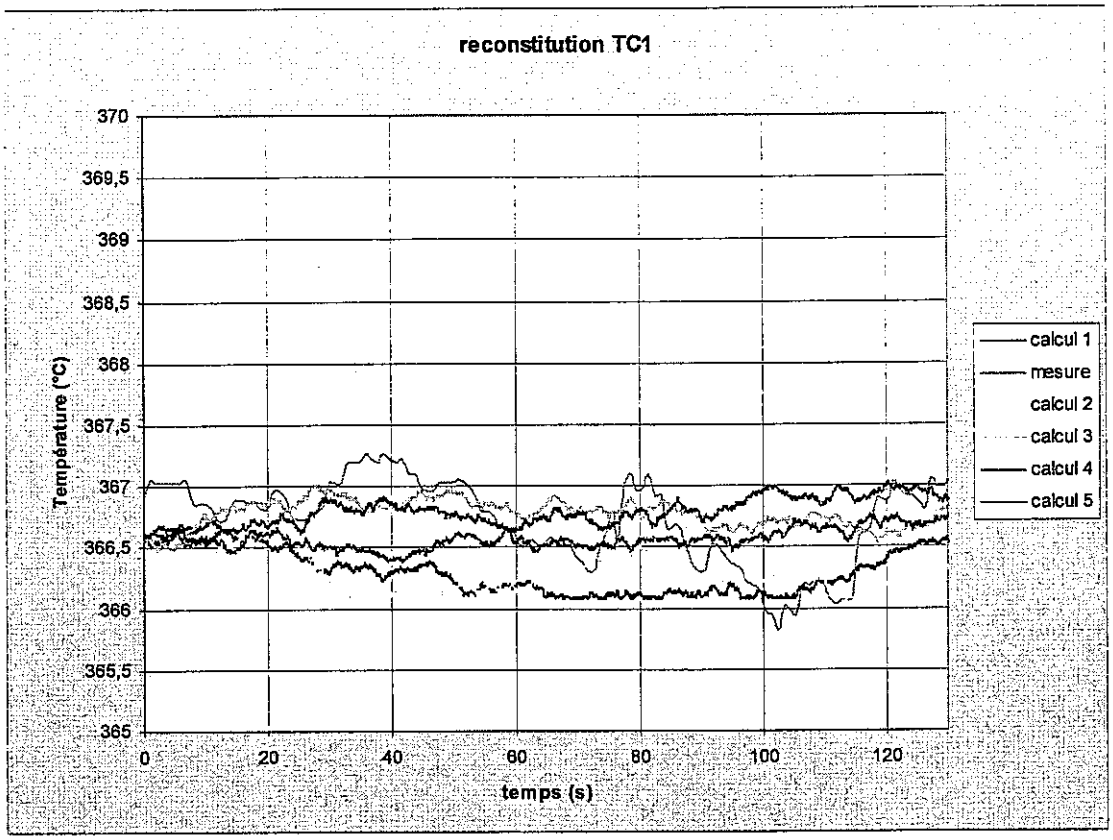

Fig. 5.4 : corresponds to dt = 0.033s,Tmax−Tmin = 1°C, n = 150

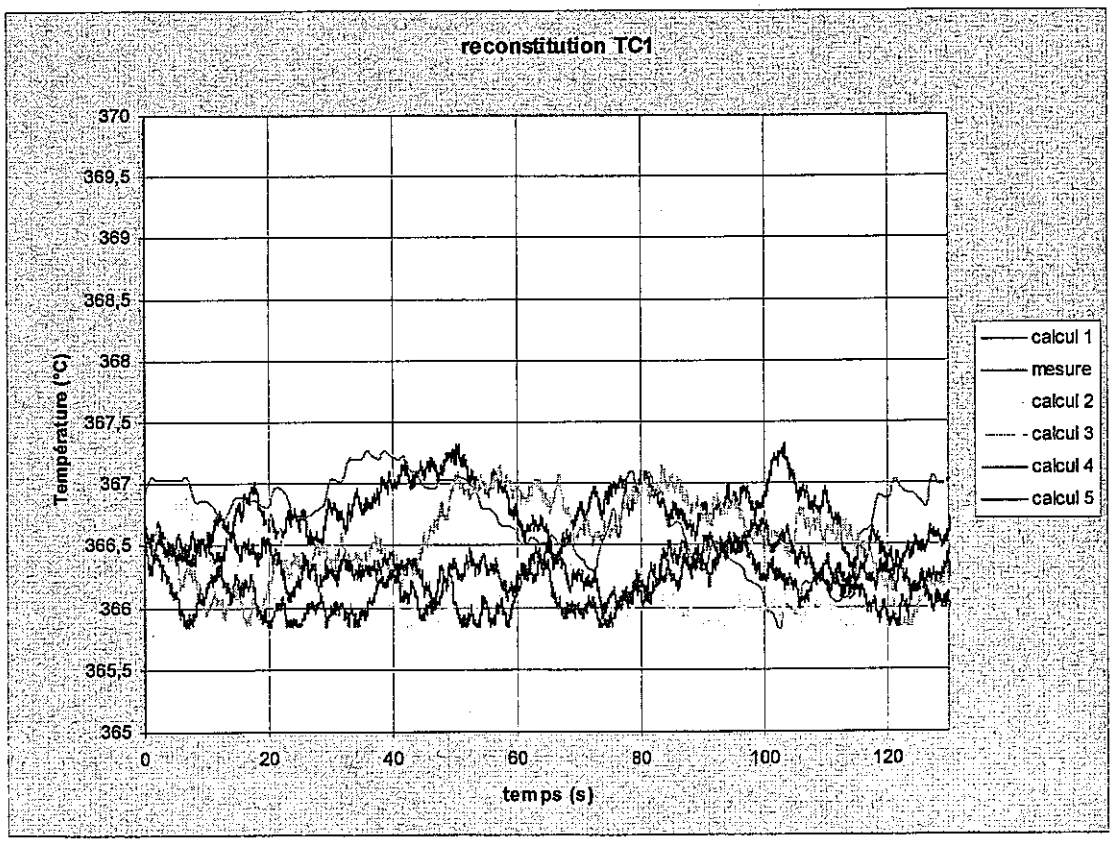

Fig. 5.5 : corresponds to dt=0.033s, Tmax−Tmin = 1.5°C, n = 75.

Another set of tests has been made with dt = 0.033s, T_{max}-T_{min} = 90°C, n = 10000 (see Fig. 5.6) in order to show the different possibilities of fitting. If calculated signals appear to be similar to the precedent, they should be completely different for very long time applications, since it is expected to reach ΔT = 90°C in the last example, what is not possible in the first.

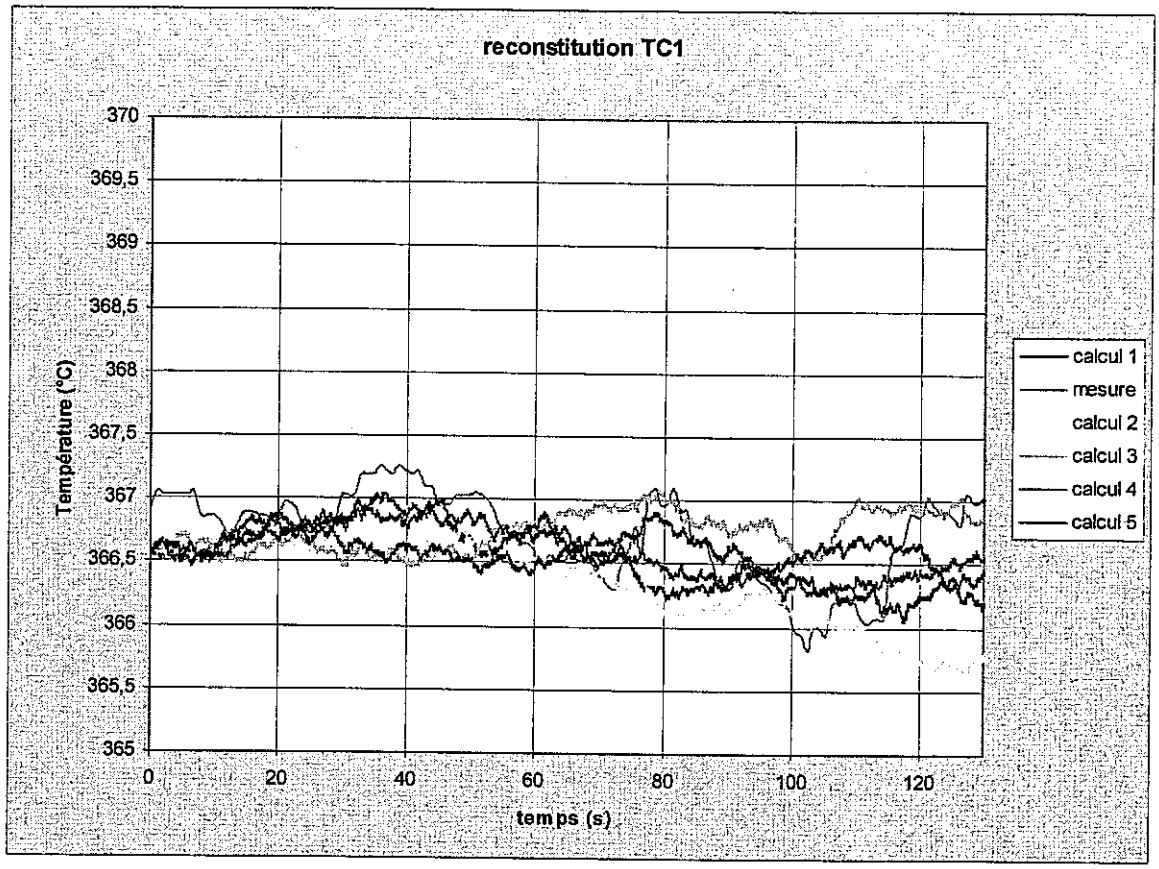

Fig. 5.6 : simulation of random walk process with dt = 0.033s, Tmax−Tmin = 90°C, n = 10000

This points out the difficulties, which may be encountered during the adjustment of the parameters.

5.4.3 CRITERIA TO DEFINE THE ACCURACY OF THE SIMULATION.

Several ways could be chosen to estimate the accuracy of the simulation.

The first possibility is to state that experimental mean temperature, variance, and other higher order moments are the reference values.

An other possibility could be to compare experimental and calculated Rainflow cycle histograms, or when applicable, to compare the differences on total fatigue damage.

Last, but not least, it could be of great interest to build the Markov matrix of the process (the elements of this matrix are the probability to reach level j when temperature is at level i). Then the comparison of experimental and calculated signals should give our criteria.

These basic ideas have not been tested in our computations, but it should be done in the future if further investigations are decided on these types of methods. In any case, as experimental signal is assumed to be not stabilised, since we want to extrapolate it, it would be difficult to compare the two signals. The comparison seems to require a rule to minimize the distance between the different set of data; in a first stage, we could try to apply a least squares regression line.

5.4.4 POSSIBLE IMPROVEMENTS

The purpose of this paragraph is to give some ideas for future improvements of the method, by a list with few comments :

- in the studied random walk process, the temperature is allowed to increase or decrease of an amount dT at each step. Of course, it could be ameliorated, giving it the right to increase or decrease of dT1, dT2, dT3,...dTn with the respective probabilities p1, p2, p3, ... pn , at each step, depending of the characteristics of the experimental signal. These characteristics are easily known by building the Markov matrix of the signal. Note that if Markov matrix is applied directly to "simulate" a new signal, it is not possible to obtain something different from the original signal ; the new signal is the exact replica of the original, statistically speaking (this can be interpreted as : the basic random walk process is a simulation, and a Markov random walk process is an adjustment on the experimental data).
- as mentioned earlier, it should be better to use a criteria and a regression

6. CONCLUSIONS

In order to evaluate actual thermal striping phenomena, the frequency response function method was extended to random fluctuation problems. One is the method based on an inverse FFT of calculated results by the frequency response function, and the other is direct fatigue analysis method in frequency domain. Through application to example problems, the former method was validated and possibility of applicability was demonstrated on the later one. Advantages of this approach are a significant reduction of stress calculation time and an understanding of damageable frequency.

Concerning methods to extrapolate signals to long time duration, theory of rare expectations is not easy to apply for the case of large numbers. This theory leads to infinite extreme values for infinite time duration. Other theories could also be applied to thermal striping signals, like random walk process. This theories should be studied more in detail, and must be imposed by Markov matrix use, and regression analysis for amelioration adjustment with experimental results.

7. DISCUSSIONS

To extrapolate short period fluctuation data to actual operation time, a statistical approach is necessary. Limitation of damageable frequency range is helpful to rationalize statistical approach. There is a possibility to apply the evaluation method in frequency domain for extrapolation. Continuous discussions are required to examine above items.

ACKNOWLEDGEMENT

It is very thankful in rain flow programs by Mr.H.Hosogai of Joyo industries. Finite element calculations of H.Takasho of Joyo industries is gratefully acknowledged. The author is also deeply indebted to Dr. C.Poette and Dr. M.T. Cabrillat of CEA-Cadarache and Dr.M.Morishita of OEC/JNC for their kindness to make a chance of cooperative work under the EJCC contract

REFERENCES

[1] Muramatsu,T., Experimental and Numerical Results on Non-Stationary Thermal Response Characteristics for a Fluid-Structure Interaction System, E-J Thermal-Hydraulics Specialist Meeting, CEA France,(1998)

[2] Kasahara,N. , Frequency response function method for evaluation of thermal striping phenomena , JNC TN9400 2001-005,(2000)

[3] Kasahara,N. and Lejeail, Y., Benchmark problems on thermal striping evaluation of FAENA and TIFFSS sodium experiments, JNC TN9400 2001-006,(2000)

[4] Kasahara,N. and Lejeail, Y. , Interpretation of FAENA and TIFFFSS experiments : Comparison of temperature evaluation methods on thermal striping JNC TN9400 2001-014,(2000)

[5] Kasahara,N. and Lejeail,Y., Interpretation of FAENA and TIFFFSS experiments : Comparison of fatigue strength evaluation methods on thermal striping , JNC TN9400 2001-013,(2000)

[6] Gelineau,O., et al., Review of predictive methods applied to thermal striping problems and recommendations, SMiRT15, F06/3, (1999)

[7] Kasahara, N. et al., 'Advanced Creep-fatigue Evaluation Rule for Fast Breeder Reactor Components : Generalization of Elastic Follow-up Model', NED 155, pp499/518, (1995)

[8] Kasahara,N. et al.,'Strain Concentration Evaluation of Smooth Structures Subjected to Thermal Stress', JSME, Proc.of Annual Meeting of JSME/MMD,315 In Japanese,(1993)

[9] E.J. Gumbel, "Statistical Theory of Extreme Values and some Practical Applications", U.S. Govt. Print. Office Washington, 1954

[10] Norman T. J. Bailey, "The elements of stochastic processes", John Wiley publications, New York, 1964